ECF-HANFORD-19-0042
Revision 0

Vadose Zone Model for B-3A/B Pond for Composite Analysis

Prepared for the U.S. Department of Energy
Assistant Secretary for Environmental Management

Contractor for the U.S. Department of Energy
under Contract DE-AC06-08RL14788

CH2MHILL
Plateau Remediation Company

P.O. Box 1600
Richland, Washington 99352

ECF-HANFORD-19-0042
Revision 0

Vadose Zone Model for B-3A/B Pond for Composite Analysis

Document Type: ECF Program/Project: EPSP

G. Tartakovsky
INTERA, Inc.

J. P. McDonald
INTERA, Inc.

S. L. Lindberg
INTERA, Inc.

C. R. Farrow
INTERA, Inc.

P. Allena
INTERA, Inc.

Date Published
September 2020

Prepared for the U.S. Department of Energy
Assistant Secretary for Environmental Management

Contractor for the U.S. Department of Energy
under Contract DE-AC06-08RL14788

CH2MHILL
Plateau Remediation Company
P.O. Box 1600
Richland, Washington 99352

APPROVED
By Lynn M. Ayers at 11:01 am, Oct 05, 2020

Release Approval Date

ENVIRONMENTAL CALCULATION COVER PAGE

SECTION 1 - Completed by the Responsible Manager

Project: Hanford Site Composite Analysis Update	RELEASE / ISSUE DATE: Oct 05, 2020 HANFORD RELEASE
Date: 05/02/2019	
Calculation Title and Description: Vadose Zone Model for B-3A/B Pond for Composite Analysis	

Qualifications Summary

Preparer(s):

Name: Guzel Tartakovsky (Model Team Leader; title page identifies all team members)

Degree, Major, Institution, Year: MS, Hydrology, University of Arizona, 2006
BS, Mathematics, Kazan State University, 1994

Professional Licenses:

Brief Narrative of Experience: Ms. Guzel Tartakovsky has well over a decade of experience in numerical modeling of flow and transport in groundwater and the vadose zone. Guzel has been applying the STOMP simulator to a variety of multiphase problems during her employment at Pacific Northwest National Laboratory and before that at Columbia Environmental Sciences. She has co-authored several peer-reviewed papers related to vadose zone flow and transport, remediation of nonaqueous phase liquids, and geologic CO2 sequestration. As a graduate research assistant at the University of Arizona, she had developed an analytical solution for the delayed aquifer response process characterizing flow to a pumping well. The solution was implemented in the aquifer test analysis software AQTESOLV.

ENVIRONMENTAL CALCULATION COVER PAGE (Continued)

Checker(s):	
Name:	Jose Lopez (Calculation Process Checking Team Leader)
Degree, Major, Institution, Year:	BA, Geography with GIS, Mapping, and Society Focus, University of Washington, 2017
Professional Licenses:	
Brief Narrative of Experience:	Jose Lopez's experience focuses on collecting, analyzing, manipulating, and developing spatial data pertaining to Geographic Information Systems (GIS). He specializes in analyzing GIS data and using it to identify trends, build geodatabases, and create interactive maps to visualize data changes. He will be applying his skills to support and assist INTERA GIS specialists with map design, GIS analysis, and modeling. Jose is also proficient with ESRI ArcGIS software, Python, Java, and Microsoft Office applications.
Name:	Mary Weber (Document Consistency Checker)
Degree, Major, Institution, Year:	MS, Geoscience, University of Iowa, 2015 BS, Geoscience, University of Iowa, 2013
Professional Licenses:	
Brief Narrative of Experience:	Mary Weber focuses her geoscientific skills on the development and application of groundwater flow and contaminant fate and transport models. She uses models to help guide environmental investigation and remediation efforts and to project future water availability as part of developing and managing groundwater resources. Mary currently provides modeling and other technical support for remedial investigations and feasibility studies being performed on one of the largest environmental restoration projects in the world at the U.S. Department of Energy's Hanford Site.

ENVIRONMENTAL CALCULATION COVER PAGE (Continued)

Senior Reviewer(s):

Name: Mart Oostrom

Degree, Major, Institution, Year: PhD, Soil Physics, Auburn University, 1991
MS, Soil Physics and Hydrogeology, Wageningen University, 1986
MA, Teaching (Mathematics), University of Idaho, 2010
BS, Soil Science, Wageningen University, 1984

Professional Licenses:

Brief Narrative of Experience: Mart Oostrom brings specialized expertise in the development and application of numerical models to evaluate groundwater flow and contaminant transport and the effectiveness of various environmental remediation methods and technologies. Some of his recent experience includes quantifying contaminant flux into groundwater at various deep-vadose zone waste disposal sites; conducting reservoir modeling for enhanced oil recovery and CO2 sequestration; remediating the vadose zone using ammonium injection, soil dessication, and/or pore-water extraction; and developing a circulation method to quantify back-diffusion of dissolved contaminants into permeable sediment. Mart is co-author of the STOMP© (Subsurface Flow over Multiple Phase) simulator, a mathematical model used to numerically simulate subsurface (multiphase) flow and transport as well as vadose zone and groundwater remediation. STOMP's target capabilities were guided by proposed or applied remediation activities at sites contaminated with volatile organic compounds and/or radioactive material. The simulator's modeling capabilities address a variety of subsurface environments, including nonisothermal conditions, fractured media, multiple-phase systems, nonwetting fluid entrapment, soil freezing conditions, nonaqueous phase liquids, first-order chemical reactions, radioactive decay, solute transport, dense brines, nonequilibrium dissolution, and surfactant-enhanced dissolution and mobilization of organics. Mart is Associate Editor of the Journal of Contaminant Hydrology and has authored over 100 refereed journal articles and contributed to book chapters on the subjects of multifluid flow, site characterization, remediation, and monitoring.

SECTION 2 - Completed by Preparer

Calculation Number: ECF-HANFORD-19-0042 | Revision Number: 0

Revision History

Revision No.	Description	Date	Affected Pages
0	Initial issue	09/17/2020	All

SECTION 3 - Completed by the Responsible Manager

Document Control:

Is the document intended to be controlled within the Document Management Control System (DMCS)? ◉ Yes ○ No

Does document contain scientific and technical information intended for public use? ◉ Yes ○ No

Does document contain controlled-use information? ○ Yes ◉ No

ENVIRONMENTAL CALCULATION COVER PAGE (Continued)

SECTION 4 - Document Review and Approval

Preparer(s):

Print First and Last Name	Position	Signature	Date
Guzel Tartakovsky	Hydrogeologist	Per Electronic Approval (attached)	

Checker(s):

Print First and Last Name	Position	Signature	Date
Jose Lopez	GIS Analyst	Per Electronic Approval (attached)	
Mary Weber	Hydrogeologist	Per Electronic Approval (attached)	

Senior Reviewer(s):

Print First and Last Name	Position	Signature	Date
Mart Oostrom	Principal Scientist	Per Electronic Approval (attached)	

Responsible Manager(s):

Print First and Last Name	Position	Signature	Date
Alaa Aly	Risk & Model Integr Mgr	Per Electronic Approval (attached)	

SECTION 5 - Applicable if Calculation is a Risk Assessment or Uses an Environmental Model

Prior to Initiating Modeling:

Required training for modelers completed:
Integration Lead:

Print First and Last Name	Signature	Date
William Nichols	Per Electronic Approval (attached)	

Safety Software Approved:
Integration Lead:

Print First and Last Name	Signature	Date
William Nichols	Per Electronic Approval (attached)	

Calculation Approved:
Risk/Modeling Integration Manager:

Print First and Last Name	Signature	Date
Alaa Aly	Per Electronic Approval (attached)	

From: PRC SharePoint
To: Nichols, William E
Subject: Electronic Approval has completed for document: ECF-HANFORD-19-0042-R0.
Date: Tuesday, September 22, 2020 2:57:28 PM

Electronic Approval has completed for document: ECF-HANFORD-19-0042-R0.

Please include this email as the Electronic Approval page.

Electronic Approval for document: ECF-HANFORD-19-0042-R0 has successfully COMPLETED.

Electronic Approval started by Nichols, William E on 9/19/2020 2:57 PM
Comment: Please approve release of ECF-HANFORD-19-0042 Rev. 0 (B-3A/B Ponds VZ Model for Composite Analysis)

Approved by Nichols, William E on 9/19/2020 2:59 PM
Comment:

Approved by Aly, Alaa H on 9/21/2020 1:43 PM
Comment:

Approved by Weber, Mary C on 9/22/2020 2:57 PM
Comment:

From: Guzel Tartakovsky
To: Nichols, William E; Jose Lopez; Mart Oostrom
Subject: RE: Electronic Approval Tasks - Please approve ECF-HANFORD-19-0042-R0
Date: Sunday, September 20, 2020 10:15:45 AM

Approve.

From: Nichols, William E <william_e_nichols@rl.gov>
Sent: Saturday, September 19, 2020 4:59 PM
To: Guzel Tartakovsky <GTartakovsky@intera.com>; Jose Lopez <JLopez@intera.com>; Mart Oostrom <MOostrom@intera.com>
Subject: Electronic Approval Tasks - Please approve ECF-HANFORD-19-0042-R0

Electronic Approval Task assigned by Nichols, William E on 9/19/2020.

Completing this task acts as your approval in place of a hard copy signature for document: ECF-HANFORD-19-0042-R0.

Due by **9/21/2020 5:00 PM**

Electronic Approval started by Nichols, William E on 9/19/2020 2:57 PM
Comment: Please approve release of ECF-HANFORD-19-0042 Rev. 0 (B-3A/B Ponds VZ Model for Composite Analysis)

To complete this task:
1. Review ECF-HANFORD-19-0042-R0. (note: HLAN link)
2. When review is complete, reply to this email with the word "**Approve**" to approve release of this document.

From: Jose Lopez
To: Nichols, William E
Subject: RE: Electronic Approval Tasks - Please approve ECF-HANFORD-19-0042-R0
Date: Monday, September 21, 2020 2:49:26 PM

Approve.

From: Nichols, William E <william_e_nichols@rl.gov>
Sent: Saturday, September 19, 2020 2:59 PM
To: Guzel Tartakovsky <GTartakovsky@intera.com>; Jose Lopez <JLopez@intera.com>; Mart Oostrom <MOostrom@intera.com>
Subject: Electronic Approval Tasks - Please approve ECF-HANFORD-19-0042-R0

Electronic Approval Task assigned by Nichols, William E on 9/19/2020.

Completing this task acts as your approval in place of a hard copy signature for document: ECF-HANFORD-19-0042-R0.

Due by **9/21/2020 5:00 PM**

Electronic Approval started by Nichols, William E on 9/19/2020 2:57 PM
Comment: Please approve release of ECF-HANFORD-19-0042 Rev. 0 (B-3A/B Ponds VZ Model for Composite Analysis)

To complete this task:

1. Review ECF-HANFORD-19-0042-R0. (note: HLAN link)
2. When review is complete, reply to this email with the word "**Approve**" to approve release of this document.

From: Mart Oostrom
To: Nichols, William E
Subject: RE: Electronic Approval Tasks - Please approve ECF-HANFORD-19-0042-R0
Date: Monday, September 21, 2020 8:50:11 PM

Approve

From: Nichols, William E <william_e_nichols@rl.gov>
Sent: Saturday, September 19, 2020 2:59 PM
To: Guzel Tartakovsky <GTartakovsky@intera.com>; Jose Lopez <JLopez@intera.com>; Mart Oostrom <MOostrom@intera.com>
Subject: Electronic Approval Tasks - Please approve ECF-HANFORD-19-0042-R0

Electronic Approval Task assigned by Nichols, William E on 9/19/2020.

Completing this task acts as your approval in place of a hard copy signature for document: ECF-HANFORD-19-0042-R0.

Due by **9/21/2020 5:00 PM**

Electronic Approval started by Nichols, William E on 9/19/2020 2:57 PM
Comment: Please approve release of ECF-HANFORD-19-0042 Rev. 0 (B-3A/B Ponds VZ Model for Composite Analysis)

To complete this task:
1. Review ECF-HANFORD-19-0042-R0. (note: HLAN link)
2. When review is complete, reply to this email with the word "**Approve**" to approve release of this document.

Contents

Appendices

Figures

Tables

This page intentionally left blank.

Terms

CA	composite analysis
ECF	environmental calculation file
EHM	Equivalent Homogeneous Media
eSTOMP	exascale Subsurface Transport Over Multiple Phases
GIS	geographic information system
Hf1	Hanford formation unit 1
Hf2	Hanford formation unit 2
Hf3	Hanford formation unit 3
HSU	hydrostratigraphic unit
ICF	Integrated Computational Framework
K_d	partition coefficient
P2R	plateau to river
PA	performance assessment
PA-TCT	power-averaging tensorial connectivity-tortuosity
RET	recharge evolution tool
Rlm	Ringold Formation member of Wooded Island – lower mud unit
RTD	remove, treat, and dispose
Rwia	Ringold Formation member of Wooded Island – unit A
SIM-v2	Hanford Soil Inventory Model
STOMP	
	Subsurface Transport Over Multiple Phases
TCT	tensorial connectivity-tortuosity
WMA C	Waste Management Area C

This page intentionally left blank.

1 Purpose

The objectives of the vadose modeling for the updated Hanford Site composite analysis (CA) are to simulate the flow and transport of water and radionuclide releases from the surface to the water table and to provide radionuclide transfer rates for the plateau to river (P2R) model, version 8.3 (CP-57037, *Model Package Report: Plateau to River Groundwater Model, Version 8.3*). Water additions include natural recharge and water discharged to the ground as a result of industrial processes associated with Hanford Site operations. Contaminant sources include radionuclides in water discharged to the ground during operations and radionuclides disposed "dry" in solid waste burial grounds or other means. The following 16 radionuclides were selected for this modeling effort; carbon-14 (C-14), chlorine-36 (Cl-36), tritium (H-3), iodine-129 (I-129), neptunium-237 (Np-237), rhenium-187 (Re-187), strontium-90 (Sr-90), technetium-99 (Tc-99), uranium-232 (U-232), uranium-233 (U-233), uranium-234 (U-234), uranium-235 (U-235), uranium-236 (U-236), uranium-238 (U-238), radium-226 (Ra-226), and thorium-230 (Th-230). The simulation time starts in 1943 and ends at 12070, which is 10,000 years after assumed Hanford Site closure in 2070.

The parallel version of the Subsurface Transport Over Multiple Phases (STOMP[1]) simulator officially named the exascale Subsurface Transport Over Multiple Phases (eSTOMP), is used to simulate flow and transport for the vadose models. The documentation for the STOMP code is comprehensive. The theoretical and numerical approaches applied in the STOMP code are documented in a published theory guide (PNNL-12030, *STOMP Subsurface Transport Over Multiple Phases Version 2.0 Theory Guide*). The code has undergone a rigorous verification procedure against analytical solutions, laboratory-scale experiments, and field-scale demonstrations. The application guide (PNNL-11216, *STOMP Subsurface Transport Over Multiple Phases Application Guide*) provides instructive examples in the application of the code to classical groundwater problems. The user's guide (PNNL-15782, *STOMP: Subsurface Transport Over Multiple Phases Version 4.0: User's Guide*) describes the general use, input file formatting, compilation, and execution of the code. The primary output of the vadose zone modeling is radionuclide transfer rates to the groundwater for input into the P2R model. The rates will be summed over the 100 by 100 m P2R grid cells that fall within the vadose zone model source domain.

The Hanford Site Central Plateau was subdivided into 26 individual vadose zone models, with 13 in the 200 East Area and 13 in the 200 West Area. Waste sites that have a completed performance assessment (PA) or past-leak analysis were not included as sources of radionuclides. Instead the vadose zone to groundwater transfer rates of the Environmental Restoration Disposal Facility, Integrated Disposal Facility, US Ecology, and Waste Management Area C (WMA C) PAs and the past-leak analysis for WMA C were used as direct input to the P2R model. Each of the vadose zone models is documented in separate environmental calculation files (ECFs). This ECF describes the B-3A/B Ponds model. The scope of this ECF is to document the development and results of the B-3 A/B Ponds vadose zone model. CP-63515, *Model Package Report: Central Plateau Vadose Zone Models*, describes the approach, assumptions, process of determining the number of models required and domain of each model, input data, and processing common to all the models. Additionally, the following documents support inputs to the models:

- CP-60925, *Model Package Report: Central Plateau Vadose Zone Geoframework*, describes the hydrostratigraphic framework.

[1] STOMP is a copyright of Battelle Memorial Institute, Columbus, Ohio, and used under the Limited Government License.

- CP-61786, *Inventory Data Package for the Hanford Site Composite Analysis*, contains the solid waste inventory.
- CP-62184, *Hanford Site Composite Analysis: Radionuclide Selection for Groundwater Pathway Evaluation*, describes the selection of the 16 radionuclides used in these simulations.
- CP-62766, *Model Package Report: Composite Analysis Solid Waste Release Model (CASWR Model)*, describes the mechanisms of release of radionuclides from solid waste based on waste type.
- CP-63883, *Vadose Zone Flow and Transport Parameters Data Package for the Hanford Site Composite Analysis,* describes the process of assigning material properties to the hydrostratigraphic units (HSUs).
- ECF-HANFORD-15-0019, *Hanford Site-wide Natural Recharge Boundary Condition for Groundwater Models*, describes the recharge evolution tool (RET) used to calculate the recharge.
- ECF-HANFORD-17-0079, *Hanford Soil Inventory Model (SIM-v2) Calculated Radionuclide Inventory of Direct Liquid Discharges to Soil in the Hanford Site's 200 Areas*, describes the aqueous sources for the CA modeling effort, which uses the source inventory found in Appendix F of ECF-HANFORD-17-0079.
- ECF-HANFORD-18-0035, *Central Plateau Vadose Zone Geoframework*, describes the updates to the hydrostratigraphy surfaces defined in CP-60925, and defines the hydrostratigraphy surfaces used by this modeling effort.
- ECF-HANFORD-19-0032, *Distribution of Infiltration in the 216-U-10 and 216-B-3 Pond Systems 1944-1997*, estimates the routing of effluent and infiltration between ditches and ponds of the 216-U-10 Pond System and between the main pond and expansion lobes of the 216-B-3 Pond System.
- ECF-HANFORD-19-0094, *Calculation of Moisture-Dependent, Anisotropic Parameters Supporting the Hanford Site's Composite Analysis, Cumulative Impact Evaluation, and Performance Assessments*, describes calculations of moisture-dependent, anisotropy of hydraulic conductivity for the HSUs.
- ECF-HANFORD-19-0112, *Solid Waste Release Calculations for the Composite Analysis Baseline Assessment*, calculates the solid waste annual release rates.
- ECF-HANFORD-19-0121, *Selection of Vadose Zone Flow and Transport Properties with Gravel Fraction Corrections for the Hanford Site Composite Analysis and Cumulative Impact Evaluation*, describes the physical and chemical properties used for these models.
- ECF-HANFORD-20-0006, *Composite Analysis Solid Waste Release Data Reduction of Activity Flux from Waste Sites to the Vadose Zone*, describes the solid waste data reduction.

2 Background

The B-3A/B Ponds model covers the 216-B-3A and 216-B-3B Expansion Ponds of the 216-B-3 Pond System located in a topographic low east of the 200 East Area (Figure 2-1). The main lobe of the pond system, 216-B-3, is addressed by the B-3 Pond model (ECF-HANFORD-19-0041, *Vadose Zone Model for B-3 Pond for Composite Analysis*), and the third expansion lobe, 216-B-3C, is covered by the B-3C Pond model (ECF-HANFORD-19-0043, *Vadose Zone Model for B-3C Pond for Composite Analysis*). The pond system operated from 1945 to 1997 and received effluents from the Plutonium Uranium Extraction Plant, B Plant, 284-E Powerhouse, and other 200 East Area facilities (DOE/RL-2008-59, *Interim Status Groundwater Monitoring Plan for the 216-B-3 Pond*). Wastewater was conveyed to the pond system mostly by ditches.

The 216-B-3A and 216-B-3B lobes were constructed in 1983 and 1984, respectively, to accommodate increased discharges from the restart of Plutonium Uranium Extraction Plant (DOE/RL-89-28, *216-B-3 Expansion Ponds Closure Plan*). 216-B-3A operated from October 1983 to April 1994 and received overflow water from the main pond (216-B-3) through a spillway. In January 1984, the dike between 216-B-3A and 216-B-3B failed and water flowed into 216-B-3B. This was the only time 216-B-3B received water. The 216-B-3A lobe was inactive from February 1984 to May 1984 while repairs to the dike were made. A trench was dug into the bottom of 216-B-3A to increase infiltration, and the lobe was fully operational again by June 1984. 216-B-3A was taken out of service in 1994 (DOE/RL-2008-59). The volume of effluent discharged to 216-B-3A and 216-B-3B was not recorded, but infiltration volumes for these lobes was estimated in ECF-HANFORD-19-0032 to support this modeling effort.

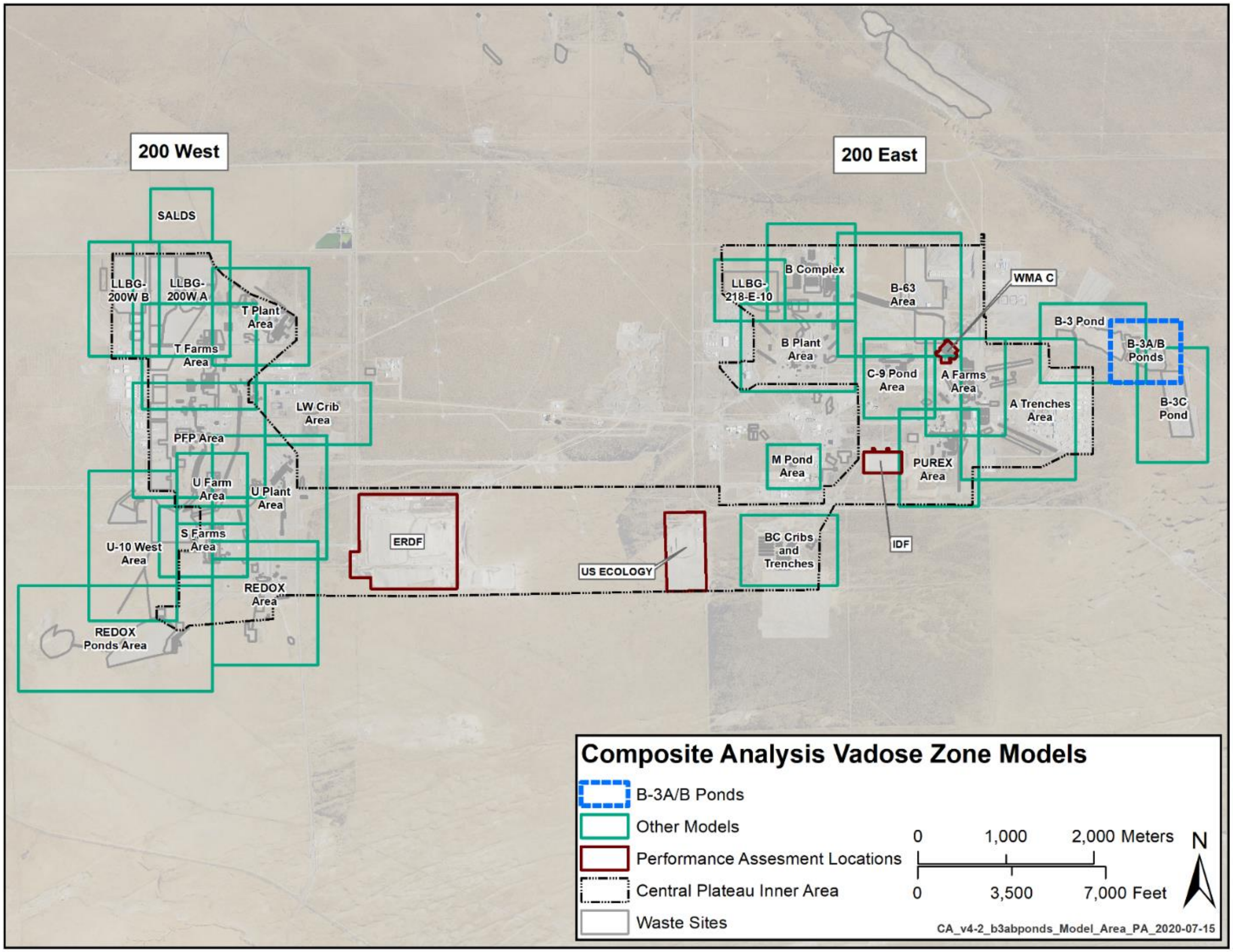

Figure 2-1. Location of the B-3A/B Ponds Model

3 Methodology

This chapter contains a discussion of configuration control, a brief overview of the methodology for creating the B-3A/B Ponds model, and a list of modifications specific to this model.

3.1 Configuration Control

A configuration control system was developed so that all vadose zone models generated for the CA would follow a consistent set of conventions and use only approved input data (e.g., geoframework, hydraulic and contaminant properties, source releases, etc.). This system was manifested as sets of qualified input data, scripts used to construct the models and post-process the results and sets of instructions for building and executing the models. Each script was reviewed, tested, and documented to qualify it for use. A list of scripts developed for the vadose zone modeling effort is found in Section 5.3 of this ECF. Each CA model used the same directory structure. A discussion of the configuration control system is found in CP-63515.

A data configuration quality-control system (hereinafter called the Integrated Computational Framework [ICF]), provides the tools necessary to verify that all model output data are correctly associated with their corresponding input data. The ICF consists of two parts: a file management system and utility scripts to support the file management system.

The ICF houses all data produced by and in support of the CA modeling effort. The ICF file management system ensures that no data can be modified, deleted, or used in a model application without being checked into the ICF, reviewed, and accepted by the ICF administrator. Separating the data flow from the modeling helps prevent accidental modification and guarantees a data review prior to acceptance of any data product into the ICF.

The utility scripts establish a pedigree for any data product stored in the ICF. The ICF allows users to ascertain all the ancestor and derivative products related to any ICF data product. By combining the file structure and software utilities, the ICF provides confidence that the CA output data are associated with a set of versioned input data.

The CA models were constructed on a central computer system, and many of the models contained over one million nodes. Along with the long time period simulated and the release of large volumes of water from liquid waste disposal sites in many of the model domains, the size of the models caused long run times. Thus, the model files were transferred to a high-power computer system, GAIA, for execution. Following completion of model runs, the input and output files were returned to the original computer system for post-processing. File fingerprinting was used to verify this transfer process and to verify that the correct input files were used for each model simulation.

3.2 Model Construction and Execution

This ECF is one of 26 similar ECFs, one for each CA vadose zone model, each of which followed the same general methodology. A detailed description of the general model construction is found in CP-63515. Adjustments are made to the methodology as needed to tailor model development to best represent the area being simulated. The steps were developed to include mass balance checks to verify model performance. A brief outline for the construction and execution of the B-3A/B Ponds model is as follows:

1. Construct the model grid.
2. Assign HSUs and material properties to the model grid nodes.

3. Generate the temporal-spatial recharge distributions for the model using the RET.
4. Execute the steady-state flow simulation to establish the initial conditions for the transient simulations.
5. Conduct post-processing of the steady-state simulation, including calculating the liquid volume balance.
6. Incorporate the transient RET results, radionuclide waste release, and liquid waste release data into the model input file. Generate input files for a historical simulation from 1943–2018, a forecast simulation from 2018–12070, and a simulation from 1943–12070 with no radionuclide decay which is used to check the mass balance.
7. Modify liquid waste releases as necessary, for example, averaging releases to improve model convergence.
8. Execute the mass balance simulation. This requires two simulations because the 16 radionuclides simulated are divided into two groups, Radionuclide Group 1 and Radionuclide Group 2, as shown in Table 3-1.
9. Conduct post-processing of the radionuclide mass balance simulations, including calculating the mass balance.
10. Execute the historical radionuclide transport simulations (1943–2018) for Radionuclide Group 1 and Radionuclide Group 2.
11. Execute the forecast radionuclide transport simulations from 2018–12070 for Radionuclide Group 1 and Radionuclide Group 2.
12. Conduct post-processing of the radionuclide transport simulations to generate contaminant transfer rates to groundwater for the P2R model.

Table 3-1. List of Modeled Radionuclides in Radionuclide Group 1 and Radionuclide Group 2

Radionuclide Group 1	Radionuclide Group 2
C-14	U-232
Cl-36	U-233
H-3	U-234
I-129	U-235
Np-237	U-236
Re-187	U-238
Sr-90	Ra-226
Tc-99	Th-230

All model inputs were checked during production. Checking documentation is found in Appendix A.

3.3 Model-Specific Modifications

Model-specific changes were required for some models. This model required model-specific modifications. These modifications are as follows: averaged aqueous sources over a number of years and extended an aqueous source application period. This is discussed in Section 4.5.2.1.

This page intentionally left blank.

4 Assumptions and Inputs

The domain and structure of the B-3A/B Ponds model, hydraulic properties, boundary and initial conditions, source releases, the types of simulations performed, and assumptions are described in the following sections.

4.1 Model Domain and Grid

The B-3A/B Ponds model was constructed to simulate radionuclide contaminant transport through the vadose zone from the waste sites at and around the B-3A/B Ponds in the 200 East Area. The extents and grid spacing of this model are shown in Figure 4-1. A general approach to grid spacing for the CA vadose zone models, both horizontal and vertical, is discussed in CP-63515. The B-3A/B Ponds model grid is aligned with the P2R model grid (CP-57037) as shown in Figure 4-2. The B-3A/B Ponds model has 80 columns from west to east (X-nodes), 70 rows from south to north (Y-nodes), and 137 layers in the vertical dimension (Z-nodes), for a total of 767,200 nodes. The total extent of the model is 800 m in the east-west direction and 700 m in the north-south direction. The southwest corner of the domain has coordinates of 577,000 m east and 136,200 m north (Washington State Plane, South Zone [4602]). The model extends vertically from the approximate water table elevation to the ground surface. Grid spacing for each model was determined through multiple iterations based on geologic layer thickness, plume extent, waste site alignment, and mass balance considerations. Preliminary model runs were used to evaluate spatial discretization, and refinements were made as necessary (e.g., to better represent source zone geometry and plume migration). Vertical spacing is 0.5 m.

This model has a source zone and a buffer zone. The dashed blue line in Figure 4-1 indicates the separation between the source and buffer zones. These regions are distinguished by how the radionuclide inventory from waste sites is distributed. Water and radionuclide releases were simulated for waste sites in the source zone, whereas only water volume releases were simulated for waste sites in the buffer zone. Water volume releases in the buffer zone were included so that their hydraulic effect on flow beneath the source zone is accounted for. Waste sites with radionuclide releases located in the buffer zone are included in the source zones of other models.

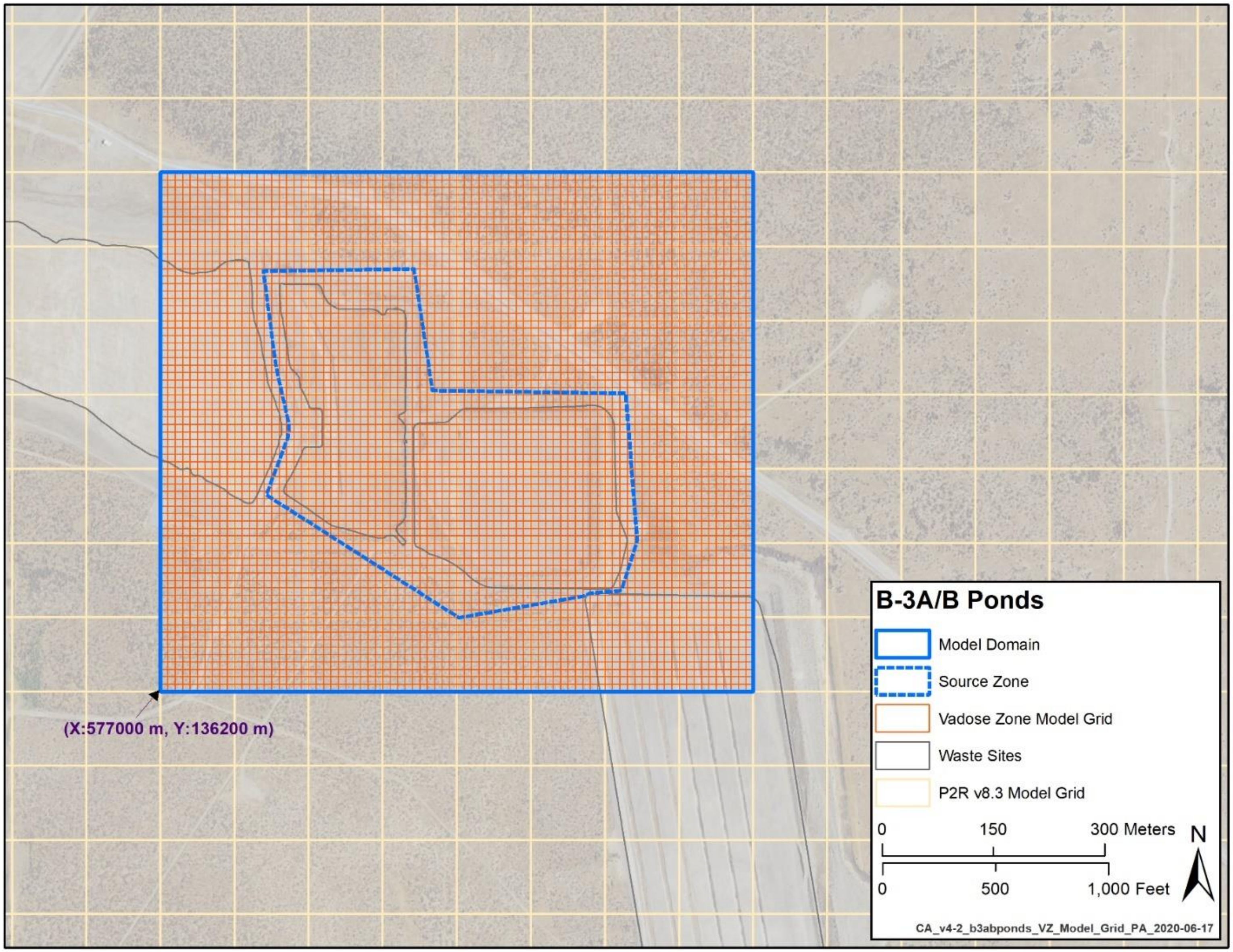

Figure 4-1. Plan View of the B-3A/B Ponds Model Grid Overlain on the P2R Grid Cells

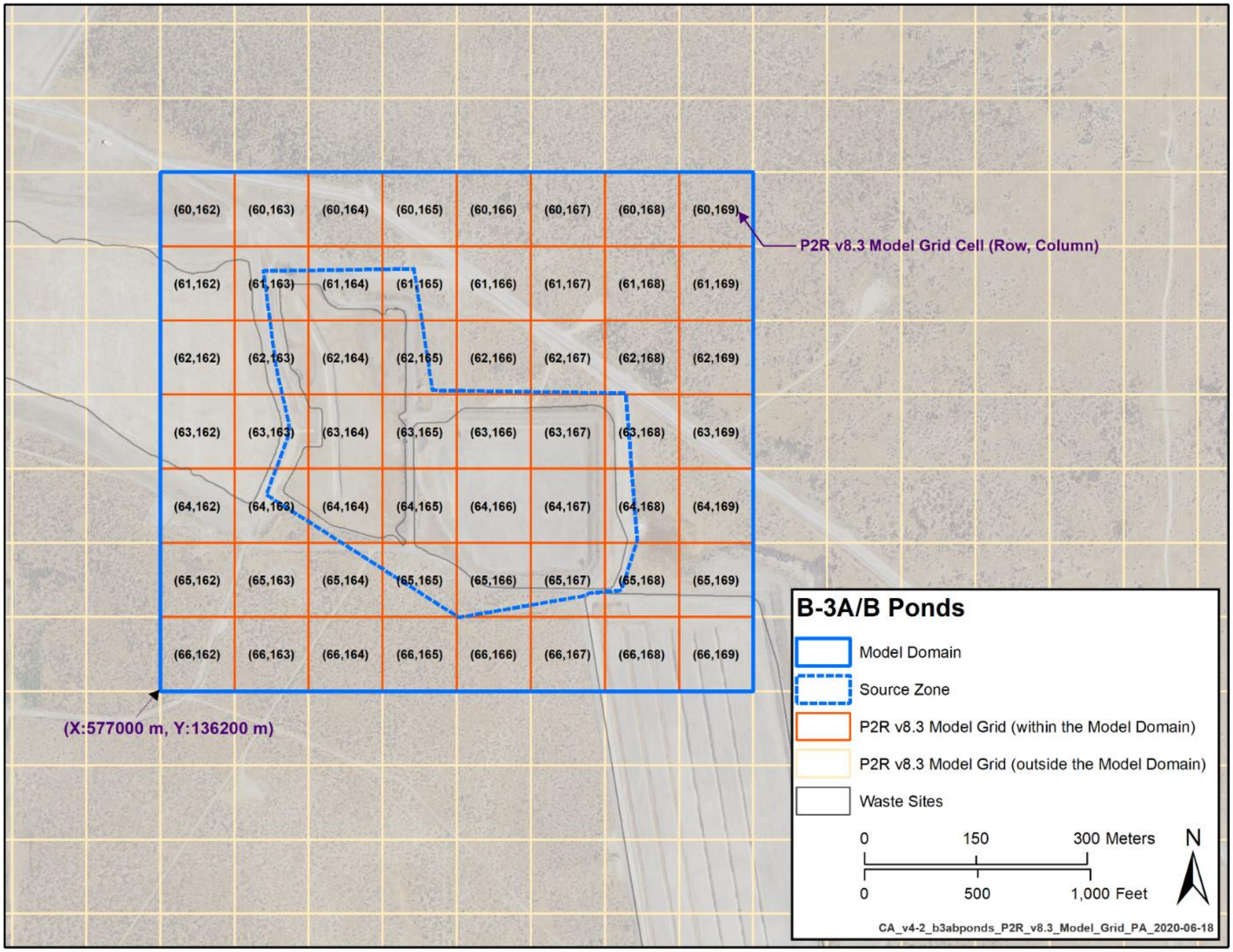

Figure 4-2. Plan View of the P2R Grid Cells in the B-3A/B Ponds Model

4.2 Model Hydrostratigraphy

The B-3A/B Ponds model includes 6 HSUs: Backfill, Hanford formation unit 1 (Hf1), Hanford formation unit 2 (Hf2), Hanford formation unit 3 (Hf3), Ringold Formation member of Wooded Island – lower mud unit (Rlm), and Ringold Formation member of Wooded Island – unit A (Rwia), in descending sequence. HSU designations were assigned to each grid node based on the surfaces in the geoframework model (ECF-HANFORD-18-0035). Properties assigned to each HSU are presented in ECF-HANFORD-19-0121 and are described in Section 4.3. CP-63515 provides a detailed description of the hydrostratigraphy for the CA vadose zone models. Figure 4-3 through Figure 4-6 show the hydrostratigraphic framework for the B-3A/B Ponds model from various orientations. A progression of cross-sections from west to east and south to north through the model are shown in Appendix B of this ECF.

The Hanford formation units (Hf1, Hf2, and Hf3) are the thickest units in the model, and their thicknesses vary throughout the model. The Rlm and Rwia are the oldest units in the model. The Rlm is at the base of the model over the southern portion of the model, and the Rwia, the oldest unit in the model, is at the base of the model over the northern portion of the model.

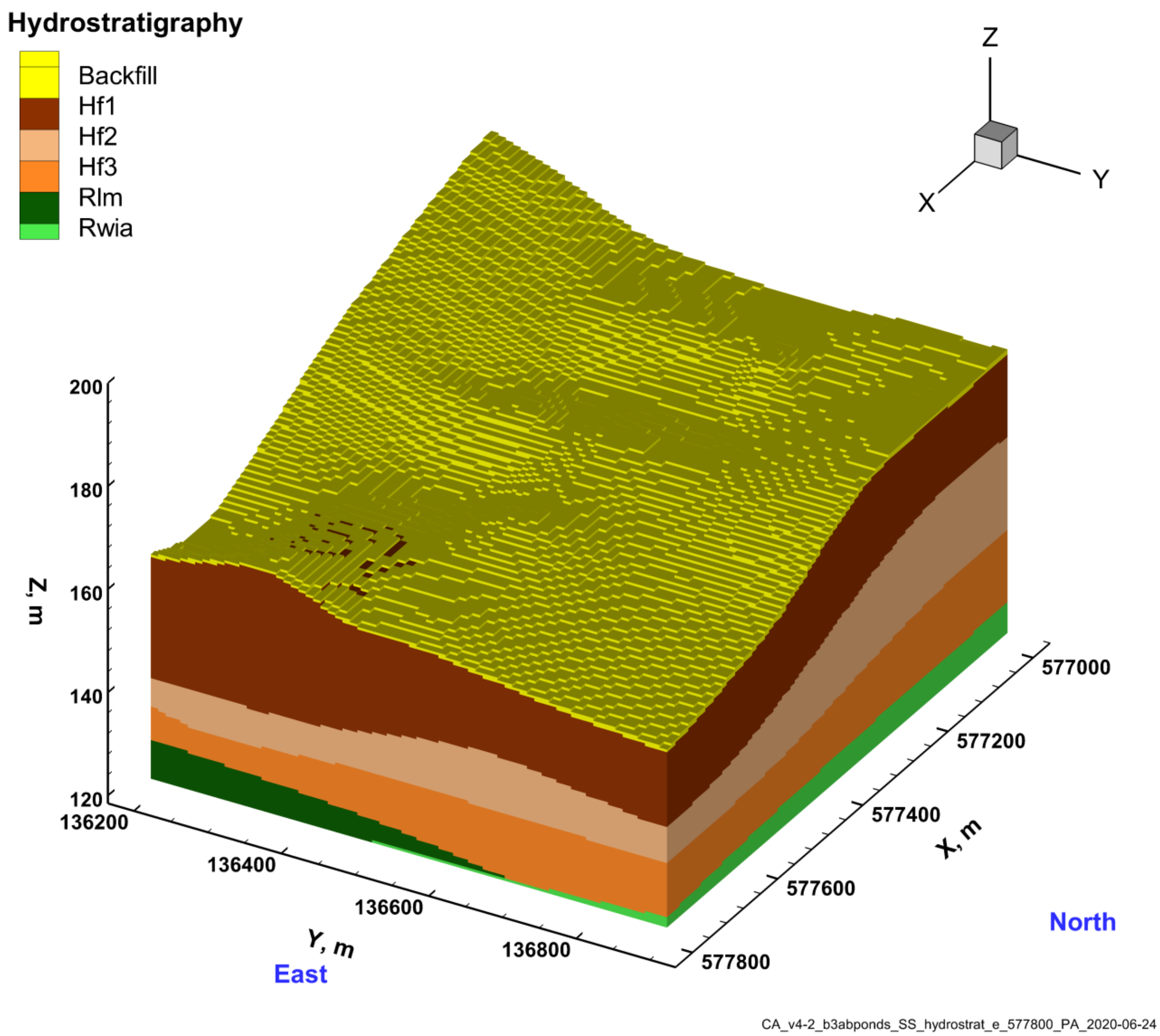

Figure 4-3. Model Hydrostratigraphy Three-Dimensional View Showing the North and East Faces

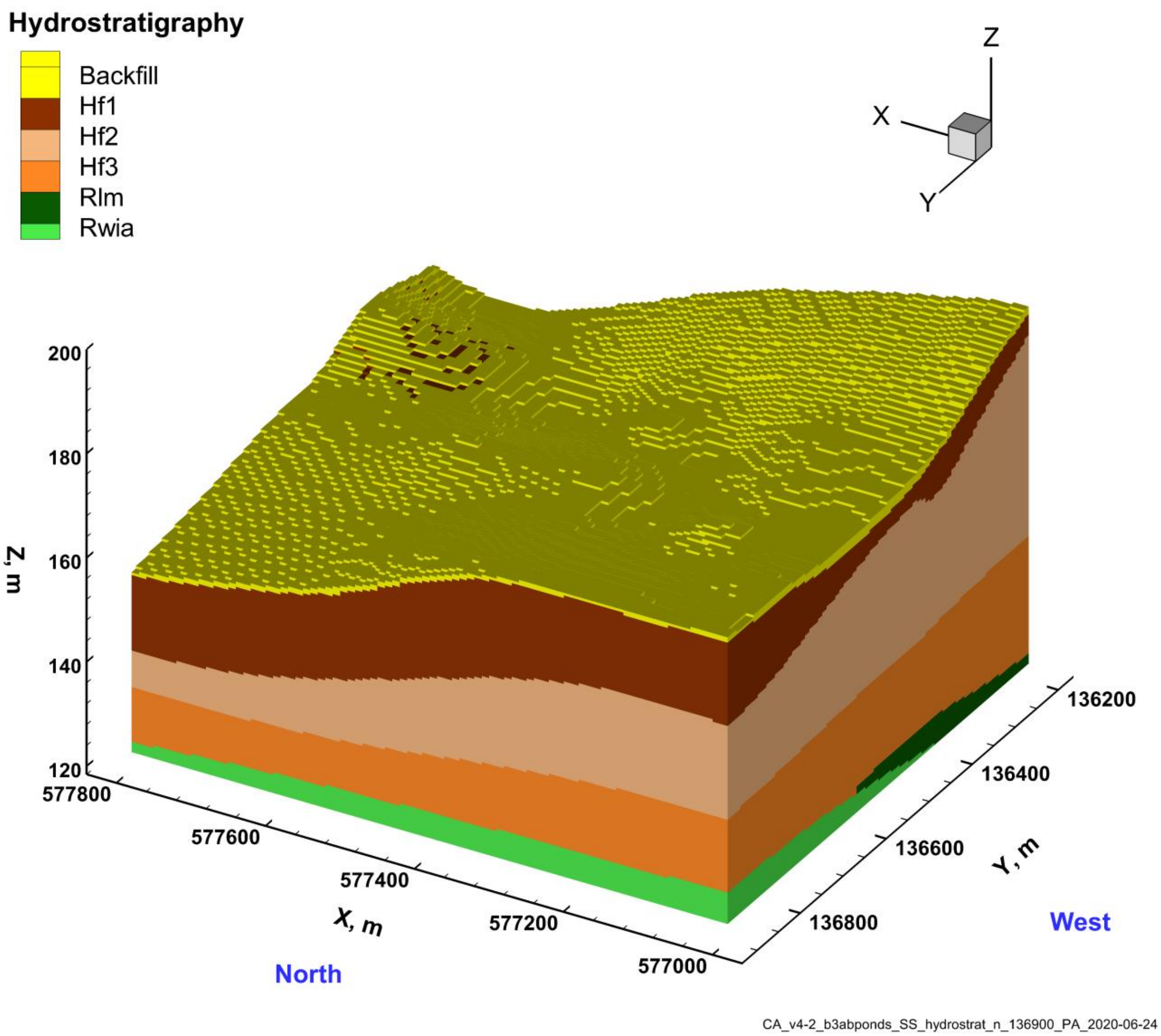

Figure 4-4. Model Hydrostratigraphy Three-Dimensional View Showing the North and West Faces

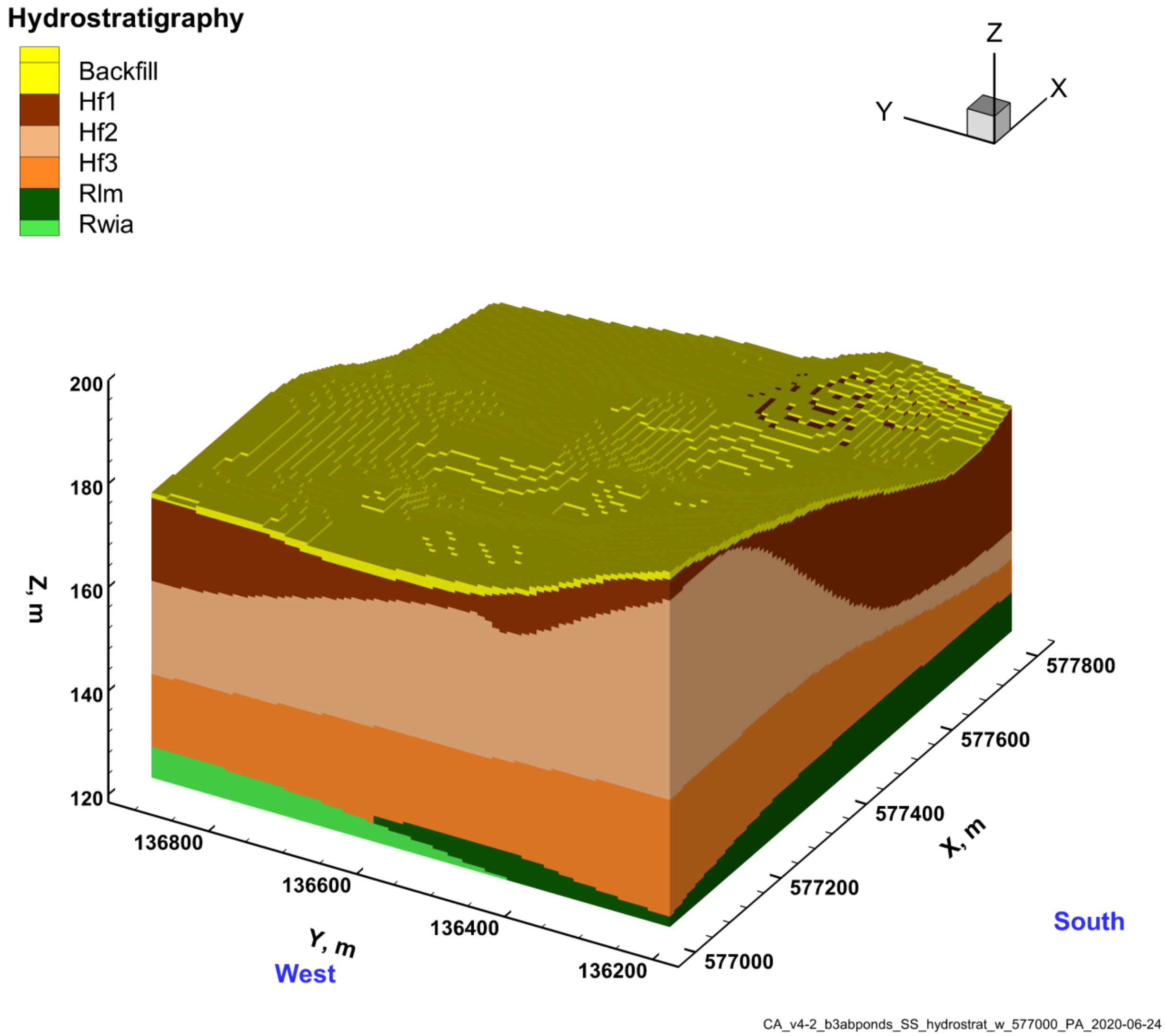

Figure 4-5. Model Hydrostratigraphy Three-Dimensional View Showing the South and West Faces

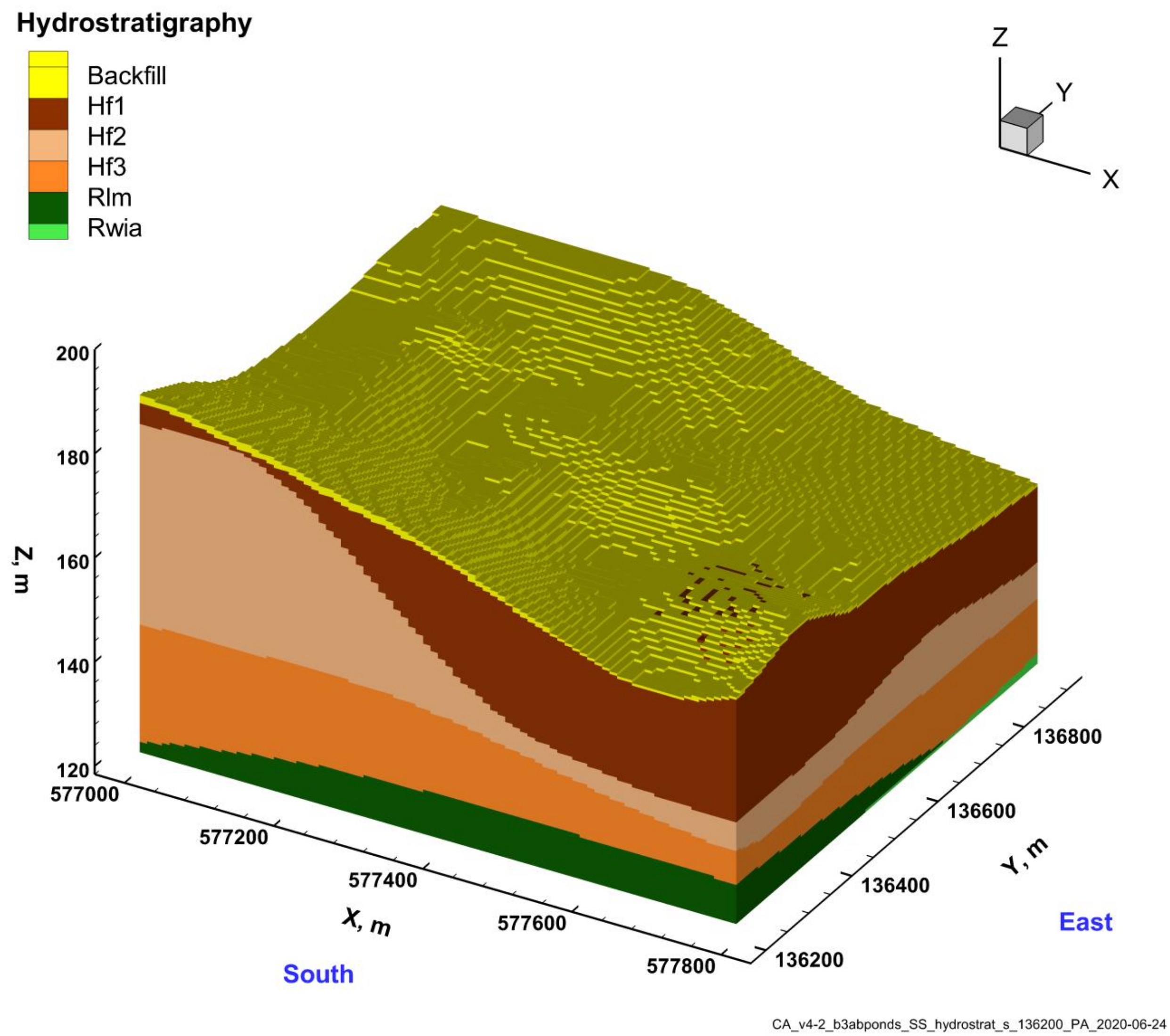

Figure 4-6. Model Hydrostratigraphy Three-Dimensional View Showing the South and East Faces

4.3 Hydraulic Properties

Hydraulic properties for the B-3A/B Ponds HSUs are shown in Tables 3, 4, 6, and 7 of ECF-HANFORD-19-0121. For most of the HSUs, hydraulic property estimates in ECF-HANFORD-19-0121 were obtained from CP-63883, which contains a detailed description of the development of these parameters for the unconsolidated sediments overlying the basalt HSU in the Central Plateau. Properties for the perched zone units and the basalt HSU were obtained from other sources.

HSUs were assumed to follow the van Genuchten (van Genuchten, 1980, "A Closed-form Equation for Predicting the Hydraulic Conductivity of Unsaturated Soils") moisture-retention constitutive relation and the Mualem-van Genuchten relative-permeability constitutive relation (Mualem, 1976, "A New Model for Predicting the Hydraulic Conductivity of Unsaturated Porous Media"), requiring values to be specified in STOMP for the following items:

- Saturated hydraulic conductivity

- Saturated moisture content
- Residual saturation, equal to the residual moisture content divided by the saturated moisture content
- van Genuchten α, proportional to the inverse of the air entry matric potential
- The dimensionless van Genuchten *n* fitting parameter
- The tensorial connectivity-tortuosity (TCT) parameters for moisture dependent anisotropy (discussion of the TCT parameters is in CP-63515 and ECF-HANFORD-19-0094).

4.4 Transport Parameters

In addition to the hydraulic properties discussed in Section 4.3, the transport simulations also require particle density, molecular diffusion rate, longitudinal and transverse dispersivity, solid-aqueous partition coefficient (K_d), and radionuclide half-life. Tables 5, 8, 9, 10, 13, 15, and 16 of ECF-HANFORD-19-0121 list the transport properties for the HSUs present in the modeled area. A detailed description of the transport properties used for the CA vadose zone models can be found in ECF-HANFORD-19-0121.

4.5 Source Releases

Within the source zone, the transport models consider radionuclide releases from both solid and liquid sources. Sources within the buffer zone are simulated as water-only releases (i.e., the radionuclide inventory is not included; these sites are included in the source zones of other models). Some sites within a model's source zone lack a radionuclide inventory and are also simulated as water-only releases (e.g., septic systems). This model contains no sites with solid releases. An index of waste sites contributing releases to the model are shown in Table 4-1. The waste sites contributing liquid releases within this model are shown in Figure 4-7. Section 4.5.1 contains a discussion of the radionuclide inventory released from waste sites in the model; liquid waste sites are addressed in Section 4.5.1.1 and solid waste sites are addressed in Section 4.5.1.2. Section 4.5.2 addresses liquid (volume) releases from waste sites, including water-only release sites.

Table 4-1. Waste Sites Included in the B-3A/B Ponds Model

Source Zone – Liquid Waste Sites with Radionuclide Releases (2)	
216-B-3A-RAD	216-B-3B-RAD
Source Zone – Liquid Waste Sites with No Radionuclide Releases (i.e., Liquid Only) (0)	
None	
Source Zone – Solid Waste Sites (0)	
None	
Buffer Zone – Waste Sites (Liquid Only) (2)	
216-B-3	216-B-3C-RAD

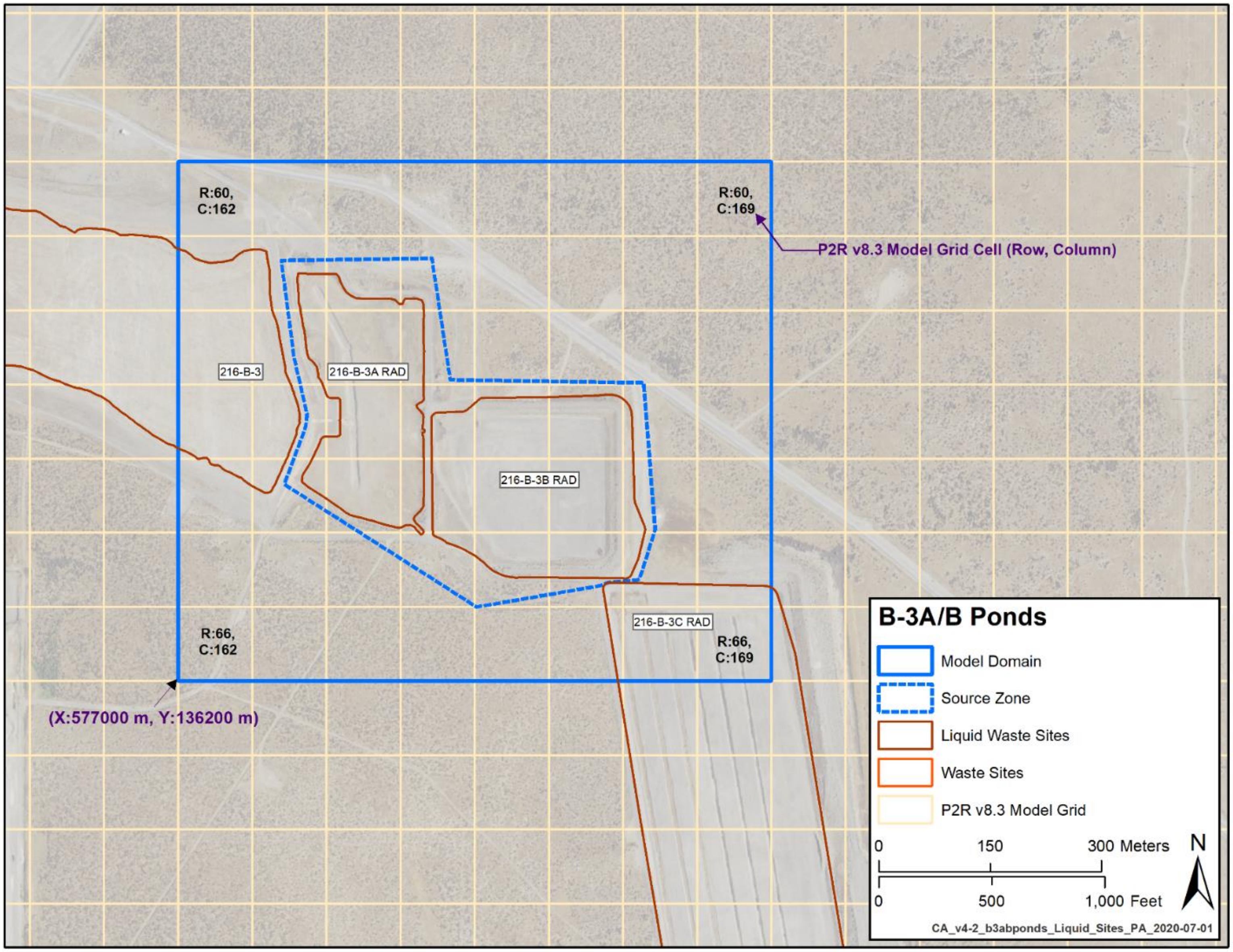

Figure 4-7. Waste Sites in the B-3A/B Ponds Model with Liquid Source Inventory

The radionuclides included in the CA vadose zone models were determined through a screening process based on prior modeling studies. CP-62184 discusses this screening process. This process identified 16 radionuclides for simulation. For computational reasons, transport of radionuclides for the CA vadose zone modeling effort was modeled in two separate groups, Radionuclide Group 1 and Radionuclide Group 2, as shown in Table 4-2. Transport properties and half-lives of the radionuclides are described in CP-62184. Not all 16 radionuclides are present in every model. No inventory is present at the waste sites in this model domain for Cl-36 and Re-187; therefore, they were not simulated. Ra-226 and Th-230 are decay products of U-234 and were included even though there was no source inventory for these radionuclides. Radionuclide activities released in the model (from liquid and solid waste sites separately, as well as the total) are shown in Table 4-2.

Table 4-2. Released Radionuclide Activities in the B-3A/B Ponds Model

Radionuclide	Total (Ci)	Liquid Waste (Ci)	Solid Waste (Ci)
Radionuclide Group 1			
C-14	1.662E+01	1.662E+01	0.000E+00
Cl-36	0.000E+00	0.000E+00	0.000E+00
H-3	2.333E+03	2.333E+03	0.000E+00
I-129	4.929E-04	4.929E-04	0.000E+00
Np-237	1.183E-02	1.183E-02	0.000E+00
Re-187	0.000E+00	0.000E+00	0.000E+00
Sr-90	2.739E+00	2.739E+00	0.000E+00
Tc-99	8.158E-03	8.158E-03	0.000E+00
Radionuclide Group 2			
U-232	7.765E-05	7.765E-05	0.000E+00
U-233	2.208E-05	2.208E-05	0.000E+00
U-234	2.078E-01	2.078E-01	0.000E+00
U-235	7.964E-03	7.964E-03	0.000E+00
U-236	2.006E-02	2.006E-02	0.000E+00
U-238	1.432E-01	1.432E-01	0.000E+00
Th-230	0.000E+00	0.000E+00	0.000E+00
Ra-226	0.000E+00	0.000E+00	0.000E+00

4.5.1 Contaminant (Activity) Releases

This section describes the releases of radionuclides to the subsurface included in this model. Simulations for the CA consider both liquid and solid waste sites but only liquid waste releases are present in the source zone of this model. These are described in Section 4.5.1.1. Releases were input to the model as annual average release rates.

4.5.1.1 Liquid Waste Site Releases

Liquid waste sites are sites where liquid wastes, often containing radionuclides, are released to the vadose zone. A map of aqueous waste sites in the B-3A/B Ponds model is shown in Figure 4-7. The waste site inventory was retrieved from ECF-HANFORD-17-0079. The radionuclides discharged to this model from liquid waste sites are shown as site totals in Figure 4-8 through Figure 4-19, and by waste site by year in Figure 4-20 through Figure 4-31. Waste sites that contributed less than 0.1% of the total radionuclide release were not included in the images for Figure 4-8 through Figure 4-19. Radionuclide releases in ECF-HANFORD-17-0079 were decayed to 2001; these were undecayed for input to the B-3A/B Ponds model.

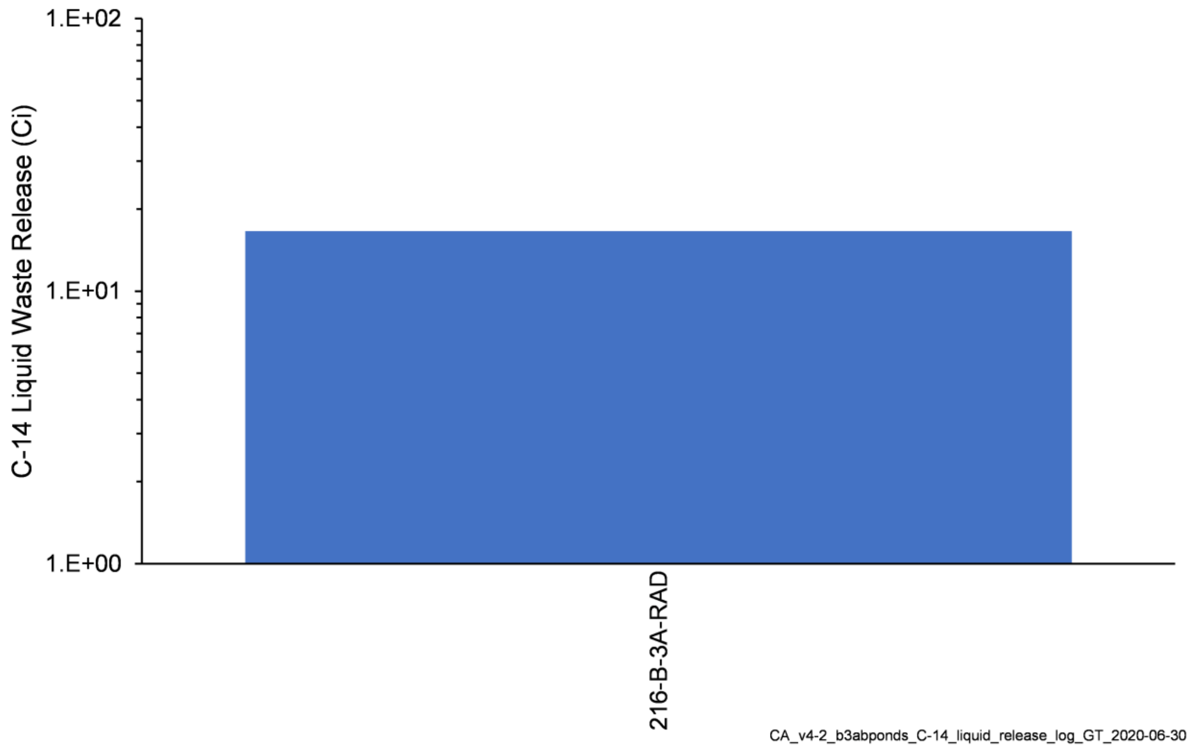

Figure 4-8. Total C-14 Activity Released from Liquid Waste Sites in the B-3A/B Ponds Model

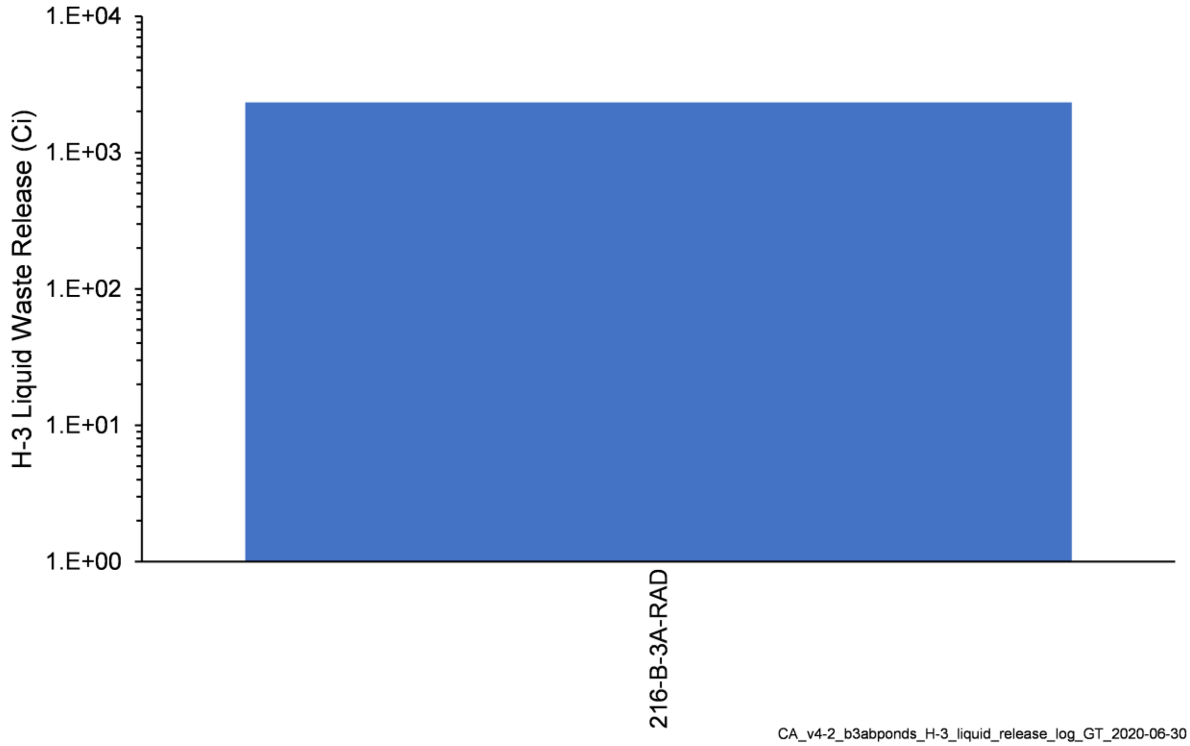

Figure 4-9. Total H-3 Activity Released from Liquid Waste Sites in the B-3A/B Ponds Model

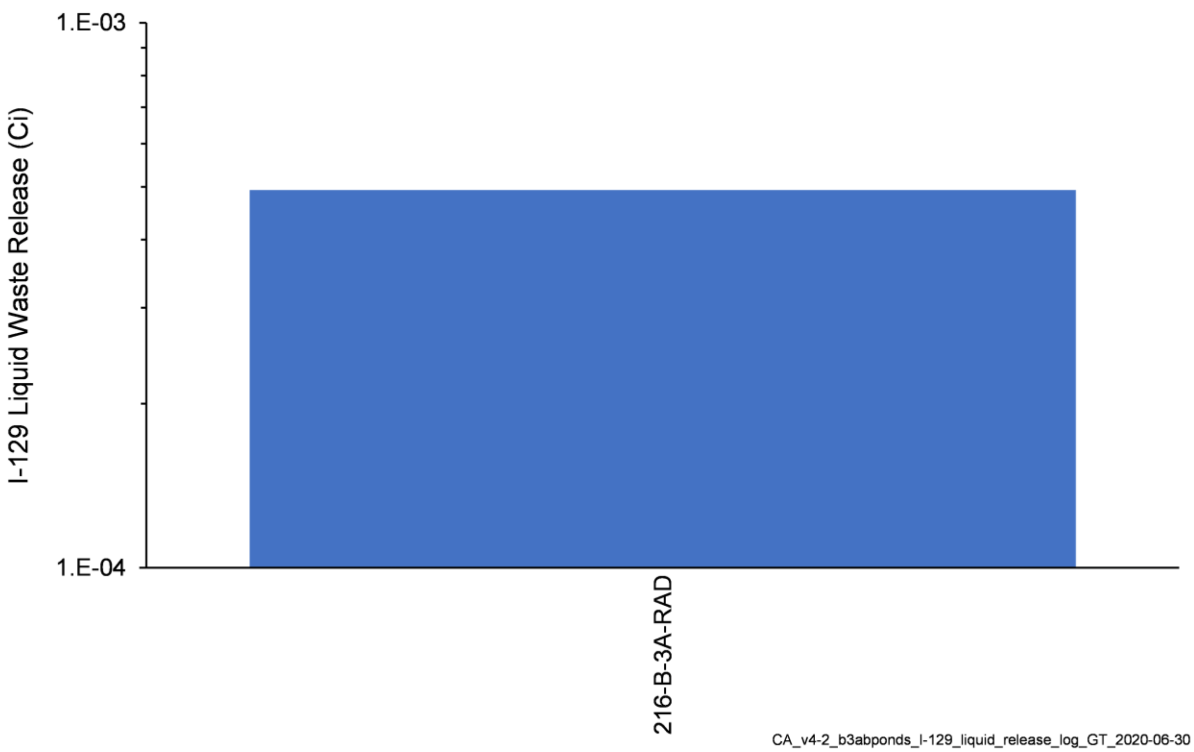

Figure 4-10. Total I-129 Activity Released from Liquid Waste Sites in the B-3A/B Ponds Model

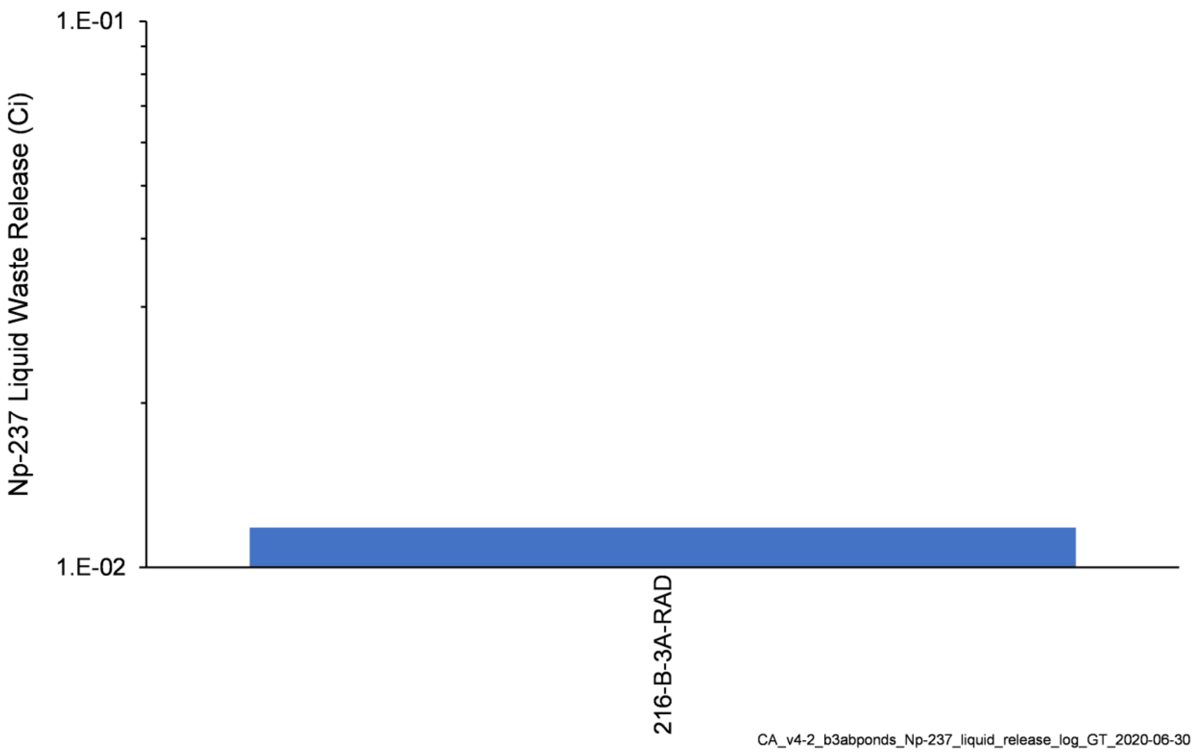

Figure 4-11. Total Np-237 Activity Released from Liquid Waste Sites in the B-3A/B Ponds Model

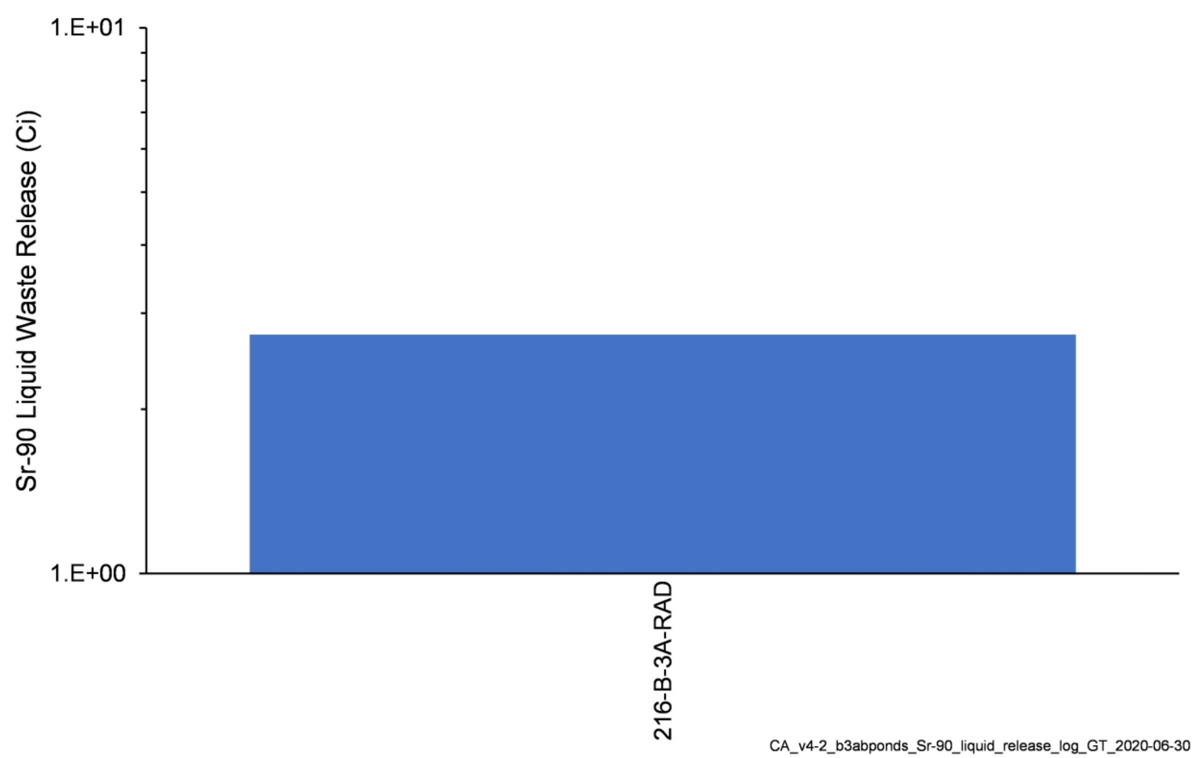

Figure 4-12. Total Sr-90 Activity Released from Liquid Waste Sites in the B-3A/B Ponds Model

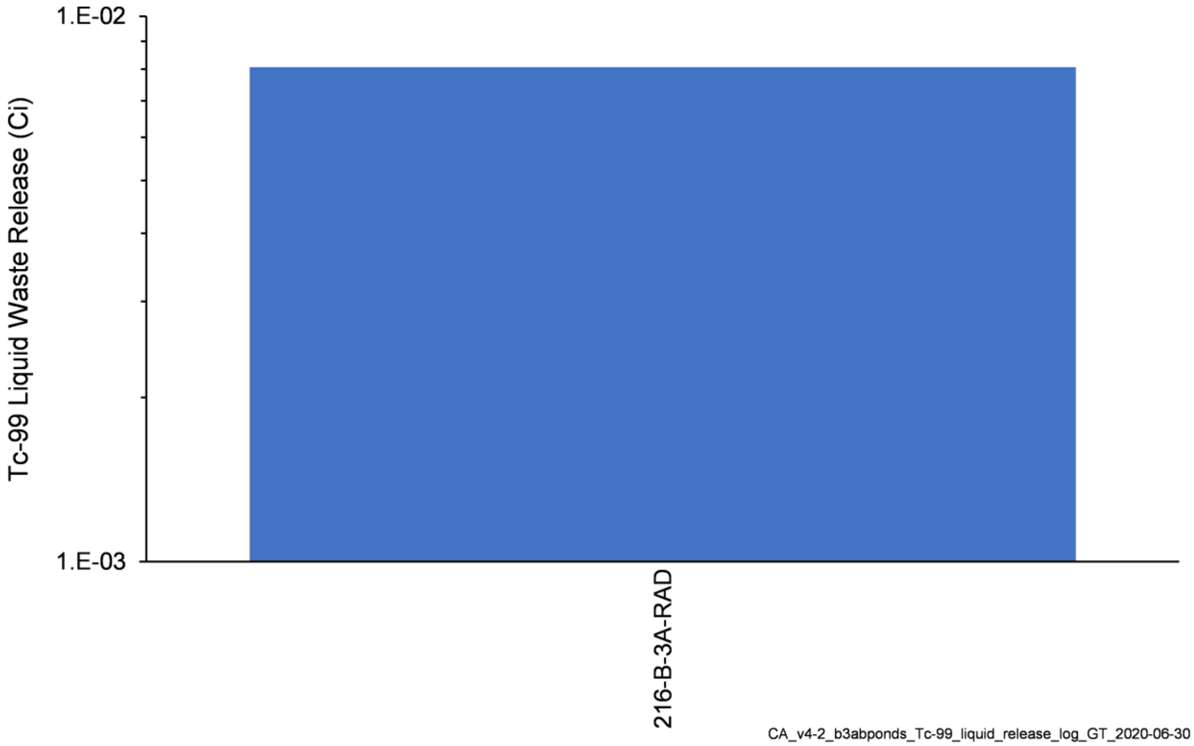

Figure 4-13. Total Tc-99 Activity Released from Liquid Waste Sites in the B-3A/B Ponds Model

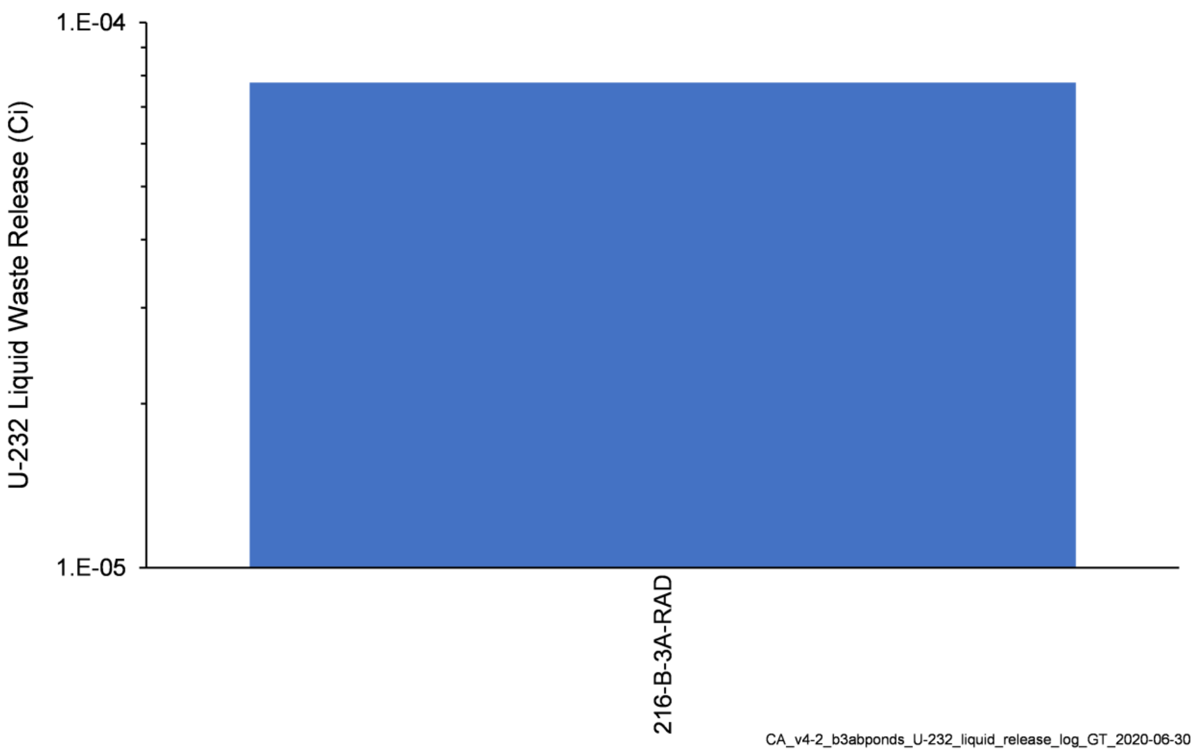

Figure 4-14. Total U-232 Activity Released from Liquid Waste Sites in the B-3A/B Ponds Model

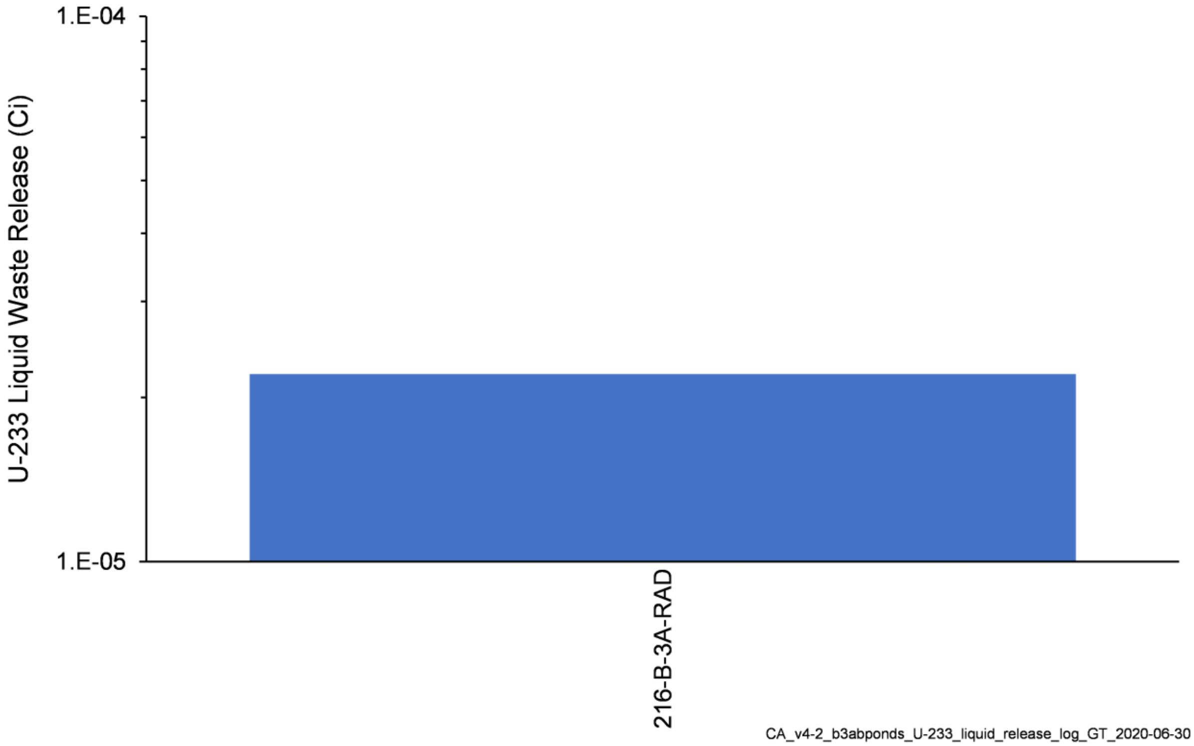

Figure 4-15. Total U-233 Activity Released from Liquid Waste Sites in the B-3A/B Ponds Model

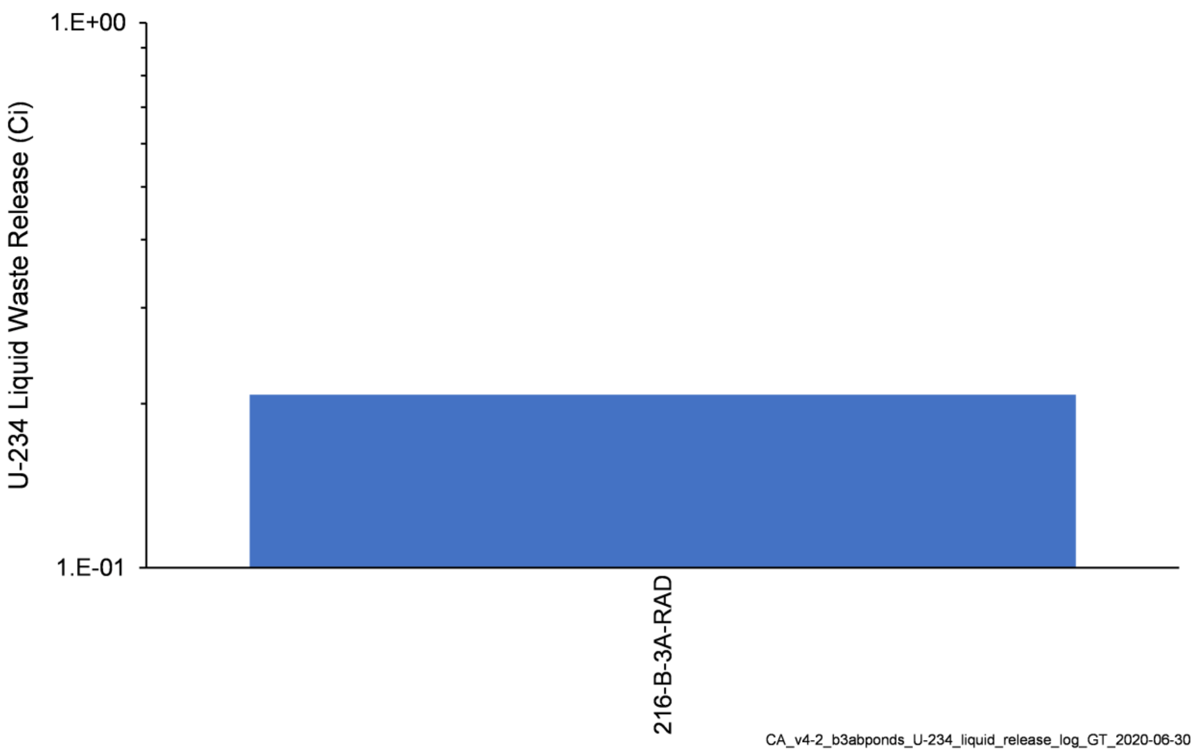

Figure 4-16. Total U-234 Activity Released from Liquid Waste Sites in the B-3A/B Ponds Model

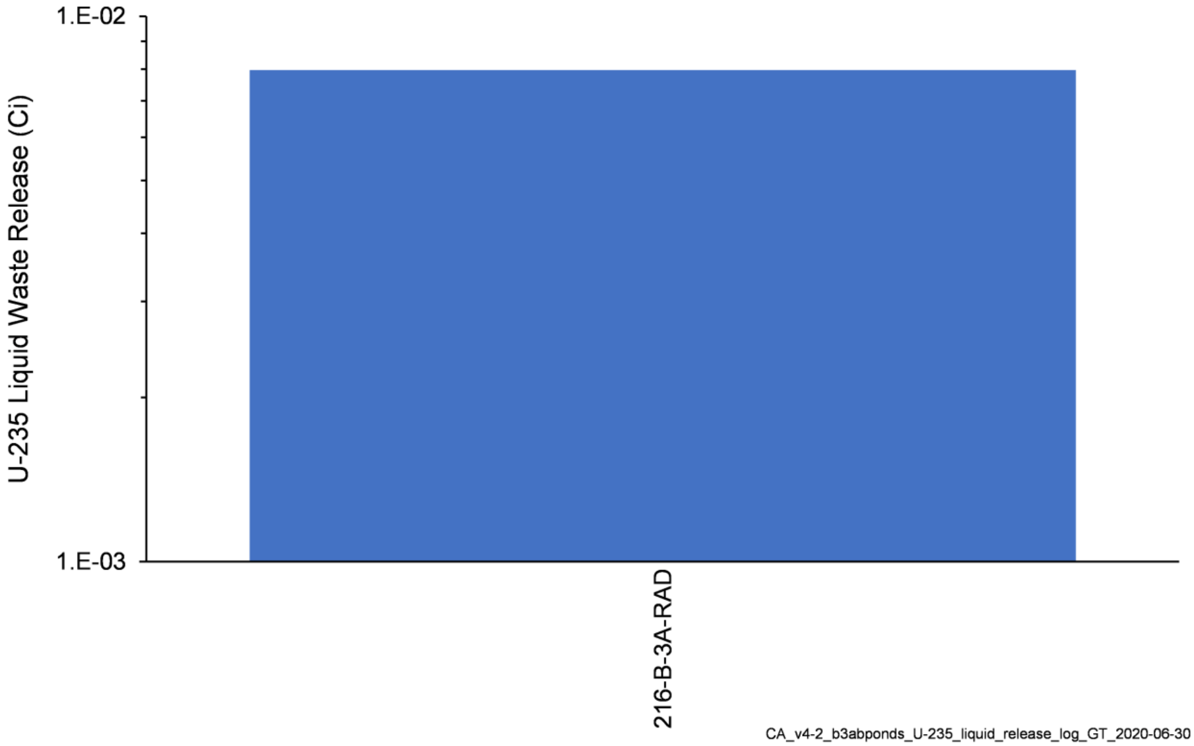

Figure 4-17. Total U-235 Activity Released from Liquid Waste Sites in the B-3A/B Ponds Model

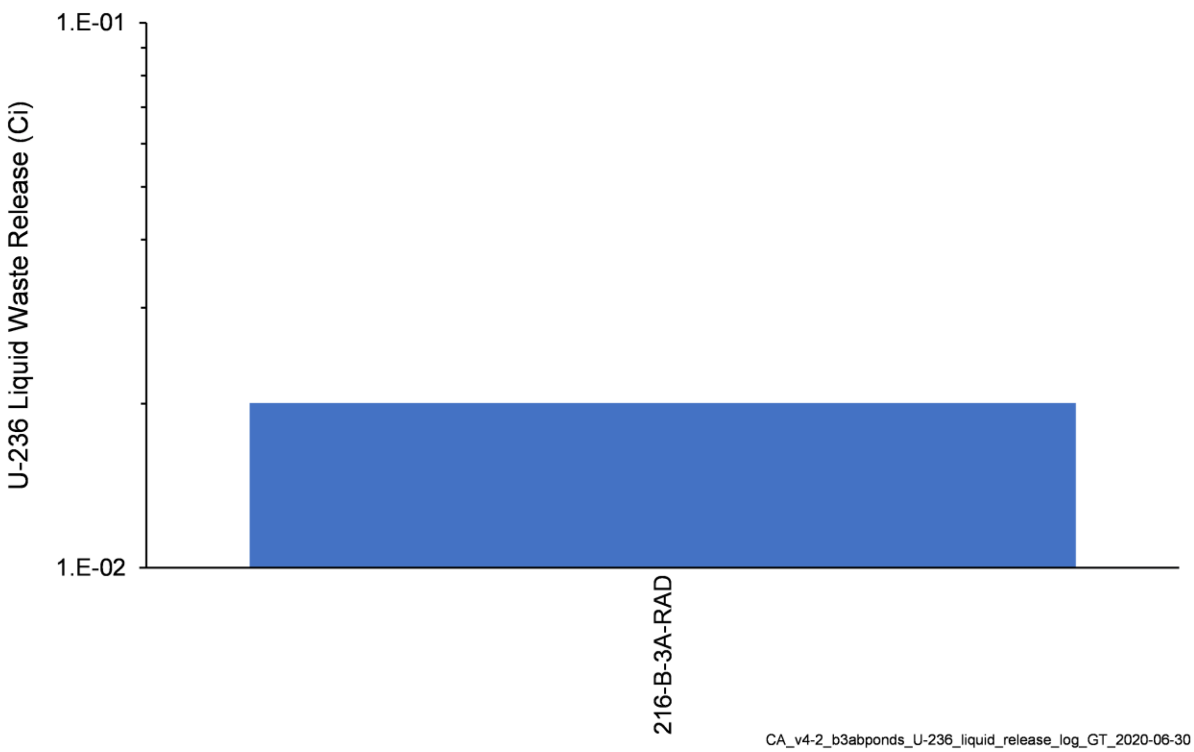

Figure 4-18. Total U-236 Activity Released from Liquid Waste Sites in the B-3A/B Ponds Model

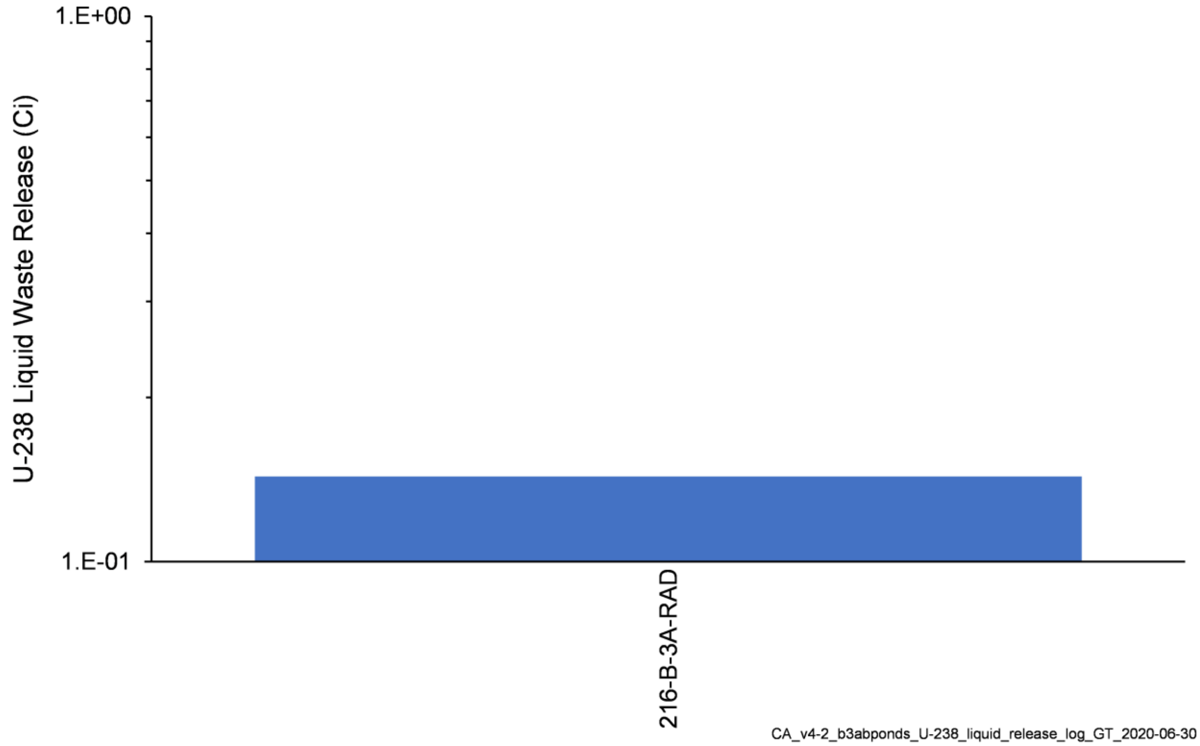

Figure 4-19. Total U-238 Activity Released from Liquid Waste Sites in the B-3A/B Ponds Model

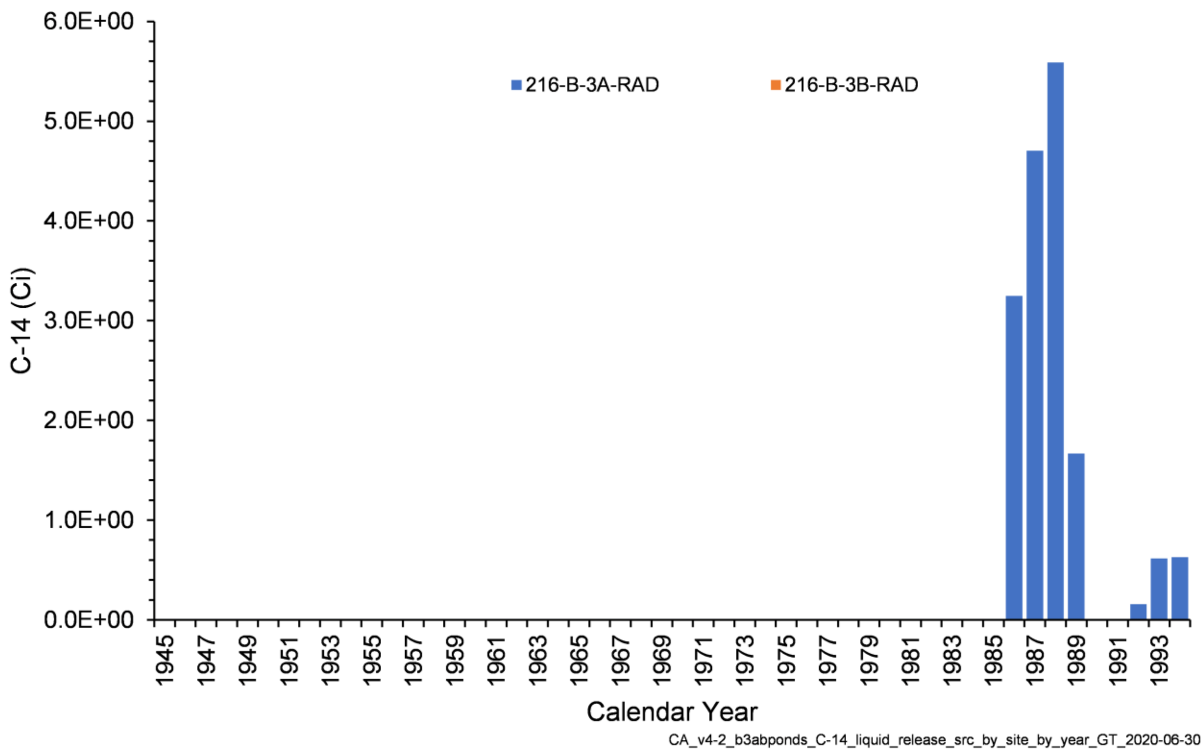

Figure 4-20. Annual C-14 Activity Released from Liquid Waste Sites in the B-3A/B Ponds Model

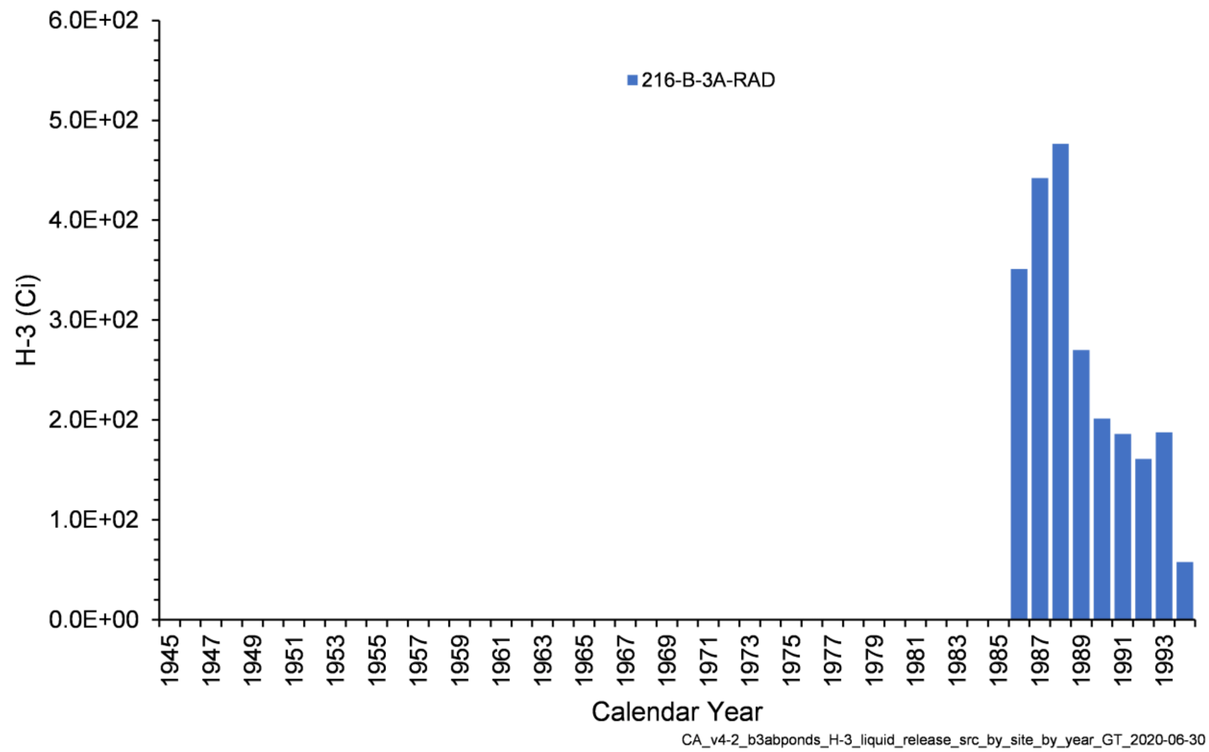

Figure 4-21. Annual H-3 Activity Released from Liquid Waste Sites in the B-3A/B Ponds Model

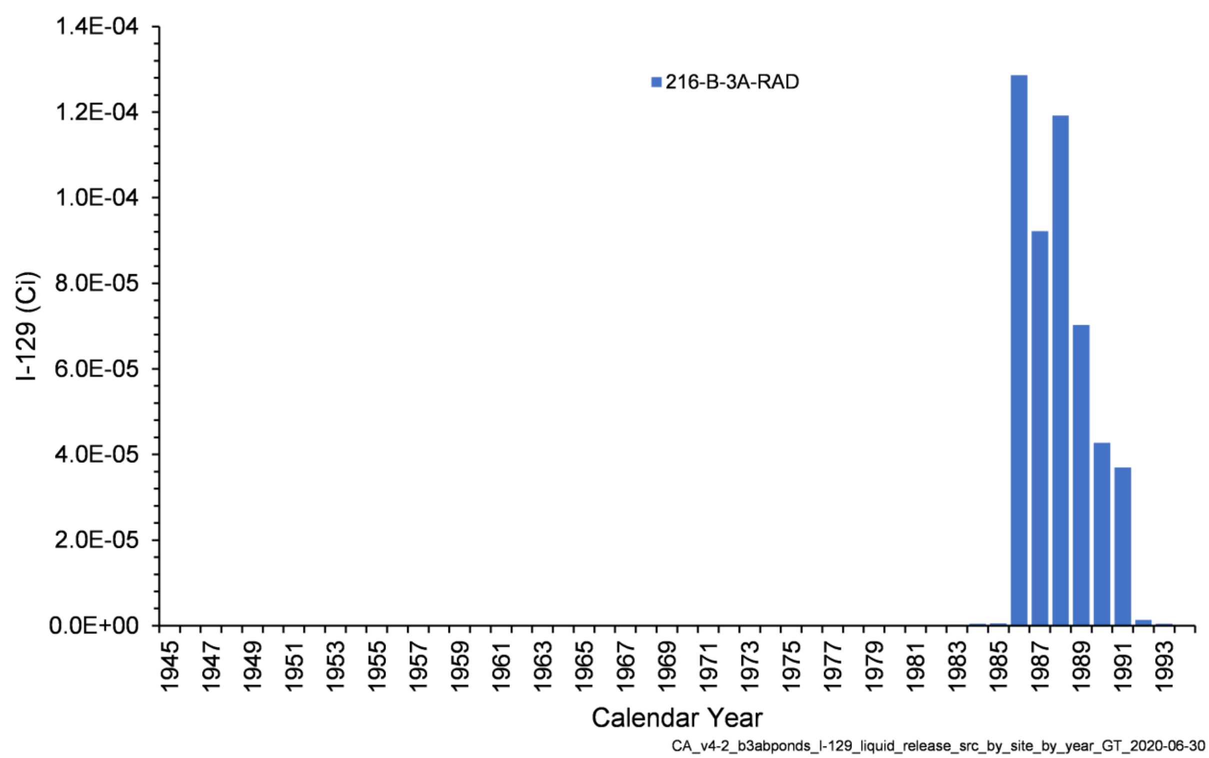

Figure 4-22. Annual I-129 Activity Released from Liquid Waste Sites in the B-3A/B Ponds Model

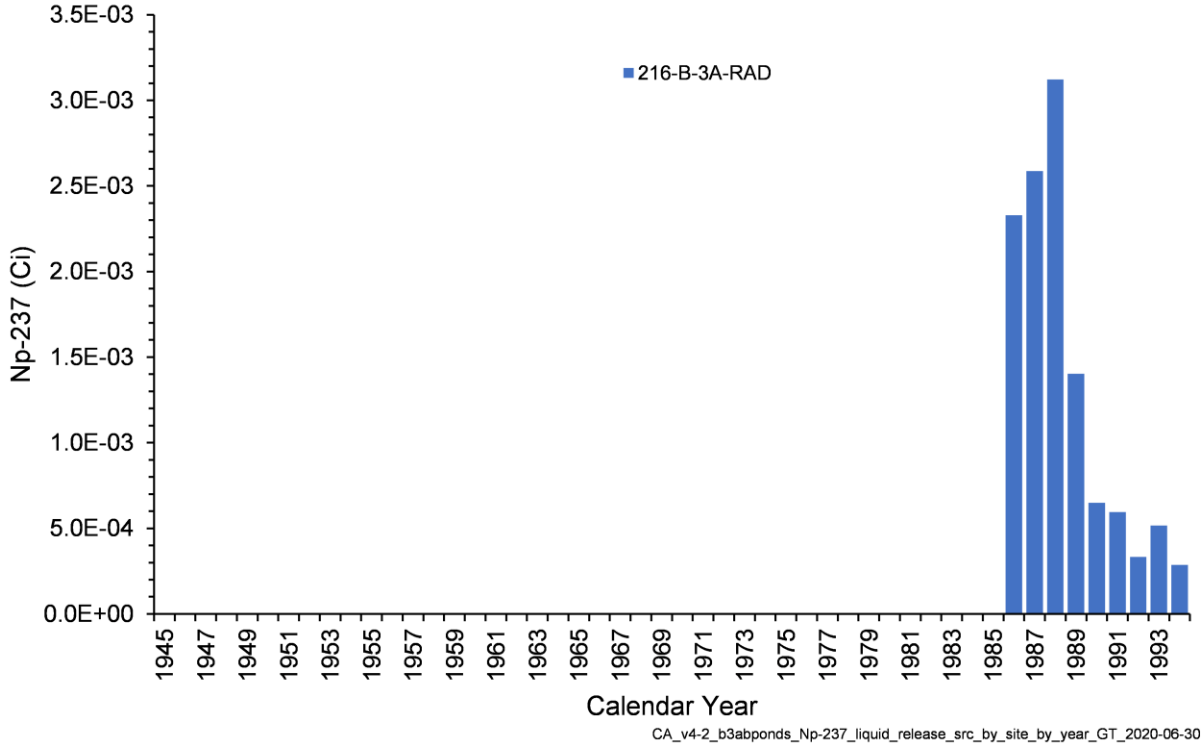

Figure 4-23. Annual Np-237 Activity Released from Liquid Waste Sites in the B-3A/B Ponds Model

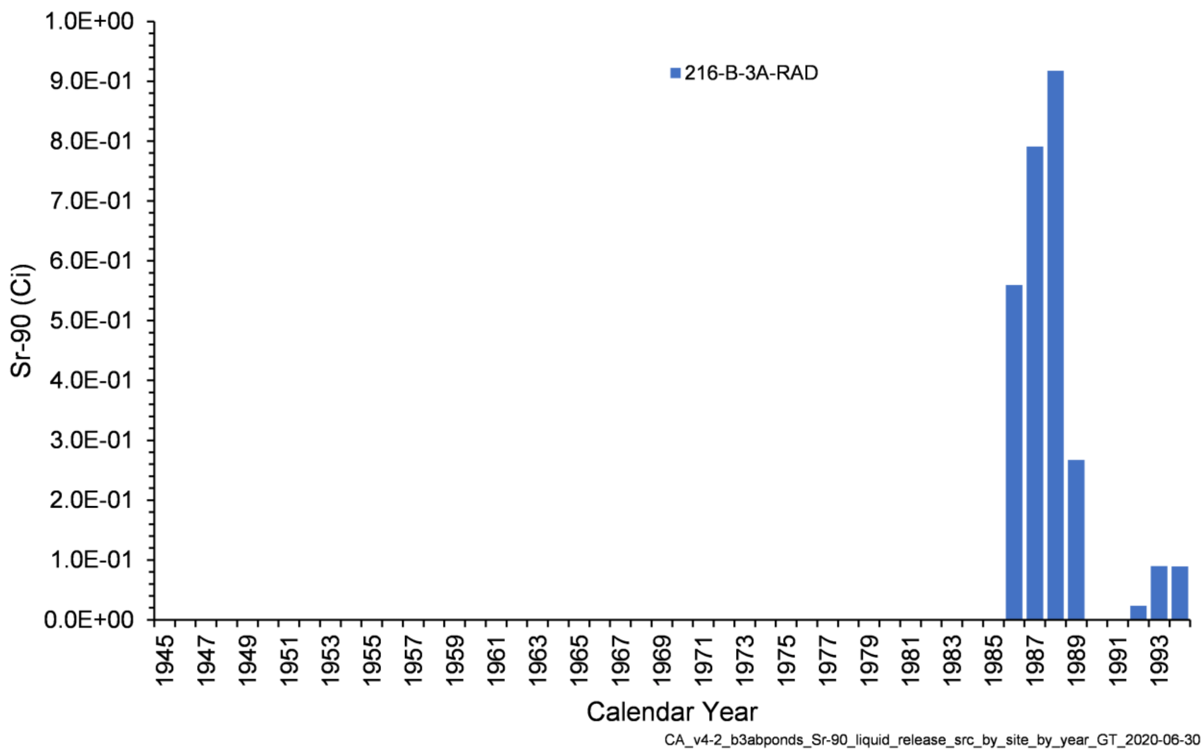

Figure 4-24. Annual Sr-90 Activity Released from Liquid Waste Sites in the B-3A/B Ponds Model

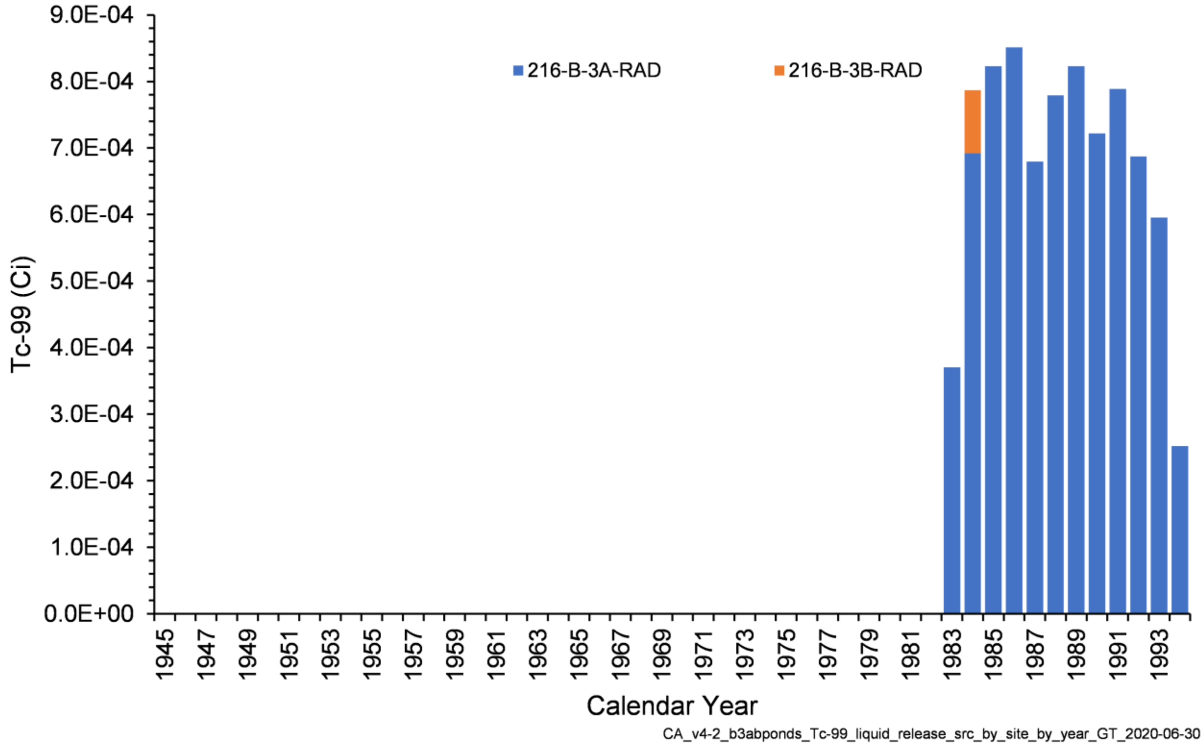

Figure 4-25. Annual Tc-99 Activity Released from Liquid Waste Sites in the B-3A/B Ponds Model

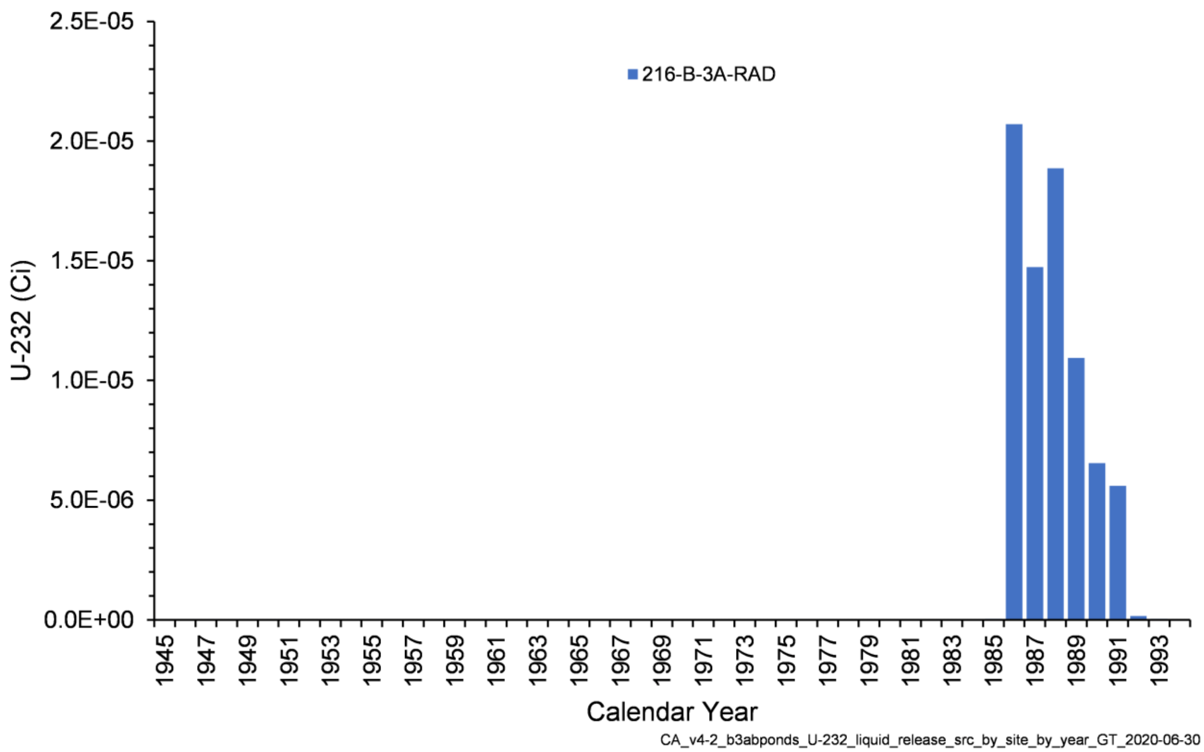

Figure 4-26. Annual U-232 Activity Released from Liquid Waste Sites in the B-3A/B Ponds Model

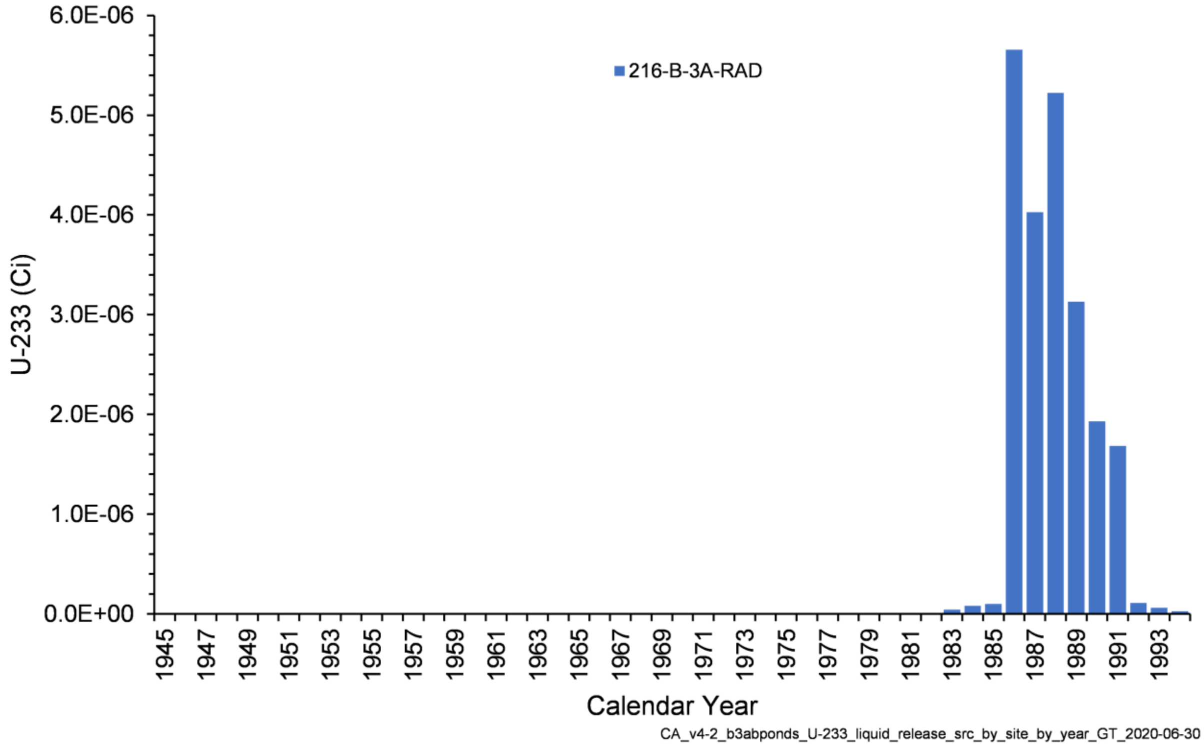

Figure 4-27. Annual U-233 Activity Released from Liquid Waste Sites in the B-3A/B Ponds Model

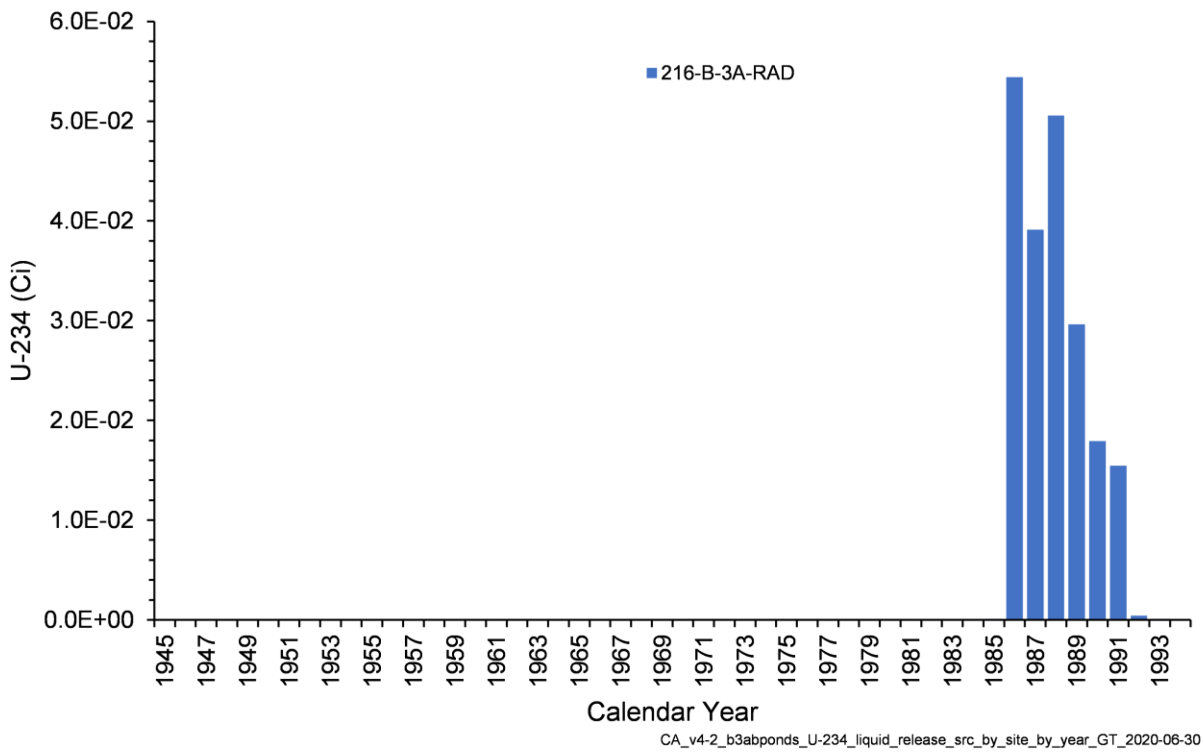

Figure 4-28. Annual U-234 Activity Released from Liquid Waste Sites in the B-3A/B Ponds Model

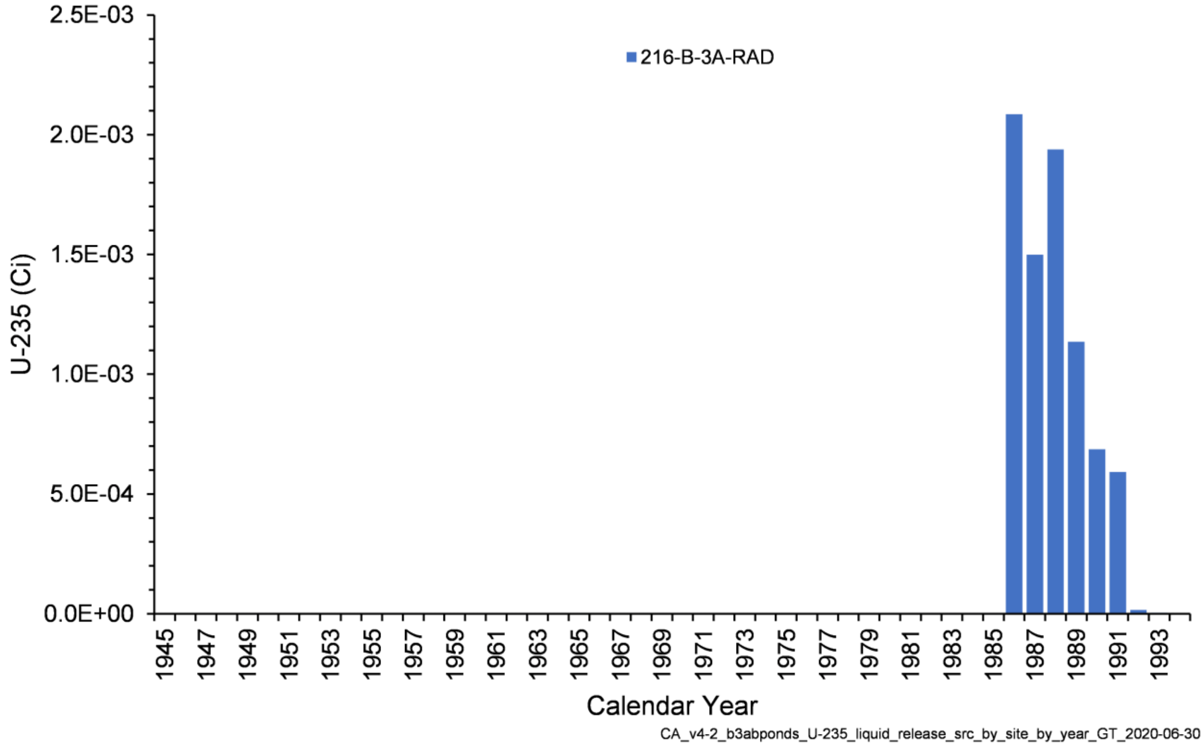

Figure 4-29. Annual U-235 Activity Released from Liquid Waste Sites in the B-3A/B Ponds Model

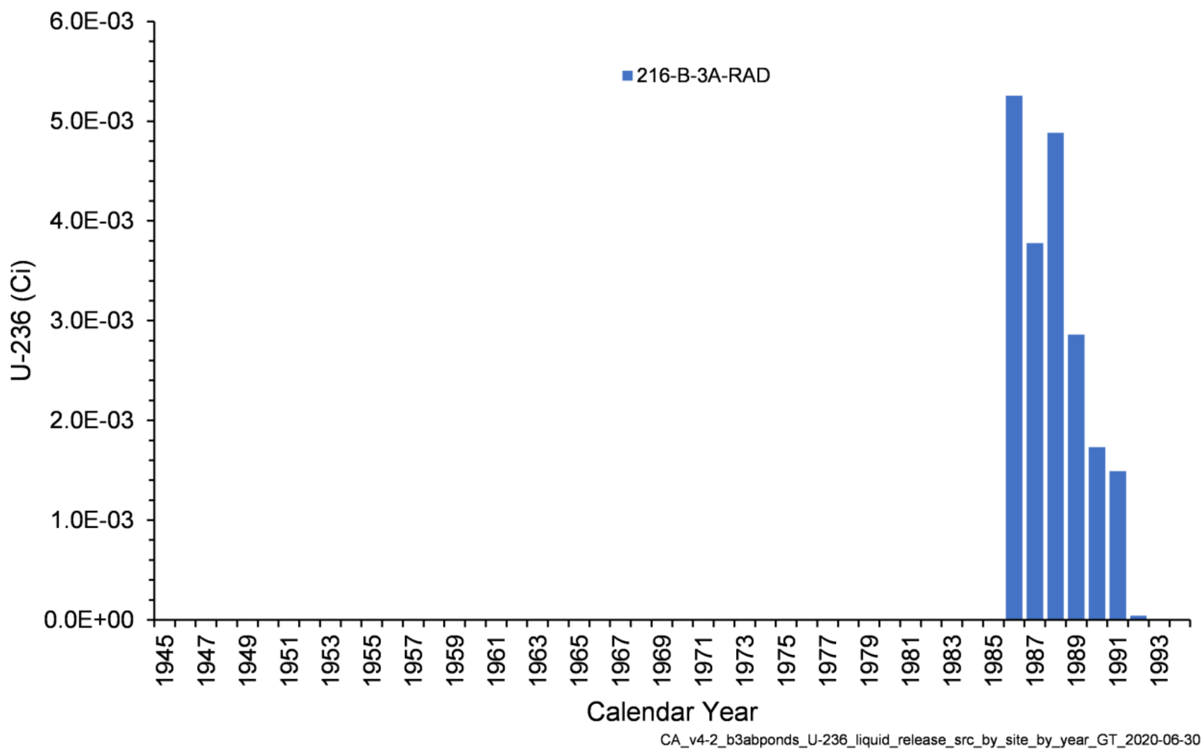

Figure 4-30. Annual U-236 Activity Released from Liquid Waste Sites in the B-3A/B Ponds Model

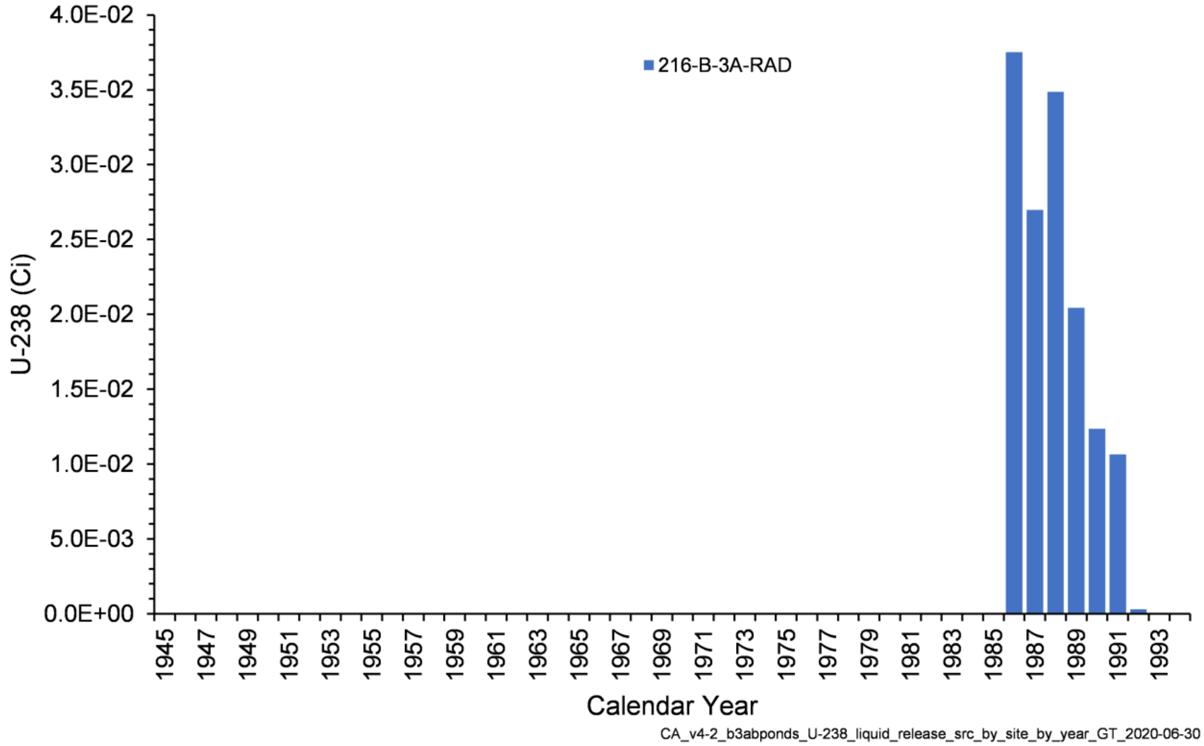

Figure 4-31. Annual U-238 Activity Released from Liquid Waste Sites in the B-3A/B Ponds Model

The assignment of radionuclide inventories to ditch/pond systems in ECF-HANFORD-17-0079 did not take into account the movement of water between components of these systems (e.g., between an influent ditch and the main pond, or between lobes of a pond system). Only a portion of the inventory assigned to a particular ditch or pond in ECF-HANFORD-17-0079 may have infiltrated from that site due to movement of the water into another segment of the system. Thus, liquid wastes assigned to the 216-U-10 Pond System and the 216-B-3 Pond System in ECF-HANFORD-17-0079 were rerouted to better account for the partitioning of infiltration within these systems as described in ECF-HANFORD-19-0032.

For the B-3A/B Ponds model, liquid waste discharged to the 216-B-3 Pond System was rerouted for this modeling effort. The 216-B-3 Pond system consisted of a main pond and 3 expansion lobes (216-B-3A, 216-B-3B-RAD, and 216-B-3C-RAD) that were operational during overlapping time periods. All of the discharges to the pond system were assigned to the main lobe, 216-B-3, in ECF-HANFORD-17-0079, hence the need to determine what fraction infiltrated from each lobe. Partitioning of infiltration and contaminant inventory between the lobes of the 216-B-3 Pond System is based on pond areal extent. For the 216-B-3 Pond System, the fraction of the total discharge that infiltrates from a particular lobe is the ratio of the area of that lobe to the total area of all lobes in operation. This calculation was performed for each operational pond configuration and the results were used to partition annual volumes by calendar year (because annual discharges are used in the vadose zone modeling). For more details, see ECF-HANFORD-19-0032.

4.5.1.2 Solid Waste Site Releases

Solid wastes are contaminated materials that have the potential to release radionuclides to the vadose zone. There are no solid waste sites present in the source zone of this model.

4.5.2 Liquid (Volume) Releases

This section provides information on liquid volumes released within the domain of the B-3A/B Ponds model. These liquids can act as a driving force for the movement of radionuclides deeper into the subsurface. Table 4-3 shows an overview of the total liquids released in the model. Figure 4-32 shows the volume of water released within the model domain by waste site, and Figure 4-33 shows the total volume of water released by year.

Table 4-3. Released Liquid Volumes in the B-3A/B Ponds Model

Total	Source Zone	Buffer Zone
106,066,100	27,518,200	78,547,900

Note: all values reported in m^3

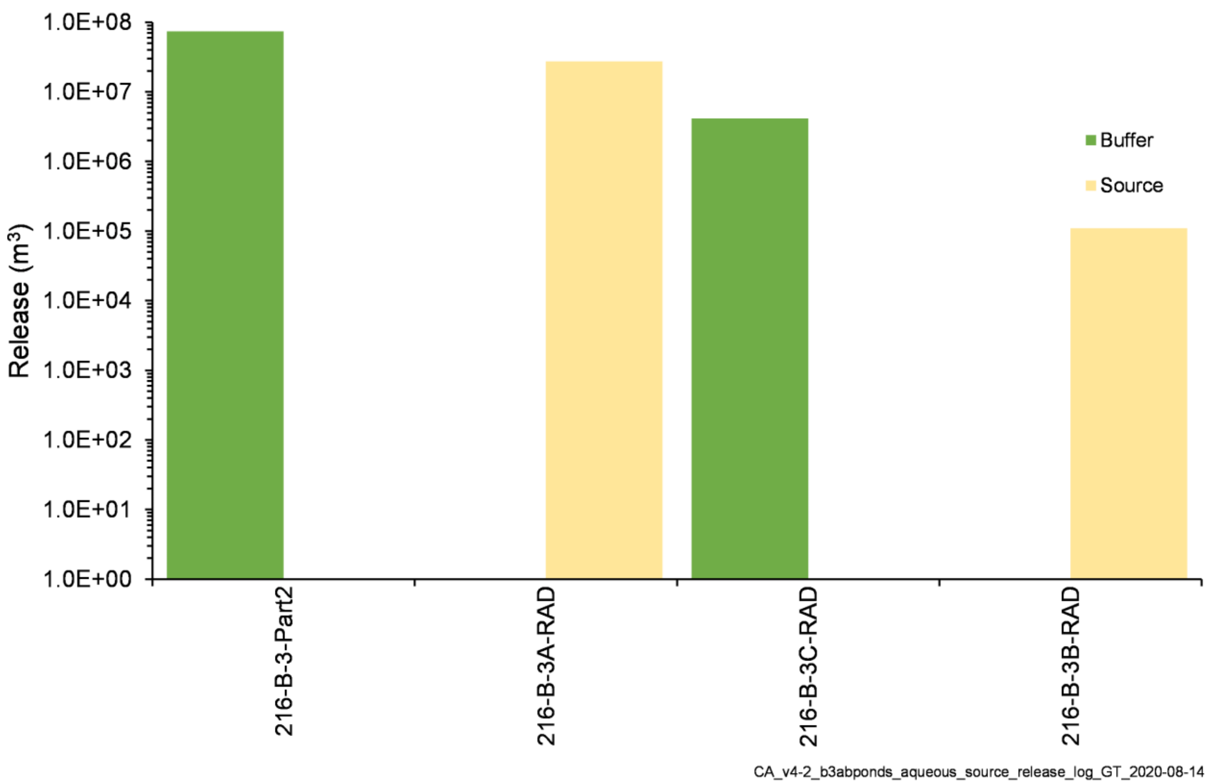

Figure 4-32. Total Volume of Water Released from Liquid Waste Sites in the B-3A/B Ponds Model

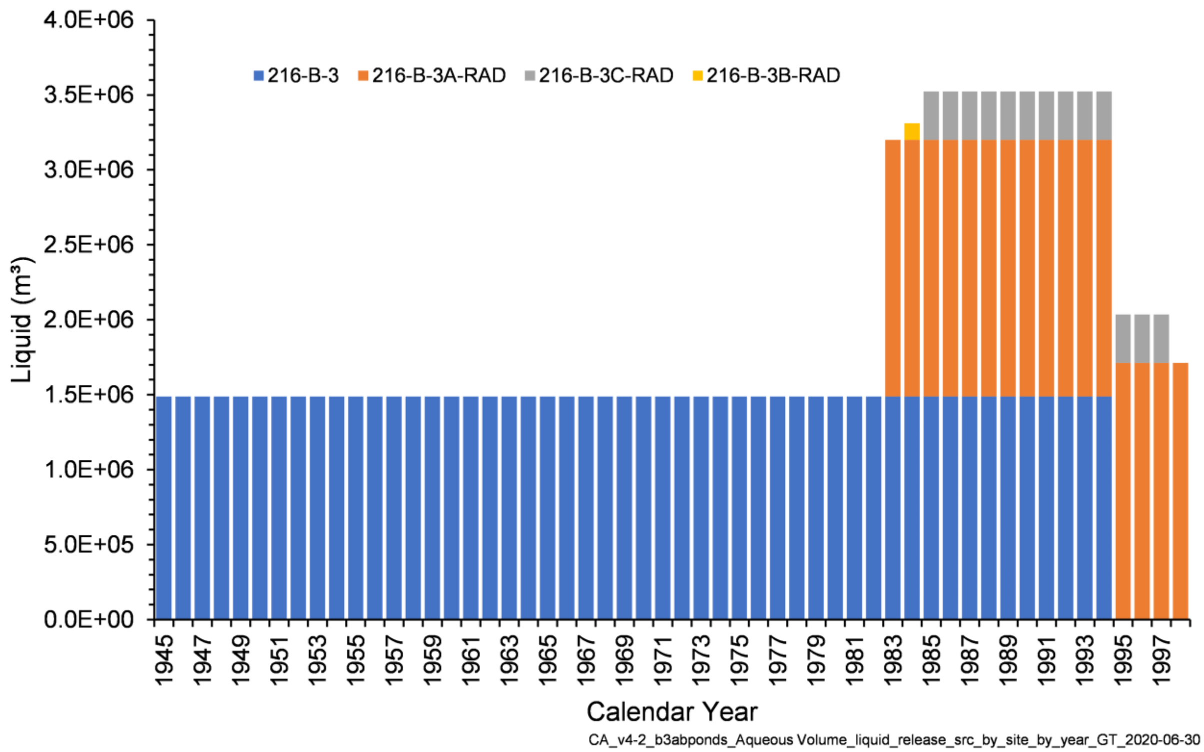

Figure 4-33. Total Volume of Water Released by Year from Liquid Waste Sites in the B-3A/B Ponds Model

4.5.2.1 Liquid Release Modifications

For some models, modifications to liquid release volumes were needed to help with convergence of the numerical solution or to provide for more representative transport through the vadose zone.

Model Convergence Resolution

This model required that the water at 216-B-3, 216-B-3A-RAD, and 216-B-3C-RAD be averaged so the numerical solution of the model governing equation may converge. For each waste site, the water discharged over a specified time period was summed, averaged, and evenly dispersed throughout the same time period, or if needed, an extended time period. The time period over which the discharge was averaged for each waste site is shown in Table 4-4. The waste site 216-B-3, located in the buffer zone, had liquid releases averaged from 1945 to 1994. The waste site 216-B-3A-RAD, located in the source zone, had liquid releases averaged from 1983 to 1998. The waste site 216-B-3C-RAD, located in the buffer zone, had liquid releases averaged from 1985 to 1997.

Table 4-4. Liquid Release Modifications for the B-3A/B Ponds Model

Site Name	Model Zone	Original Start Year	Original End Year	Modified Start Year	Modified End Year	Averaged Release Rate (m^3/yr)
216-B-3A-RAD	Source	1983	1994	1983	1998	1,713,027
216-B-3	Buffer	1945	1994	1945	1994	1,487,433
216-B-3C-RAD	Buffer	1985	1997	1985	1997	321,248

4.6 Simulations

Three different types of simulations were performed. Constant recharge conditions were used in a flow-only simulation to set the initial aqueous pressure conditions in the model. A mass balance simulation was conducted to evaluate model performance, and transport simulations were performed to estimate radionuclide activity entering the saturated zone. These are discussed in the following sections.

4.6.1 Flow-Only (Steady-State) Simulation

The flow-only simulation was performed using recharge estimated for 1943, which was prior to the start of Hanford Site operations. This was a transient simulation, but it is referred to hereinafter as the steady-state simulation because recharge was held constant at the 1943 values and the simulation was run for 10,000 years to ensure steady-state conditions were achieved within the model domain. The results were used as the initial aqueous pressure conditions for the radionuclide transport simulations starting in 1943.

4.6.2 Mass/Activity Balance Simulation

A mass/activity balance simulation was conducted to evaluate model performance. This simulation was run for 10,000 years using the source releases described in Section 4.5 and the initial aqueous pressure conditions from the steady-state simulation, but radionuclide half-lives were set to 1.0E+20 years to eliminate radiological decay and allow for the mass/activity balance to be evaluated directly. The mass/activity of each constituent leaving the model over 10,000 years and the mass/activity present in the model at the end of the simulation were summed, and the results were compared to the mass/activity released from the sources.

4.6.3 Transport Simulations

Transport simulations were performed to estimate the radionuclide activity entering the saturated zone. These were done in stages. The time period for the CA evaluation is 2018 to 12070. To set the initial radionuclide concentrations in the model domain for simulations of that time period (i.e., forecast period), a historical simulation of radionuclide releases was performed from 1943 up to but not including 2018. The radionuclide distribution in the model domain at the end of this simulation became the starting concentrations for the forecast runs.

The forecast simulations were performed for 2018 to 12070. The forecast simulation was performed in a single stage because this model contains no waste sites with a disposition of remove, treat, and dispose (RTD). If it had contained such sites, the forecast period would have been simulated in two stages. After starting in 2018, execution of the model would have been stopped at the year RTD was planned to reset concentrations in the model to zero at the RTD locations, and then the model would have been restarted from that year.

4.7 Initial Conditions

The simulations performed for the B-3A/B Ponds model require that initial aqueous pressure conditions and radionuclide concentrations in the model domain be specified, depending on the simulation. Initial-aqueous pressure conditions for the steady-state, flow-only simulation are based on hydrostatic conditions assuming that the base of the model is at the water table. This is input to STOMP as an aqueous pressure of 101,325 Pa at the water table and a z-direction gradient of -9,793.52 Pa/m.

For the historical transient simulations (i.e., 1943 to 2018), initial aqueous pressure conditions are the steady-state conditions taken from the end of the steady-state simulation. Since the purpose of the historical simulations was to define the starting radionuclide concentrations and aqueous pressure conditions for the forecast runs by simulating source release during the entirety of Hanford Site operations, the initial radionuclide concentrations were zero.

Aqueous pressure conditions and radionuclide concentration results of the historical simulation were used as the initial conditions for the forecast simulations. This model does not contain any RTD sites, so the forecast simulation was performed as a single run. If this model did have an RTD site, this would have been simulated by stopping model execution at the year designated for the RTD action, concentrations in the model where RTD would have occurred would have been set to zero, and then model execution resumed.

4.8 Boundary Conditions

Boundary conditions for the B-3A/B Ponds model include recharge to the top of the model, water table conditions at the base of the model, and no-flow conditions along the sides of the model. The boundary conditions are described in further detail in the rest of this section.

4.8.1 Natural Recharge – Top Boundary Condition

Model recharge was estimated using the RET (ECF-HANFORD-15-0019). The RET assigns soil infiltration rates for the CA vadose zone models based on land use, surface cover information from multiple sources (including existing buildings and structures, waste site footprints, and natural vegetative cover), and soil survey information. Planned future actions for waste site closure are used to develop future recharge estimates through the end of the modeling period. The RET generates spatial representations of recharge estimates for each year from 1943 until recharge reaches a final post-closure condition. These yearly recharge estimates for the model domain are then post-processed to generate the STOMP boundary condition input. The steady-state simulation uses the 1943 RET recharge values for the entire simulation under the assumption that the 1943 recharge is representative of pre-Hanford Site conditions. Recharge rates from every output year from the RET are used as the transient boundary conditions.

Natural recharge within the model domain is spatially variable. Figures of the spatial distribution of RET recharge estimates for the B-3A/B Ponds model are shown for every year there is a change in any recharge estimate in Appendix C. Figure 4-34 to Figure 4-37 show the RET recharge estimates for the B-3A/B Ponds model for 1943, 1983, 2050, and 2550. The pre-Hanford Site recharge rate distribution is determined by the soil types Rupert Sand and Burbank Loamy Sand covered with mature shrub-steppe plant communities (Figure 4-34). The recharge rates for these soils with mature vegetation are 4.0 and 3.0 mm/yr, respectively. The model area is covered by Rupert Sand in the center, and Burbank Loamy Sand in the eastern and southern parts of the model. As shown in Figure 4-7, pond development resulted in variable recharge rates over time. Development, including excavation, caused surface disturbances resulting in increased recharge rates. The 216-B-3A and 216-B-3B Ponds were in use by 1983 with an estimated recharge rate of 63 mm/yr (Figure 4-35) for the area of the ponds. In 2050, a partial surface infiltration barrier with an assumed recharge rate of 0.5 mm/yr is planned to cover the 216-B-3A Pond (Figure 4-36). The surface barrier is assumed to have a design life of 500 years, after which the affected area returns to natural conditions with an assigned recharge rate of 4.0 mm/yr (Figure 4-37).

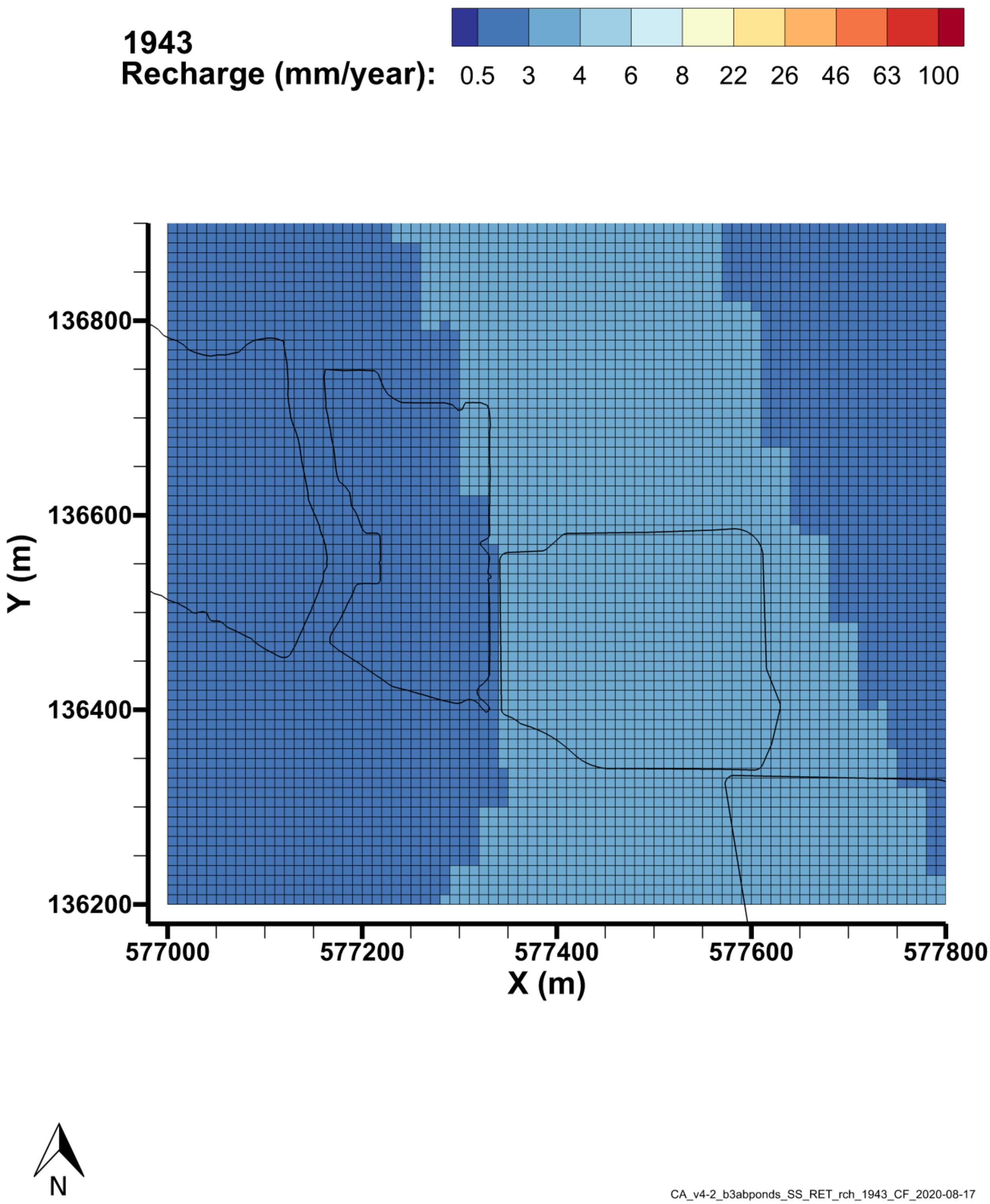

Figure 4-34. Transient Recharge Estimates for the B-3A/B Ponds Model, 1943

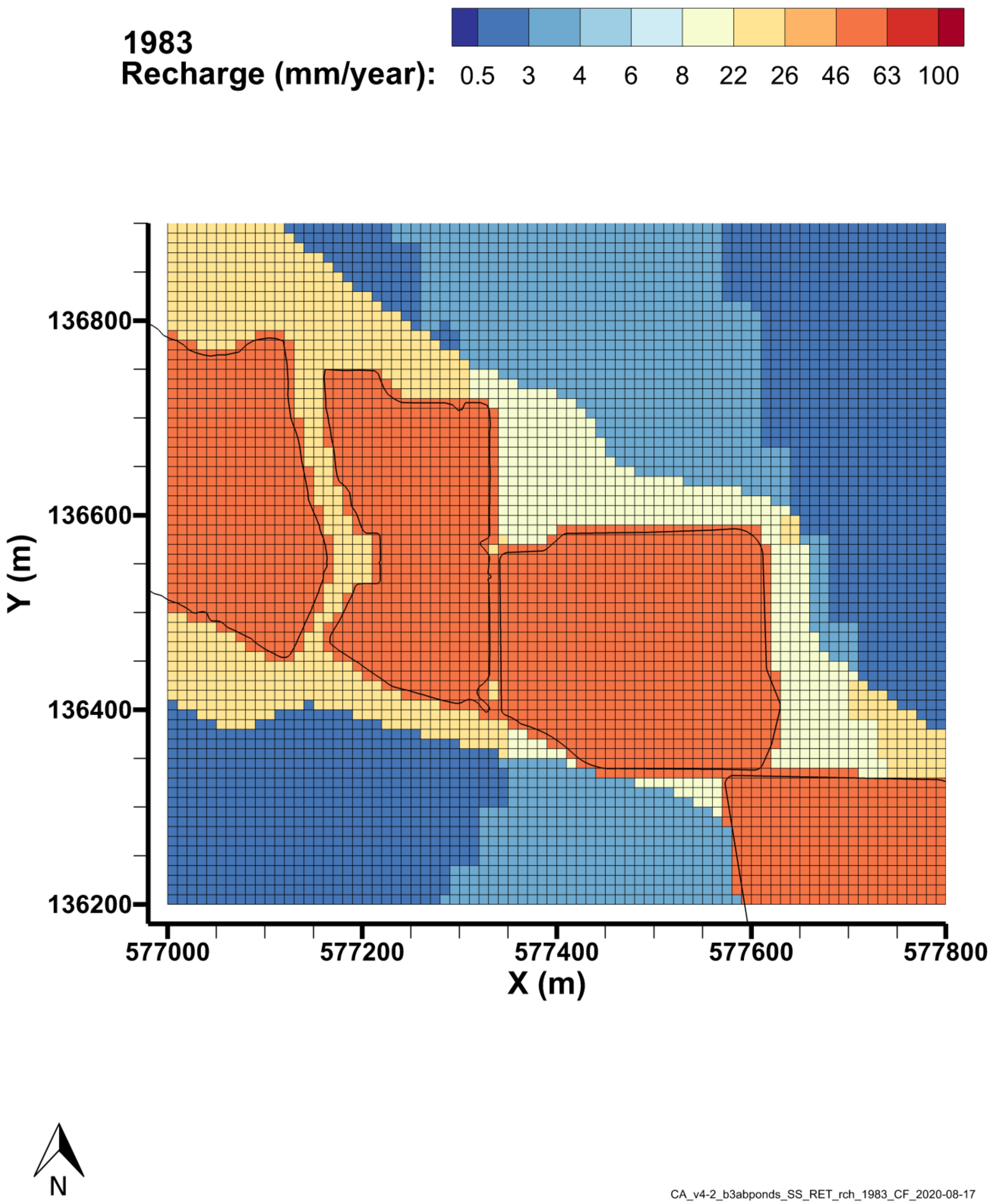

Figure 4-35. Transient Recharge Estimates for the B-3A/B Ponds Model, 1983

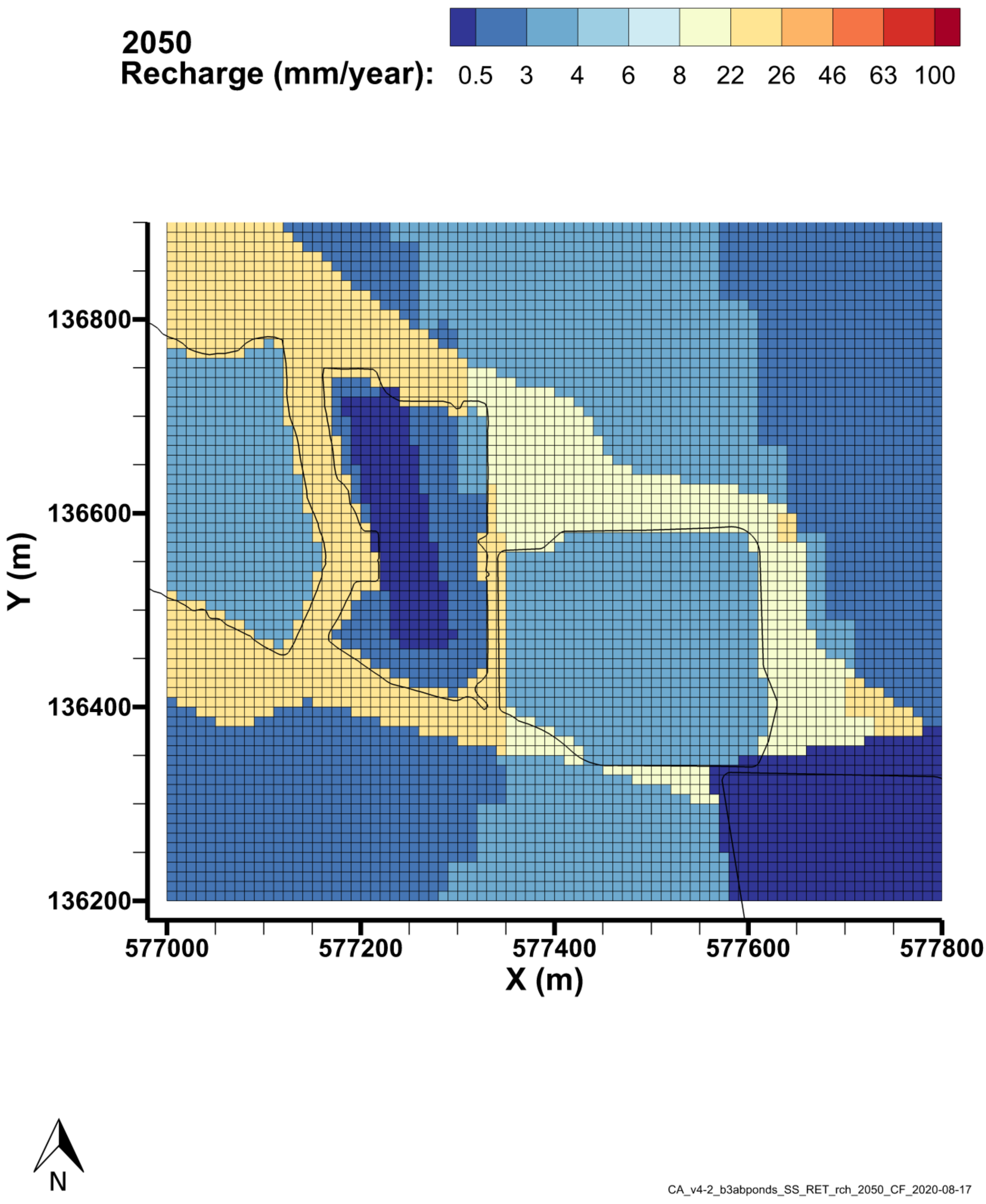

Figure 4-36. Transient Recharge Estimates for the B-3A/B Ponds Model, 2050

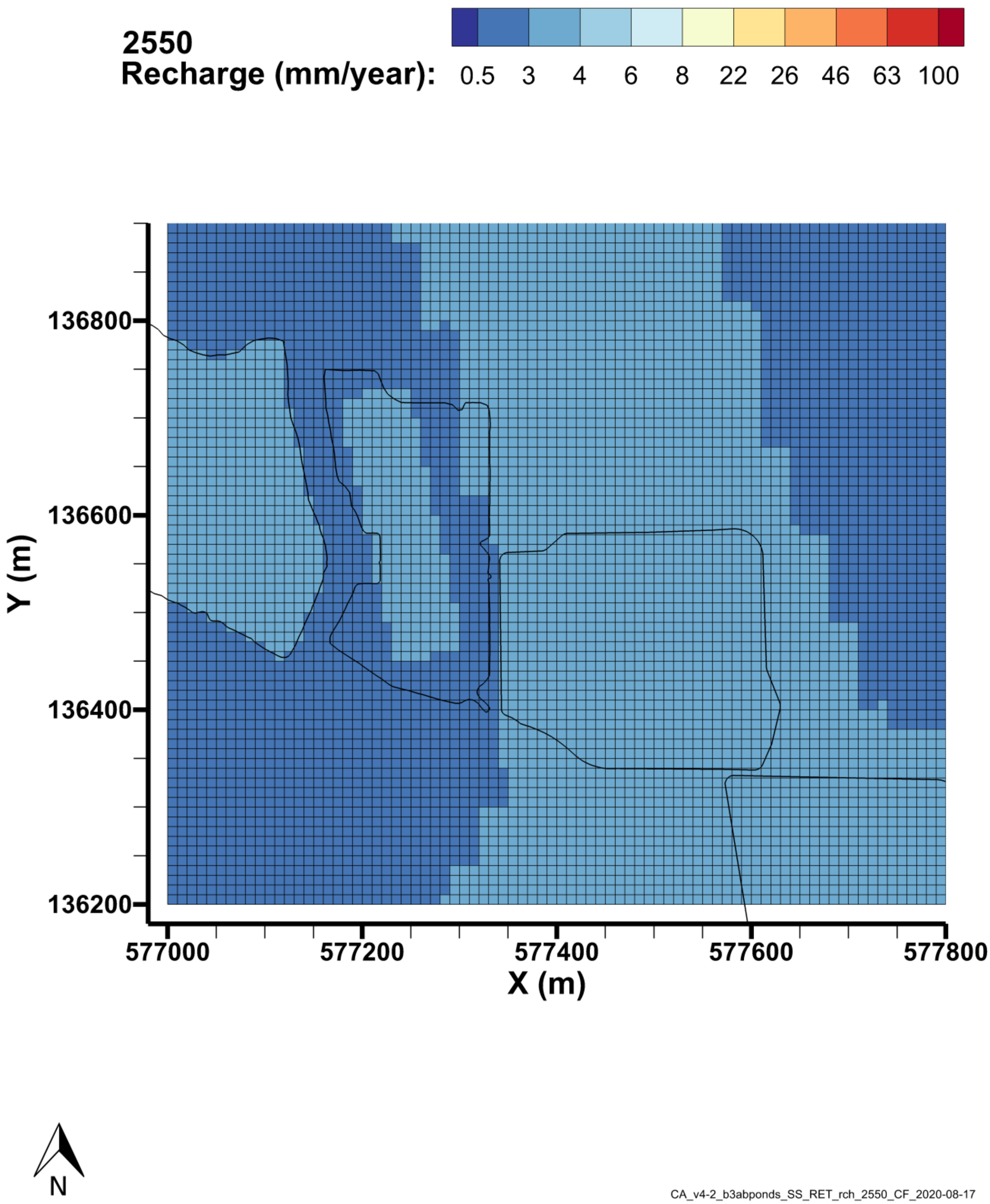

Figure 4-37. Transient Recharge Estimates for the B-3A/B Ponds Model, 2550

Example time series charts of natural recharge rates for selected locations within the model domain (locations shown in Figure 4-38) are shown in Figure 4-39 through Figure 4-41. The locations A and C on Figure 4-38 represent sites on 216-B-3A and 216-B-3B, respectively (location A, 216-B-3A, Figure 4-39, location C, 216-B-3B, Figure 4-41). The pre-Hanford Site recharge rate is 3.0 and 4.0 mm/yr for location A and C, respectively, as determined by the soil types covered with mature shrub-steppe plant communities. After Hanford Site construction began in 1943, an initial increase in recharge occurred depending on the activities that took place within the model boundary. At both locations, a disposition of "disturbed sand" due to excavation activities and other disturbances is reached at some time, with an assigned recharge rate of 63 mm/yr. This value is consistent with rates measured in unvegetated sands (Table 4.15 in PNNL-14702, *Vadose Zone Hydrogeology Data Package for Hanford Assessments*). Before reaching the high recharge rates, a cheatgrass cover appears at both locations with a recharge rate of 26 mm/yr for location A on Burbank Loamy Sand and 22 mm/yr at location B for Rupert Sand. Location A receives a surface barrier in 2050 with an assumed rate of 0.5 mm/yr for an expected design life of 500 years. After the expected design life, a final estimated recharge rate of 4 mm/yr is assumed at this location. No surface barrier is placed on location C and the recharge rate from 2050–12070 is assumed to be 4.0 mm/yr.

Location B (Figure 4-40) is not located on one of the ponds. The recharge rate initially increases to 22 mm/yr due to the appearance of a cheatgrass cover on Rupert Sand. A revegetation cycle with a linear rate decrease over 30 years down to 4.0 mm/yr is imposed in 2070. There is no barrier emplaced at this location and the 4.0 mm/yr rate is therefore used from 2100–12070.

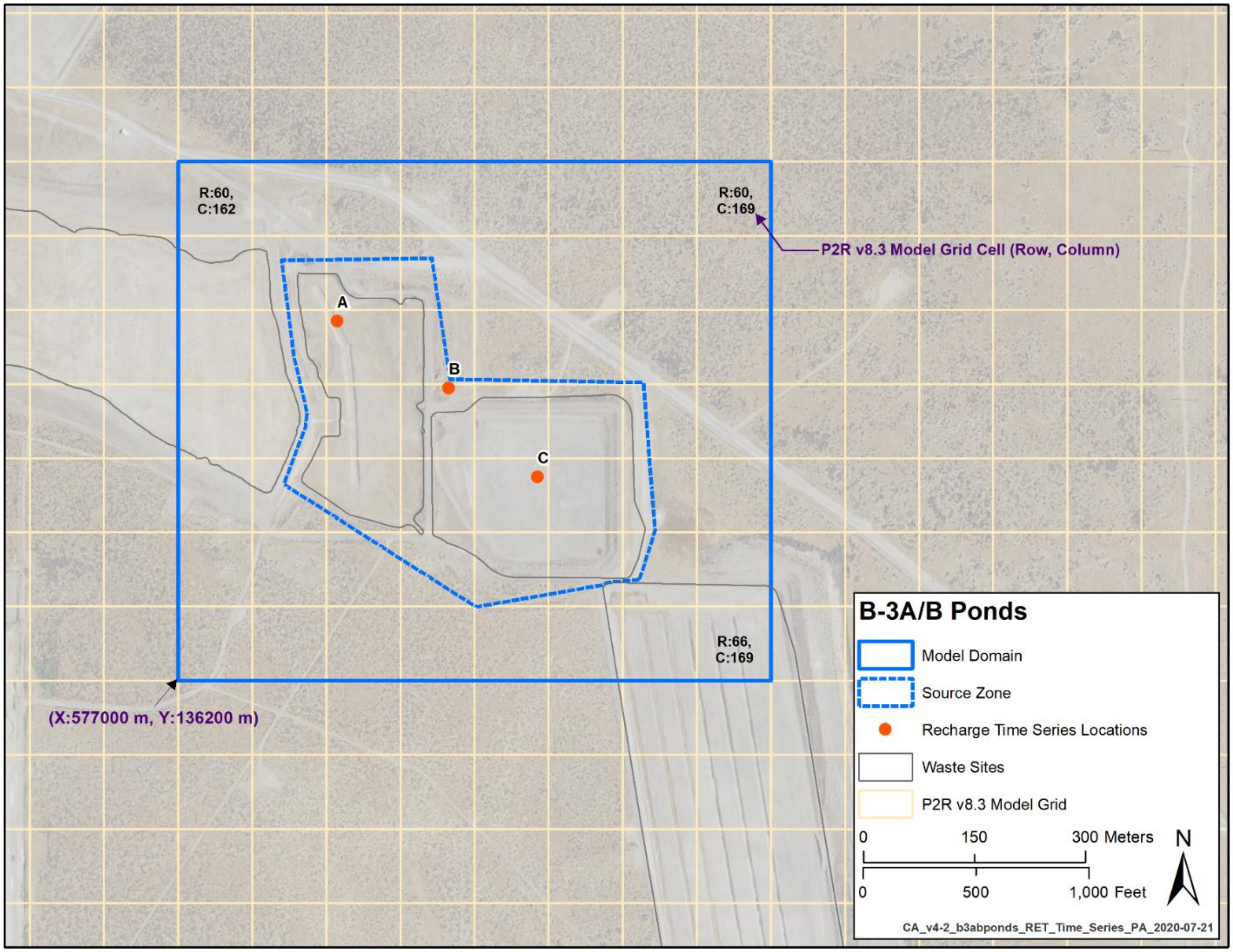

Figure 4-38. Locations of Recharge Rate Time Series Examples

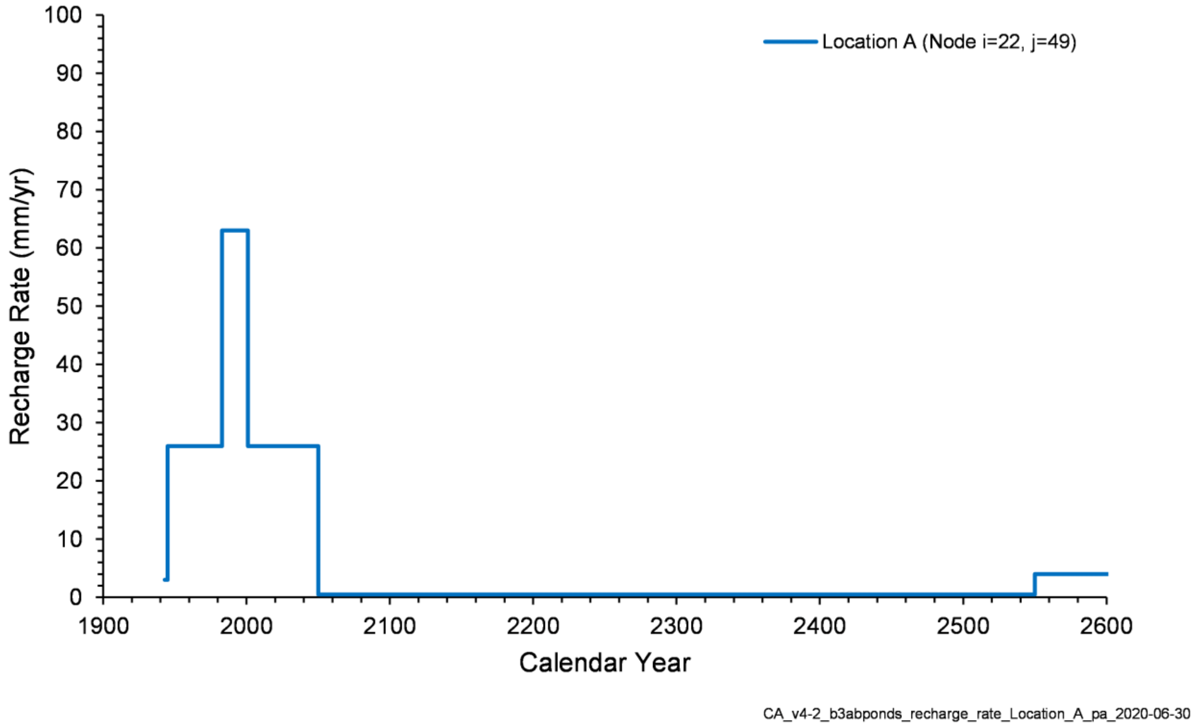

Figure 4-39. Time Series of Natural Recharge Rates, Location A

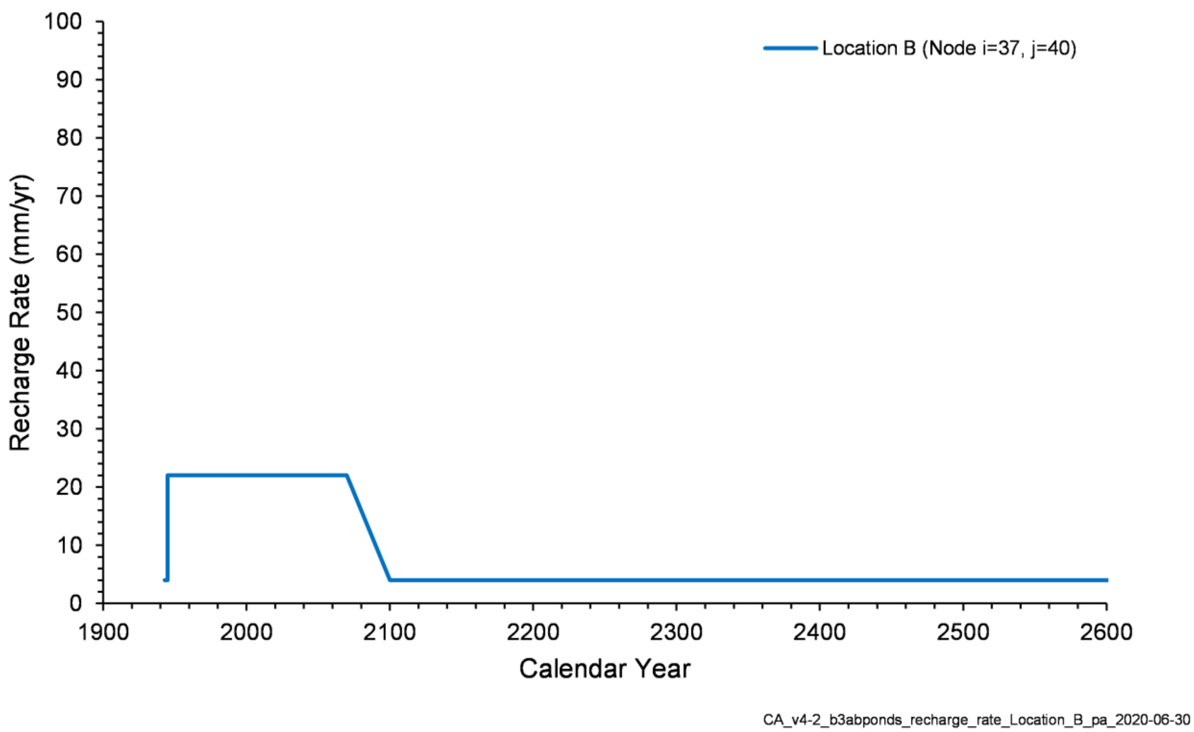

Figure 4-40. Time Series of Natural Recharge Rates, Location B

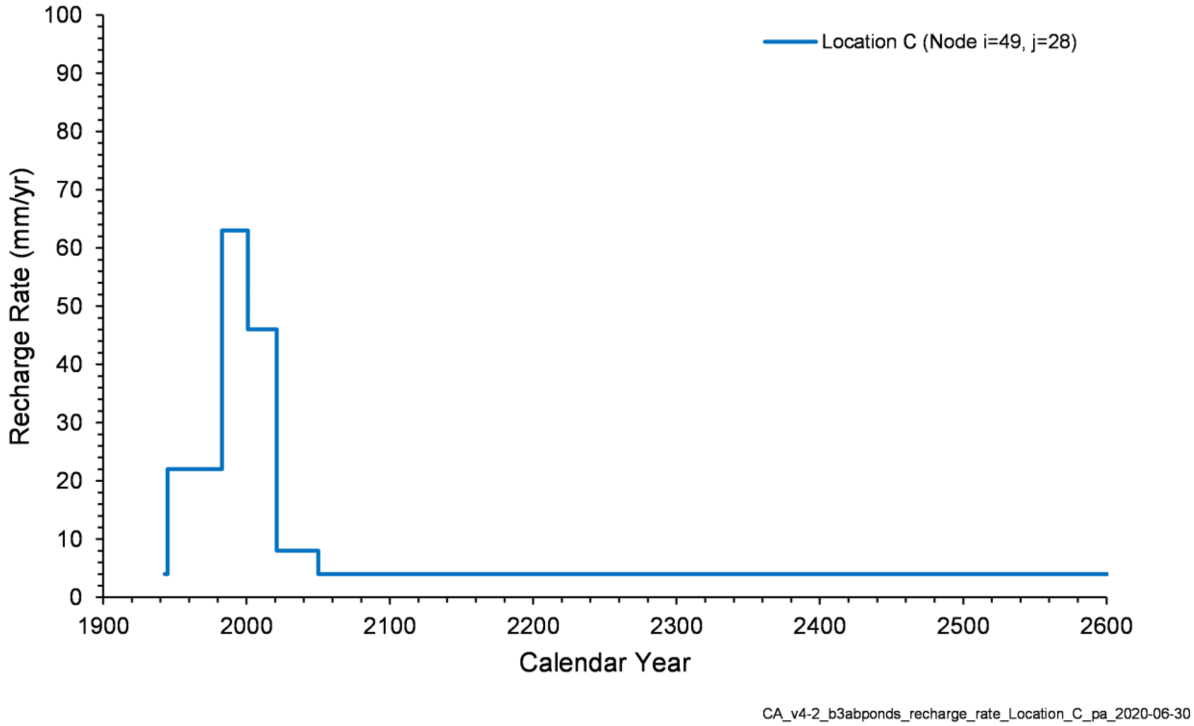

Figure 4-41. Time Series of Natural Recharge Rates, Location C

4.8.2 Lateral and Bottom Boundaries

Lateral boundaries for the model are assumed to be zero-flux boundaries for both contaminant transport and water flow. The locations of the lateral boundaries were selected in an iterative procedure to ensure that the contaminant plumes would not reach the model boundary. Source zone waste sites with radionuclide and liquid releases were at least 100 m away from the model boundary so that the releases would not affect soil moisture or contents at or near the boundary. For elongated waste sites extending into adjacent models, the assumption is that bifurcation of a waste site by a model boundary does not lead to soil moisture gradients across the boundary and that zero-flux boundaries are therefore appropriate for such waste sites.

The bottom of the model was assumed to be coincident with the water table at the model location, as estimated from the 2017 water table elevation (ECF-HANFORD-17-0120, *Preparation of the March 2017 Hanford Site Water Table and Potentiometric Surface Maps*). This boundary was represented by a Dirichlet boundary condition with a pressure of 101,325 Pa.

4.9 Source Nodes

Radionuclides and water discharged from waste sites are introduced to this model at source nodes. The distribution of these source nodes is shown in Figure 4-42. The STOMP Source Cards (i.e., specific information on source location and releases in the STOMP input file) were built using waste site footprints, source inventory, and the model grid. A discussion of the source node allocation process is found in CP-63515.

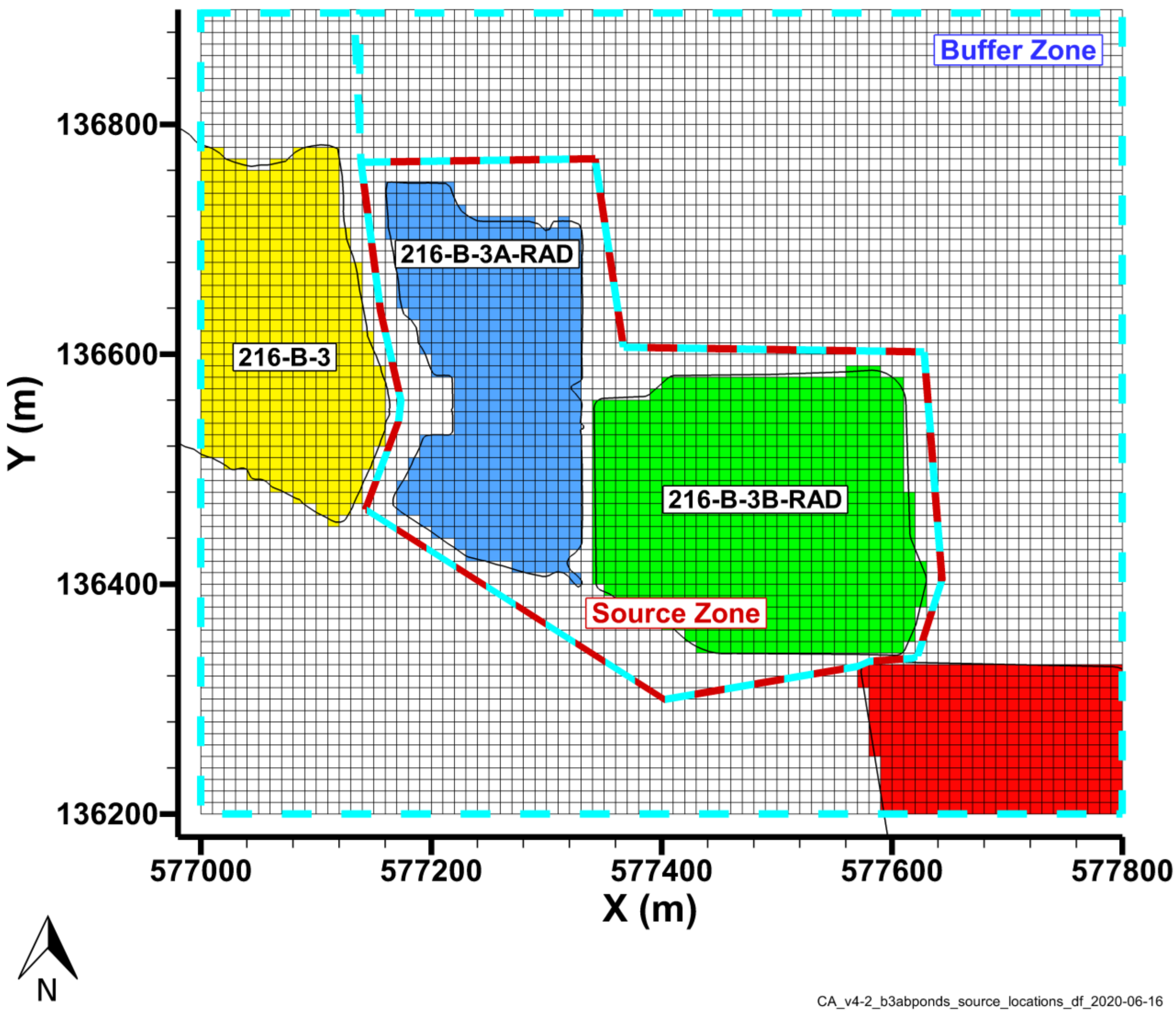

Note: Black cells indicate source nodes with input from multiple sites.

Figure 4-42. Distribution of Source Nodes in the B-3A/B Ponds Model

4.9.1 Data Reduction

The solid waste inventory from ECF-HANFORD-19-0112 described in Section 4.5.1.2 is released over approximately 10,000 years, with the total release timespan varying by waste site. These long release periods had many timesteps, resulting in large STOMP Source Cards. To accommodate the size limitations of STOMP Source Cards, the original inventory datasets were modified to release the solid waste inventory in a number of timesteps that is compatible with the Source Card size limitations. The reduced datasets were checked to ensure they adequately represent the original inventory amounts and release rates. Additional information regarding the data reduction methodology is documented in ECF-HANFORD-20-0006.

4.10 Modeling Assumptions

The development of the B-3A/B Ponds model required several conceptual and simulation assumptions. The major assumptions are as follows:

- The vadose zone model consists of a system of HSUs derived from the Central Plateau Vadose Zone Geoframework Model (CP-60925). The geoframework is a three-dimensional representation of the subsurface beneath the Central Plateau, vertically extending from the ground surface to the top of the Columbia River Basalt Group. The geoframework model is constructed using a combination of lithologic and sequence stratigraphic interpretations, leading to the definition of a series of HSUs. With this approach, correlated, hydraulically significant units are mapped while still representing the interpretations of lithologically heterogeneous features. The HSU surfaces used in generating the B-3A/B Ponds model are from an update to CP-60925, ECF-HANFORD-18-0035.

- The anisotropic Equivalent Homogeneous Media (EHM) approach is used to simulate flow and transport in the heterogeneous Central Plateau HSUs. The EHM approach is recommended by Yeh et al., 2015, "Flow Through Heterogeneous Geologic Media," for systems with large-scale HSUs. With this approach, an HSU has two main characteristics: (1) representative hydraulic property and parameter values are applied that are equivalently homogeneous (i.e., constant) in space, and (2) the effects of heterogeneity on flow are described using an anisotropic unsaturated hydraulic conductivity. An important feature of an anisotropic EHM model representation is that it captures the mean or the bulk flow characteristics of the vadose zone moisture plumes, as demonstrated by Zhang and Khaleel, 2010, "Simulating Field-Scale Moisture Flow Using a Combined Power-Averaging and Tensorial Connectivity-Tortuosity Approach." Therefore, the contaminant peak arrival time under recharge-dominated flow conditions is adequately captured by an anisotropic EHM model representation. The anisotropic EHM approach is commonly used to model flow and transport at the Hanford Site. For instance, recent PA vadose modeling for WMA C (RPP-ENV-58782, *Performance Assessment of Waste Management Area C, Hanford Site, Washington*) used this approach to simulate subsurface flow and transport.

- For simulation of flow in unsaturated Hanford Site sediments, the soil water retention relation (i.e., the relation between soil moisture content and capillary pressure) and the unsaturated hydraulic conductivity relation (i.e., the relation between moisture content and unsaturated hydraulic conductivity) need to be provided. The unsaturated hydraulic conductivity is the product of the saturated hydraulic conductivity and the aqueous phase relative permeability. The nonhysteretic van Genuchten equation (van Genuchten, 1980) is used for the soil water retention relation. The Mualem relation (Mualem, 1976) is used for the unsaturated hydraulic conductivity relation.

- For the heterogeneous stratified sediments at the Central Plateau, upscaled hydraulic properties based on small-scale laboratory measurements are used to simulate the large, field-scale behavior. This assumption requires that each heterogeneous HSU be replaced by an anisotropic EHM with upscaled hydraulic properties. The hydraulic properties used in the CA model are on a grid-block scale which are much larger than the cores that are typically analyzed in the laboratory.

- The upscaled grid-block-scale parameter values for the water retention and relative permeability relations are obtained by applying averaging procedures to core-scale data. For the soil water retention relation, the linear upscaling scheme (Green et al., 1996, "Upscaled Soil-Water Retention Using Van Genuchten's Function") is applied. For the unsaturated hydraulic conductivity, the power-averaging tensorial connectivity-tortuosity (PA-TCT) method (Zhang et al., 2003, "A Tensorial Connectivity–Tortuosity Concept to Describe the Unsaturated Hydraulic Properties of Anisotropic Soils"; Zhang and Khaleel, 2010) is used to determine directionally-dependent saturated hydraulic conductivity and relative permeability tortuosity parameters that are functions of the soil moisture content. The PA-TCT upscaling method leads to a soil-moisture-dependent anisotropic unsaturated hydraulic. Applying the PA-TCT method allows for an assessment of the effects of heterogeneity on lateral flow and contaminant spreading, including plume commingling at the HSU scale. The method has been successfully applied to evaluate various water infiltration tests performed at the Sisson and Lu field experiment site in the 200 East Area (Ye et al., 2005, "Stochastic Analysis of Moisture Plume Dynamics of a Field Injection Experiment"; Zhang and Khaleel, 2010). The field applications of the upscaled vadose zone property values based on the PA-TCT method suggests that it provides a reasonable framework for upscaling core-scale measurements, as well as an accurate simulation of moisture flow in the heterogeneous vadose zone under the Central Plateau.

- The CA vadose zone models use a "forward" modeling approach for contaminant transport in the subsurface: model transport simulations initiate at a time when contamination is not present in the subsurface, and the contaminant activity is introduced in the models as sources over time. This approach has been used to simulate Hanford Site contaminant transport resulting from liquid waste disposal (e.g., Oostrom et al., 2017, "Deep Vadose Zone Contaminant Flux Evaluation at the Hanford BY-Cribs Site Using Forward and Imposed Concentration Modeling Approaches") and past leaks (RPP-RPT-59197, *Analysis of Past Waste Tank Leaks and Losses in the Vicinity of Waste Management Area C, Hanford Site, Washington*).

- Contaminant activity is assumed to be transported in the vadose zone by advection and hydrodynamic dispersion, which is the sum of molecular diffusion and mechanical dispersion. The two components of hydrodynamic dispersion are described by a single hydrodynamic dispersion coefficient and treated as a diffusive flux proportional to the concentration gradient. Advective transport and mechanical dispersion are computed using the flow field obtained when solving the water conservation equation. The contaminants are considered to be solutes, without affecting fluid properties like density and viscosity.

- Mechanical dispersion is assumed to be directionally dependent with a constant macroscopic macrodispersivity value for each HSU. The use of a constant (asymptotic) macrodispersivity for large-scale vadose zone CA modeling is considered appropriate (NUREG/CR-5965, *Modeling Field Scale Unsaturated Flow and Transport Processes*). Macrodispersivity values for the HSUs in the longitudinal direction, are obtained from Hanford Site field-scale numerical simulations and field experiments. Hanford Site-specific datasets include Khaleel et al., 2002, "Upscaled Flow and Transport Properties for Heterogeneous Unsaturated Media"; and PNNL-25146, *Scale-Dependent Solute Dispersion in Variably Saturated Porous Media*. In the absence of unsaturated media experimental data, the CA transport models used a transverse macrodispersivity value that is 1/10th of the obtained longitudinal value.

- Contaminant sorption is simulated using a reversible linear sorption isotherm with a linear K_d. The linear sorption model approach is assumed to be adequate for modeling transport at the Hanford Site (PNNL-13895, *Hanford Contaminant Distribution Coefficient Database and Users Guide*). An important benefit of the linear adsorption assumption is that an extensive database of K_d values applicable to Hanford Site sediments is available for the contaminants of most concern over a broad range of conditions (e.g., PNNL-17154, *Geochemical Characterization Data Package for the Vadose Zone in the Single-Shell Tank Waste Management Areas at the Hanford Site*). Use of reversible linear K_d isotherms is computationally efficient and appropriate for the scale of the CA problem. Recognizing that experimental K_d values are mostly determined using sediment grain sizes <2 m, corrections for gravel content using equations provided in PNNL-17154 are used to adjust measured values for the finer fraction applicable to HSUs with considerable gravel content.

- The spatial and temporal variable natural recharge rate is used to define the upper boundary conditions for the water conservation equation. The natural recharge rate is a term applied to define the net infiltration that migrates through the vadose zone to reach the water table. At the Hanford Site, this rate is primarily a function of the surface soil type and type/density of vegetative cover. Effects of climate change on natural recharge over the next 10,000 years are not accounted for in the simulations.

- No moisture or contaminants are allowed to migrate across the lateral boundaries of the model domain. During development of the model domain, the proper locations of the zero flux lateral boundaries were determined in an iterative procedure.

- The simulations use a fixed water table representing 2018 conditions to increase efficiency and reduce complexity during implementation of the vadose zone models. The effects of the transient water table on contaminant transfer after 2018 to the aquifer were evaluated to validate this approach in Farrow et al., 2019, "Prediction of Long-Term Contaminant Flux from the Vadose Zone to Groundwater for Fluctuating Water Table Conditions at the Hanford Site." Simulations for selected vadose zone models with continuing sources demonstrated that a simplification of the water table boundary condition (i.e., a static water table), could be adequately used to compute long-term predictions of contaminant flux to groundwater.

- The liquid volumes and waste site inventories are obtained from the Hanford Soil Inventory Model (SIM-v2) (ECF-HANFORD-17-0079). Non-radiological site liquid volumes were obtained from site-specific literature. Using geometry information, waste and non-radiological site shapes were assigned to vadose zone model grid surfaces, according to EMDT-GR-0035, *Waste Site and Structure Footprint Shapefiles for Inclusion in Updated Composite Analysis*. Water volumes and SIM-v2 contaminant inventories were assigned to the model grid cells at the lowest topographic location within the site footprints.

5 Software Applications

Three types of calculation software are used in this modeling effort: the numerical modeling simulator eSTOMP, support software (spreadsheet and geographic information system [GIS] applications), and custom utility calculation software. Custom utility calculations software is documented under CHPRC-04032, *Composite Analysis / Cumulative Impact Evaluation (CACIE) Utility Codes Integrated Software Management Plan* and described in further detail in Section 5.3 of this ECF.

5.1 Approved Software

The eSTOMP numerical simulator has been used for the flow and transport calculations reported in this ECF. The application of the simulator is managed under the requirements of CHPRC-00176, *STOMP Software Management Plan*. Use of this software is consistent with the intended uses of STOMP at the Hanford Site as defined in CHPRC-00222, *STOMP Functional Requirements Document*. The STOMP software is actively managed by the CH2M HILL Plateau Remediation Company and approved for use at the Hanford Site as Level C software under a procedure that implements the requirements of DOE O 414.1D, *Quality Assurance*.

Build 6 of the STOMP software was used in the implementation of the model described in this document. This version was approved for use at the Hanford Site based on acceptance testing results reported in CHPRC-00515, *STOMP Acceptance Test Report*. The status of requirements for this software are maintained in CHPRC-00269, *STOMP Software Requirements Traceability Matrix*. All acceptance testing was performed to the requirements of CHPRC-00211, *STOMP Software Test Plan*. Installation testing is also required for any computer system on which STOMP is run. The installation test is specified in CHPRC-00211.

The STOMP simulator was developed by Pacific Northwest National Laboratory to simulate flow and transport over multiple phases in a subsurface environment. The water mode of the simulator uses numerical approximation techniques to solve partial differential equations that describe the conservation of aqueous mass and radionuclide activity in variably saturated porous media. These governing conservation equations, along with a corresponding set of constitutive relations that relate variables within the conservation equations, are solved numerically by using integrated-volume, finite-difference discretization to the physical domain and first- or second-order Euler discretization to the time domain. The resulting equations are nonlinear, coupled algebraic equations that are solved using the Newton-Raphson iteration.

The theoretical and numerical approaches applied in the STOMP simulator are documented in a published theory guide (PNNL-12030). The simulator has undergone a rigorous verification procedure against analytical solutions, laboratory-scale experiments, and field-scale demonstrations. The application guide (PNNL-11216) provides instructive examples in the application of the code to classical groundwater and vadose zone flow and transport problems. The user's guide (PNNL-15782) describes the general use, input file formatting, compilation, and execution of the code.

- Software Title: STOMP, parallel implementation (eSTOMP), executable eSTOMP1-chprc06-20200204-g.x
- Software Version: CHPRC Build 6
- Hanford Information System Inventory Identification Number: 2471

- Workstation type and property number (from which software is run): GAIA Subsurface Flow and Transport Modeling Platform, Nodes compute-0-0 through compute-0-8 inclusive, property tags: WF32991, WF32992, WF32993, WF32994, WF32995, WF32996, WF32997, WF32998, WF32999

5.1.1 Software Installation and Checkout

The software installation and checkout form for STOMP simulation software is provided as Appendix D to this ECF.

5.1.2 Statement of Valid Software Application

The application of the eSTOMP software to the vadose zone flow and transport systems is correct. The software has been used within the limits discussed in the simulator's theory guide (PNNL-12030) and user's guide (PNNL-15782). The water mode of the STOMP simulator is designed to simulate flow and transport over multiple phases in a subsurface environment, including unsaturated systems like the Hanford Site vadose zone. The simulator solves partial differential equations describing conservation of aqueous mass and radionuclide activity in variably saturated porous media, consistent with aqueous flow and contaminant transport in Hanford Site sediments. The STOMP code has been executed at research institutions and universities to address vadose zone flow and contaminant transport problems comparable to the CA unsaturated systems.

The STOMP code, including the eSTOMP parallel implementation, is developed and tested to NQA-1, *Quality Assurance Requirements for Nuclear Facility Applications*, standards by Pacific Northwest National Laboratory "by option" wherein testing conducted option by option. Therefore, an "NQA-1 Options Analysis" is provided for the model application documented in this ECF (as well as other related model applications) in CP-63515 to demonstrate that all eSTOMP code options used in this model are NQA-1 qualified.

5.2 Support Software

The following programs are classified as Support Software:

- **Microsoft® Excel®** (version 2010): The tool was used to generate inventory plots and contaminant release and transfer timeseries.
- **ArcGIS®** (version 10.3.1): The tool was used to create of spatial model discretization and waste site location maps.
- **Tecplot® 360 EX** (version 2018R1): The tool was used to generate source location, recharge distribution, and mass transfer to groundwater plots.

5.3 Support Scripts

Generation of model input files and post-processing of model results was mostly performed with utility codes (scripts) that are managed, tested, and controlled in accordance with CHPRC-04032. CHPRC-04032 provides a common foundation for the management of several custom-developed scripts to manage pre- and post-processing operations and inter-facet information passing between major software packages efficiently for the CA. It also provides direction for electronic management of

® Microsoft and Excel are registered trademarks of the Microsoft Corporation in the United States and other countries.

® ArcGIS® is a registered trademark of the Environmental Systems Research Institute, Inc., Redlands, California.

® Tecplot is a registered trademark or trademarks of Tecplot, Inc. in the United States and other countries.

documentation requirements at the script level with respect to individual tool functional requirements, software requirements specification, software design description, requirements tracing, test plans and reporting, and user documentation. The utility scripts developed for this project, in alphabetical order, are as follows:

- **aq_mod_avg.exe:** The Aqueous Source Averaging Tool averages aqueous source rates for user-specified waste sites and times.
- **ca_build_surface_flux.py:** The Build Surface Flux Tool maps the STOMP grid into the MODFLOW grid.
- **ca-dups.pl:** The Duplicate Source Nodes Tool identifies any source nodes that overlap spatially and writes information regarding the duplicate source node(s) to an output file.
- **ca-getmod_srf.pl:** The Surface File to P2R Tool aggregates solute flux and cumulative discharge data exiting the vadose zone model by P2R grid cell.
- **ca-ipp.pl:** The Inventory Pre-Processor Tool creates a comprehensive dataset consisting of radionuclide and aqueous volume releases as a function of time for Central Plateau sites. The dataset is input for the SRC2STOMP Tool.
- **ca-merge_srf.pl:** The STOMP Surface Merge Tool merges STOMP surface file data from two consecutive STOMP simulations (e.g., surface files for the 2018 to 12070 simulation).
- **ca-patchbowl.pl:** The Patchbowl Tool modifies STOMP soil zonation files to patch holes in the silt layers of the perching silt layer in the 200 East Area.
- **ca_RET2STOMP.py**: The RET2STOMP Tool generates the natural recharge Boundary Condition Cards for the STOMP model input file using output generated by the RET.
- **ca-rtdic.pl:** The RTD Initial Conditions Card Tool generates Initial Conditions Cards at RTD years for models with RTD sites using an input source card file and a steady-state STOMP input file.
- **ca-src2stomp.pl**: The SRC2STOMP Tool combines the site spatial information with the corresponding radionuclide inventory and creates a STOMP-readable Source Card file containing grid cell definitions of solute and/or liquid sources.
- **K2S_ROCSAN.exe:** The Kingdom2Stomp Tool reads an input file representing each node in the model and generates an output file like the input file with the addition of which geologic formation each model node represents.
- **ModelSetupFY18.jar:** The Composite Analysis STOMP Tool is a graphical user interface tool that produces STOMP input files based on user input model dimensions and material properties.
- **OC_SS_gen.exe:** The Steady-State Output Card Generator Tool reads files generated by the Composite Analysis STOMP Tool and generates a STOMP Output Control Card for the steady-state simulation.
- **OC_rad_gen.exe:** The Transport Output Card Generator Tool Creates a STOMP Output Control Card used for mass balance and transport production simulations.
- **reroute_sources.exe:** The Source Rerouting Tool redistributes wastewater volumes and contaminant inventories for the 216-U-10 Pond System and the 216-B-3 Pond System.

- **splitKingdomLayer.pl:** The SplitKingdomLayer Tool is used to split one geology surface layer file into two sub-unit surface layer files based on the information specified in the polygon file.
- **srcloc_modify.exe:** The Source Node Moving Tool moves source nodes from the locations selected by the SRC2STOMP Tool.
- **SS_input_gen.exe*:*** The Steady-state STOMP Input File Generator Tool generates the STOMP input file for the steady-state simulation.
- **xprt_2018_input_gen.exe:** The 2018 STOMP Input File Generator Tool generates the 1943–2018 STOMP transport input file.
- **xprt_12070_input_gen.exe:** The 12070 STOMP Input File Generator Tool generates the 2018 (or RTD year if the model has RTD remediation sites)–12070 STOMP transport input file. This code reads and modifies the 1943–2018 STOMP input file created by the 2018 STOMP Input File Generator Tool.
- **xprt_mb_input_gen.exe:** The Mass Balance STOMP Input File Generator Tool generates the mass balance STOMP transport input file. This code reads and modifies the STOMP input file created by the 2018 STOMP Input File Generator Tool.
- **xprt_RTD_input_gen.exe:** The RTD STOMP Input File Generator tool generates the 2018 – RTD year STOMP transport input file. This code reads and modifies the 1943–2018 STOMP input file created by the 2018 STOMP Input File Generator Tool.

6 Calculation

The fate and transport calculations for the B-3A/B Ponds model were performed using a suite of STOMP simulations: a steady-state simulation, mass balance transport simulations, and historical and forecast transport simulations (as discussed in Section 4.6). This section describes the mass balance calculations for the steady-state and transport simulations.

6.1 Steady-State Simulation

The purpose of the steady-state simulation was to verify model performance and to generate the initial primary variable (i.e., aqueous pressure) conditions within the model domain for the historical transport simulations, as discussed in Section 4.6.1. Contaminants are not simulated in the steady-state simulation, only flow. Pre-Hanford Site boundary conditions (i.e, natural recharge rates for 1943) are applied for a period of 10,000 years (from year zero to 10,000) to allow the simulation to reach steady-state conditions. Figure 6-1 compares the steady-state recharge flux into the top of the model to the flux leaving the base of the model, which represents discharge to groundwater from the model. Conditions reach equilibrium (i.e., flux in equals flux out) and remain unchanged through the end of the simulated time period, indicating that steady-state conditions have been achieved.

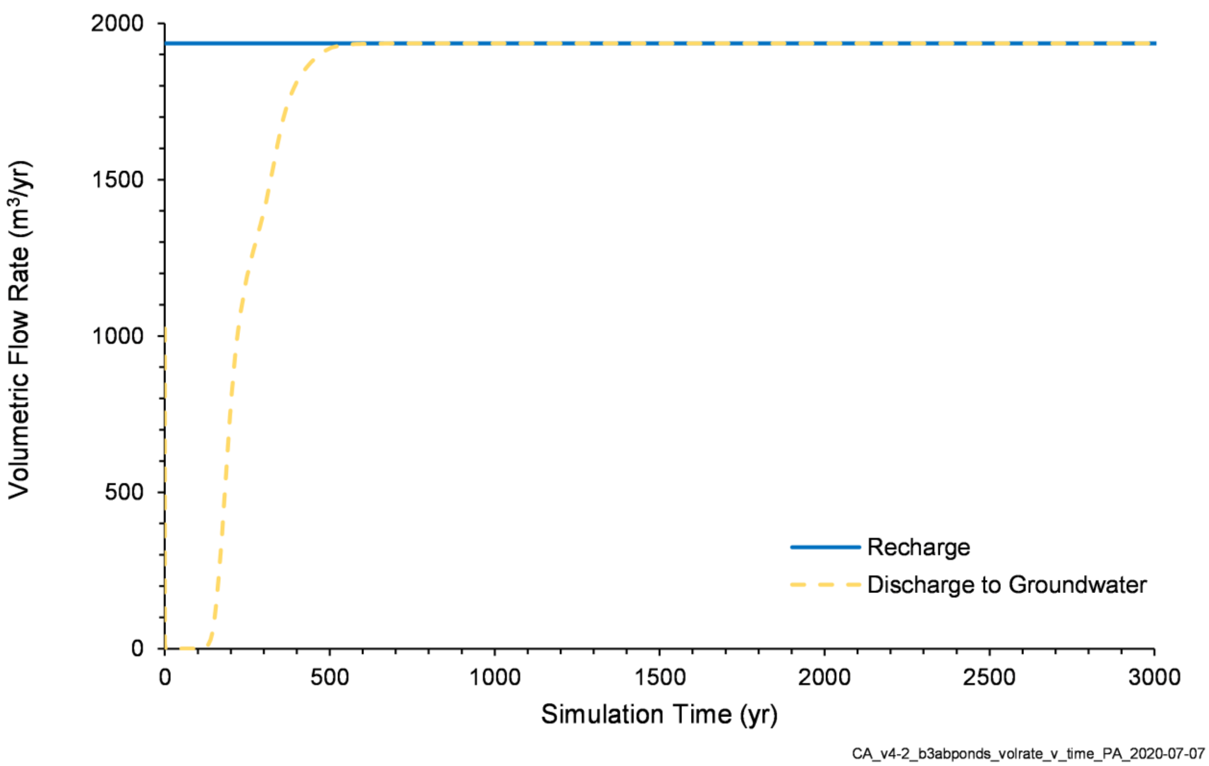

Figure 6-1. Steady-State Recharge Compared to Discharge to Groundwater Over Time

The steady-state liquid volume balance (also called mass balance) error (E) is calculated as shown in Equation 6-1 (all variables have units of volume):

$$E = (S + O) - R_P \quad \textbf{(Eq. 6-1)}$$

where:

E = liquid volume balance error

S = change in liquid storage within the model domain
O = total liquid outflow from the model domain
R_P = total pre-Hanford natural recharge.

The percent relative error (*%RE*) of the aqueous volume balance is calculated as shown in Equation 6-2:

$$\%RE = 100|E/R_P| \quad \textbf{(Eq. 6-2)}$$

where %RE is the liquid volume percent relative error.

Change in liquid storage (*S*) is the difference between liquid in the model at year 10,000 and year 0. Total liquid water outflow from the model (*O*) is the cumulative liquid volume that passed through the bottom of the model boundary at the end of 10,000 years. The pre-Hanford natural recharge (R_P) is the cumulative volume of recharge applied to the top layer of the model during the simulation. The flow-only steady-state liquid volume balance is shown in Table 6-1.

Table 6-1. Liquid Volume Balance for B-3A/B Ponds Model Steady-State Simulation

Natural Recharge (R_P) [a]	Change in Liquid Storage (*S*) [a,b]	Total Liquid Outflow (*O*) [a,b]	Error (*E*) [a]	Percent Relative Error (*%RE*)
19,352,000	472,954	18,879,170	124	6.429E-04

a. Volume units in m^3.

b. Calculated by STOMP.

%RE = liquid volume percent relative error
E = liquid volume balance error
O = total liquid outflow from the model domain
R_P = total pre-Hanford natural recharge
S = change in liquid storage within the model domain
STOMP = Subsurface Transport Over Multiple Phases

6.2 Contaminant Transport Volume and Activity Simulations

Transient simulations were used to calculate liquid volume and activity balances, also referred to as mass balances. These simulations use the steady-state model final aqueous pressure distribution as initial aqueous pressure conditions, the transient natural recharge described in Section 4.8.1, and the waste site sources described in Section 4.5. Although run as single simulations for each radionuclide group, two sets of radionuclide activity balance evaluations were performed: the first for the historical time period from 1943 to 2018, and the second for the entire transient model duration from 1943 to 12070. Radionuclide half-life values were set to 1.0E+20 years to virtually eliminate radioactive decay. Therefore, decay corrections were not necessary, and the radionuclide activity balance could be evaluated directly.

The liquid volume balance error (*E*) is calculated as shown in Equation 6-3 (all variables have units of volume):

$$E = (S + O) - (I + R) \quad \textbf{(Eq. 6-3)}$$

where:

E = liquid volume balance error

S	=	change in liquid storage within the model domain
O	=	total liquid outflow from the model domain
I	=	liquid inventory entering the model domain from liquid waste site releases
R	=	total natural recharge.

The percent relative error ($\%RE$) of liquid volume balance is calculated as shown in Equation 6-4:

$$\%RE = 100|E/(I+R)| \quad \textbf{(Eq. 6-4)}$$

where %RE is the liquid volume percent relative error.

The change in liquid storage within the model domain (*S*) is the difference between the volume of water in the model at the beginning of the simulation (1943) and the end of the mass balance analysis period (either 2018 or 12070). The total liquid outflow from the model domain (*O*) is the cumulative liquid volume that passed through the bottom of the model boundary by the end of the mass balance analysis period. The liquid inventory entering the model domain from liquid waste site releases (*I*) is the cumulative volume of liquids released to the model from liquid waste sites in the source and buffer zones during the mass balance analysis period. The natural recharge (*R*) is the cumulative volume of liquid applied to the top of the model from natural recharge during the mass balance analysis period. The liquid volume balance for the B-3A/B Ponds model for the simulation for Radionuclide Group 1 is shown in Table 6-2, the liquid volume balance for Radionuclide Group 2 is not included as it is functionally the same.

Table 6-2. Transient Liquid Volume Balances for the B-3A/B Ponds Model Radionuclide Group 1 Simulations

Liquid Inventory (*I*) [a]	Natural Recharge (*R*) [a]	Change in Liquid Storage (*S*) [a,b]	Total Liquid Outflow (*O*) [a,b]	Error (*E*) [a]	Percent Relative Error (*%RE*)
1943–2018					
106,066,060	882,975	247,211	106,701,900	76	7.079E-05
1943–12070					
106,066,060	21,177,584	5,526	127,237,700	-418	3.285E-04

a. Volume units in m^3.

b. Calculated by STOMP.

%RE	=	liquid volume percent relative error
E	=	liquid volume balance error
I	=	liquid inventory entering the model domain from liquid waste site releases
O	=	total liquid outflow from the model domain
R	=	total natural recharge
S	=	change in liquid storage within the model domain
STOMP	=	Subsurface Transport Over Multiple Phases

The radionuclide activity balance error (E_R) is calculated as shown in Equation 6-5 (all variables have units of activity):

$$E_R = (S_R + O_R) - I_R \qquad \textbf{(Eq. 6-5)}$$

where:

E_R	=	radionuclide activity balance error
S_R	=	radionuclide storage within the model domain at the end of the simulation
O_R	=	total radionuclide outflow from the model domain
I_R	=	radionuclide inventory entering the model domain from waste site releases.

The percent relative error ($\%RE_R$) of the radionuclide activity balance is calculated as shown in Equation 6-6:

$$\%RE_R = 100|E_R/I_R| \qquad \textbf{(Eq. 6-6)}$$

where $\%RE_R$ is the radionuclide activity balance percent relative error.

The total radionuclide outflow (O_R) is the cumulative activity of a particular radionuclide that migrated through the bottom boundary of the vadose zone model from the beginning of the simulation (1943) to the end of the mass balance analysis period (either 2018 or 12070). The radionuclide storage (S_R) is the difference in total activity of a particular radionuclide in the model from the beginning of the simulation (1943) and the end of the mass balance analysis period (2018 or 12070). Because there were no radionuclides in the model from anthropogenic sources in 1943, this can be understood as the change in total activity of a radionuclide in the model domain. The radionuclide inventory that entered the model domain from waste site releases (I_R) is the cumulative activity of the radionuclide released to the model from the liquid waste release sites in the source zone. Table 6-3 and Table 6-4 show the activity balance for the B-3A/B Ponds model no-decay transport simulations for Radionuclide Group 1 and Radionuclide Group 2, respectively.

Table 6-3. Transient No-Decay Activity Balances for the B-3A/B Ponds Model Radionuclide Group 1 Simulations

Radionuclide	Released Radionuclide Inventory (I_R) [a]	Radionuclide Storage (S_R) [a,b]	Radionuclide Outflow (O_R) [a,b]	Error (E_R) [a]	Relative Error ($\%RE_R$)
1943–2018					
C-14	1.662E+01	1.752E-02	1.661E+01	9.757E-03	5.871E-02
Cl-36	0.000E+00	0.000E+00	0.000E+00	See note c	See note c
H-3	2.333E+03	2.828E+00	2.331E+03	3.833E-01	1.643E-02
I-129	4.929E-04	2.392E-06	4.938E-04	3.211E-06	6.513E-01
Np-237	1.183E-02	1.179E-02	4.504E-05	1.148E-05	9.704E-02
Re-187	0.000E+00	0.000E+00	0.000E+00	See note c	See note c
Sr-90	2.739E+00	2.741E+00	1.292E-15	1.188E-03	4.338E-02
Tc-99	8.158E-03	9.780E-05	8.067E-03	6.404E-06	7.850E-02

Table 6-3. Transient No-Decay Activity Balances for the B-3A/B Ponds Model Radionuclide Group 1 Simulations

Radionuclide	Released Radionuclide Inventory (I_R) [a]	Radionuclide Storage (S_R) [a,b]	Radionuclide Outflow (O_R) [a,b]	Error (E_R) [a]	Relative Error ($\%RE_R$)
1943–12070					
C-14	1.662E+01	2.019E-19	1.663E+01	9.689E-03	5.830E-02
Cl-36	0.000E+00	0.000E+00	0.000E+00	See note c	See note c
H-3	2.333E+03	2.641E-17	2.334E+03	3.725E-01	1.596E-02
I-129	4.929E-04	2.423E-13	4.962E-04	3.212E-06	6.515E-01
Np-237	1.183E-02	1.165E-02	1.904E-04	1.191E-05	1.007E-01
Re-187	0.000E+00	0.000E+00	0.000E+00	See note c	See note c
Sr-90	2.739E+00	2.741E+00	3.075E-14	1.200E-03	4.381E-02
Tc-99	8.158E-03	1.048E-22	8.164E-03	5.946E-06	7.288E-02

a. Units are in Curies.

b. Calculated by STOMP.

c. The radionuclide has no inventory.

$\%RE_R$ = percent relative error of the radionuclide mass balance

E_R = radionuclide mass balance error

I_R = radionuclide inventory entering the model domain from waste site releases

O_R = total radionuclide outflow from the model domain

S_R = radionuclide outflow from the model domain

STOMP = Subsurface Transport Over Multiple Phases

Table 6-4. Transient No-Decay Activity Balances for the B-3A/B Ponds Model Radionuclide Group 2 Simulations

Radionuclide	Released Radionuclide Inventory (I_R) [a]	Radionuclide Storage (S_R) [a,b]	Radionuclide Outflow (O_R) [a,b]	Error (E_R) [a]	Relative Error (%RE_R)
1943–2018					
U-232	7.765E-05	1.138E-06	7.678E-05	2.616E-07	3.369E-01
U-233	2.208E-05	3.378E-07	2.182E-05	7.735E-08	3.504E-01
U-234	2.078E-01	3.053E-03	2.054E-01	6.912E-04	3.327E-01
U-235	7.964E-03	1.170E-04	7.874E-03	2.650E-05	3.327E-01
U-236	2.006E-02	2.948E-04	1.984E-02	6.676E-05	3.327E-01
U-238	1.432E-01	2.105E-03	1.416E-01	4.765E-04	3.327E-01
Th-230	0.000E+00	0.000E+00	0.000E+00	See note c	See note c
Ra-226	0.000E+00	0.000E+00	0.000E+00	See note c	See note c
1943–12070					
U-232	7.765E-05	1.598E-07	7.776E-05	2.625E-07	3.380E-01
U-233	2.208E-05	4.650E-08	2.211E-05	7.775E-08	3.522E-01
U-234	2.078E-01	4.286E-04	2.080E-01	6.935E-04	3.338E-01
U-235	7.964E-03	1.643E-05	7.974E-03	2.659E-05	3.338E-01
U-236	2.006E-02	4.139E-05	2.009E-02	6.698E-05	3.338E-01
U-238	1.432E-01	2.955E-04	1.434E-01	4.782E-04	3.338E-01
Th-230	0.000E+00	0.000E+00	0.000E+00	See note c	See note c
Ra-226	0.000E+00	0.000E+00	0.000E+00	See note c	See note c

a. Units are in Curies.

b. Calculated by STOMP.

c. The radionuclide has no inventory.

%RE_R = percent relative error of the radionuclide mass balance

E_R = radionuclide mass balance error

I_R = radionuclide inventory entering the model domain from waste site releases

O_R = total radionuclide outflow from the model domain

S_R = radionuclide outflow from the model domain

STOMP = Subsurface Transport Over Multiple Phases

7 Results

This chapter presents the results of the transport simulations. These results include the calculation of cumulative radionuclide activity transferred to the groundwater and the cumulative activity remaining in the vadose zone at the end of the historical simulation (1943–2018) and the CA evaluation (i.e., forecast) simulation (2018–12070).

For each of the 16 radionuclides, Table 7-1 and Table 7-2 list the total activity discharged to the groundwater and the total activity remaining in the vadose zone. Table 7-1 shows these data at the end of the historical simulation (1943–2018), and Table 7-2 shows these data at the end of the forecast simulation (2018–12070).

The data presented in Table 7-1 and Table 7-2 are presented graphically in Section 7.1 through 7.16. These sections each present the data for one radionuclide. The cumulative activity of radionuclides discharged to the groundwater presented in Table 7-1 are shown spatially, aggregated by P2R grid cell, in Figure 7-1 and similar figures. The cumulative activity discharged to groundwater and the cumulative inventory released to the model shown in Table 7-1for 1943–2018 and Table 7-2 for 2018–12070, is shown through time, first by figures which show the data from 1943–2018 (like Figure 7-3) and then by figures which show the data from 1943–12070 (like Figure 7-4). Additional figures showing radionuclide arrival to the groundwater through time for P2R grid cells in this model are shown in Appendix E.

Table 7-1. B-3A/B Ponds Model Radionuclide Activity Transfer to Groundwater from 1943–2018 and Remaining Activity in the Vadose Zone at 2018

Radionuclide	1943–2018 Inventory Released to Vadose Zone (Ci)	1943–2018 Activity Transferred to Groundwater (Ci)	1943–2018 Percent Activity Transferred to Groundwater [a]	Activity Remaining in Vadose Zone at 2018 (Ci)	Percent Activity Remaining in Vadose Zone at 2018 [a]
Radionuclide Group 1					
C-14	1.662E+01	1.661E+01	99.9	1.746E-02	0.1
Cl-36	0.000E+00	0.000E+00	See note b	0.000E+00	See note b
H-3	2.333E+03	2.287E+03	98.0	5.985E-01	<0.1
I-129	4.929E-04	4.938E-04	100.2	2.392E-06	0.5
Np-237	1.183E-02	4.504E-05	0.4	1.179E-02	99.7
Re-187	0.000E+00	0.000E+00	See note b	0.000E+00	See note b
Sr-90	2.739E+00	8.726E-16	<0.1	1.341E+00	49.0
Tc-99	8.158E-03	8.067E-03	98.9	9.779E-05	1.2

Table 7-1. B-3A/B Ponds Model Radionuclide Activity Transfer to Groundwater from 1943–2018 and Remaining Activity in the Vadose Zone at 2018

Radionuclide	1943–2018 Inventory Released to Vadose Zone (Ci)	1943–2018 Activity Transferred to Groundwater (Ci)	1943–2018 Percent Activity Transferred to Groundwater [a]	Activity Remaining in Vadose Zone at 2018 (Ci)	Percent Activity Remaining in Vadose Zone at 2018 [a]
Radionuclide Group 2					
U-232	7.765E-05	7.557E-05	97.3	8.469E-07	1.1
U-233	2.208E-05	2.182E-05	98.8	3.378E-07	1.5
U-234	2.078E-01	2.054E-01	98.9	3.053E-03	1.5
U-235	7.964E-03	7.874E-03	98.9	1.170E-04	1.5
U-236	2.006E-02	1.984E-02	98.9	2.948E-04	1.5
U-238	1.432E-01	1.416E-01	98.9	2.105E-03	1.5
Th-230	0.000E+00	3.750E-09	See note b	1.168E-06	See note b
Ra-226	0.000E+00	1.468E-11	See note b	2.580E-10	See note b

a. The percentage or sum of percentages could differ slightly from 100 due to numerical error.

b. The radionuclide has no 1943–2018 inventory.

Table 7-2. B-3A/B Ponds Model Radionuclide Activity Transfer to Groundwater from 2018–12070 and Remaining Activity in the Vadose Zone at 12070

Radionuclide	1943–12070 Inventory Released to Vadose Zone (Ci)	2018–12070 Activity Transferred to Groundwater (Ci)	2018–12070 Percent Activity Transferred to Groundwater [a]	Activity Remaining in Vadose Zone at 12070 (Ci)	Percent Activity Remaining in Vadose Zone at 12070 [a]
Radionuclide Group 1					
C-14	1.662E+01	1.714E-02	0.1	5.938E-20	<0.1
Cl-36	0.000E+00	0.000E+00	See note b	0.000E+00	See note b
H-3	2.333E+03	1.045E-01	<0.1	0.000E+00	0.0
I-129	4.929E-04	2.392E-06	0.5	2.419E-13	<0.1
Np-237	1.183E-02	1.451E-04	1.2	1.161E-02	98.2
Re-187	0.000E+00	0.000E+00	See note b	0.000E+00	See note b
Sr-90	2.739E+00	4.375E-17	<0.1	0.000E+00	0.0
Tc-99	8.158E-03	9.730E-05	1.2	1.014E-22	<0.1

Table 7-2. B-3A/B Ponds Model Radionuclide Activity Transfer to Groundwater from 2018–12070 and Remaining Activity in the Vadose Zone at 12070

Radionuclide	1943–12070 Inventory Released to Vadose Zone (Ci)	2018–12070 Activity Transferred to Groundwater (Ci)	2018–12070 Percent Activity Transferred to Groundwater [a]	Activity Remaining in Vadose Zone at 12070 (Ci)	Percent Activity Remaining in Vadose Zone at 12070 [a]
Radionuclide Group 2					
U-232	7.765E-05	4.504E-08	0.1	0.000E+00	0.0
U-233	2.208E-05	2.862E-07	1.3	4.450E-08	0.2
U-234	2.078E-01	2.595E-03	1.2	4.165E-04	0.2
U-235	7.964E-03	1.007E-04	1.3	1.643E-05	0.2
U-236	2.006E-02	2.536E-04	1.3	4.137E-05	0.2
U-238	1.432E-01	1.811E-03	1.3	2.954E-04	0.2
Th-230	0.000E+00	2.524E-08	See note b	4.174E-05	See note b
Ra-226	0.000E+00	2.508E-08	See note b	7.771E-07	See note b

a. The percentage or sum of percentages could differ slightly from 100 due to numerical error.

b. The radionuclide has no 1943–12070 inventory.

Further description of the fate and transport of each radionuclide is outlined in Sections 7.1 through 7.16. Results presented in the sections show cumulative activity of the radionuclide discharged to groundwater over the historical (1943–2018) and forecast (2018–12070) simulations, and figures showing the cumulative activity released from the sources compared to the transfer rate to groundwater for the historical (1943–2018) and entire (1943–12070) modeled periods. For H-3, a constituent with a relatively large inventory that could potentially contribute to dose, additional figures were included detailing the radionuclide flux to groundwater.

7.1 C-14 Fate and Transport Results

This model simulated the release and transport of C-14. The cumulative discharge of C-14 into groundwater is shown aggregated by P2R grid cell in Figure 7-1 and Figure 7-2 for 1943–2018 and 2018–12070, respectively. The inventory released to the B-3A/B Ponds model and the transfer of C-14 to groundwater are shown from 1943–2018 in Figure 7-3 and from 1943–12070 in Figure 7-4.

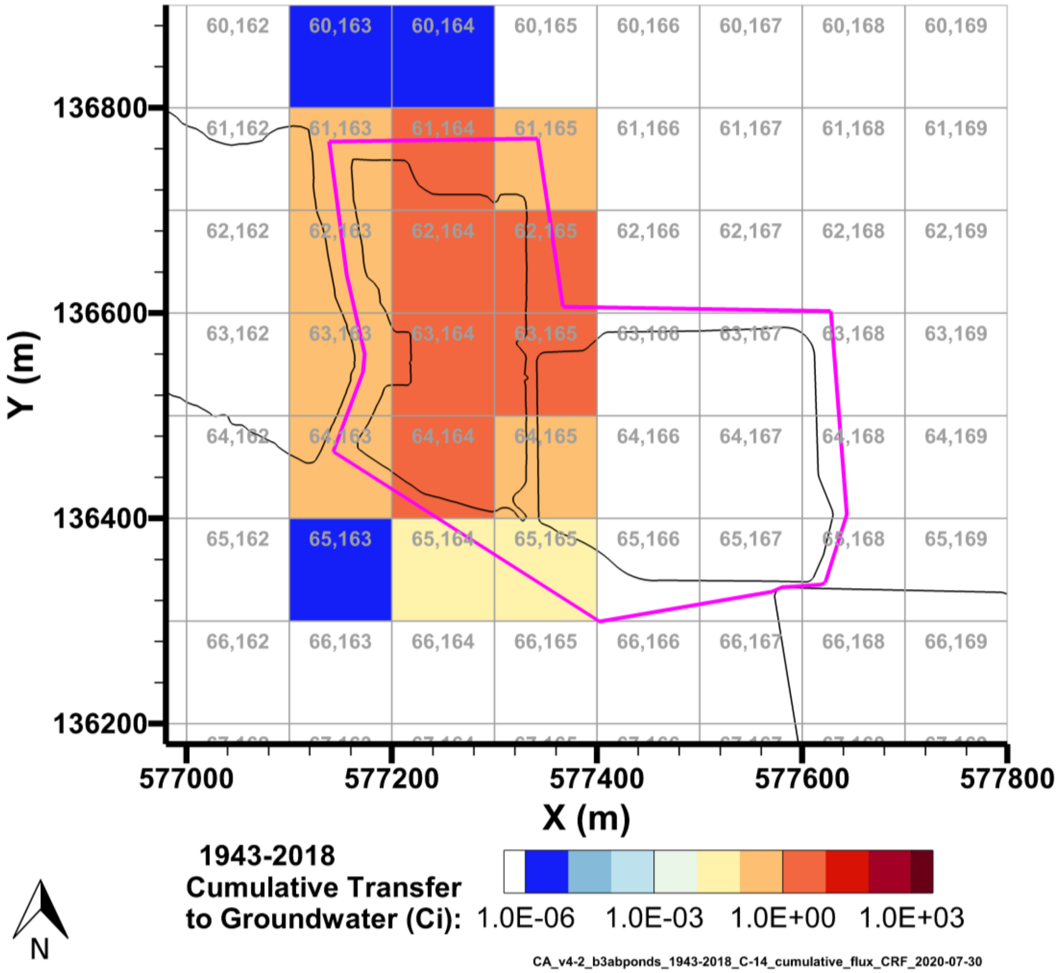

Note: source zone outlined in pink.

Figure 7-1. Cumulative C-14 Activity Discharged to Groundwater from the B-3A/B Ponds Model from 1943–2018 per P2R Grid Cell

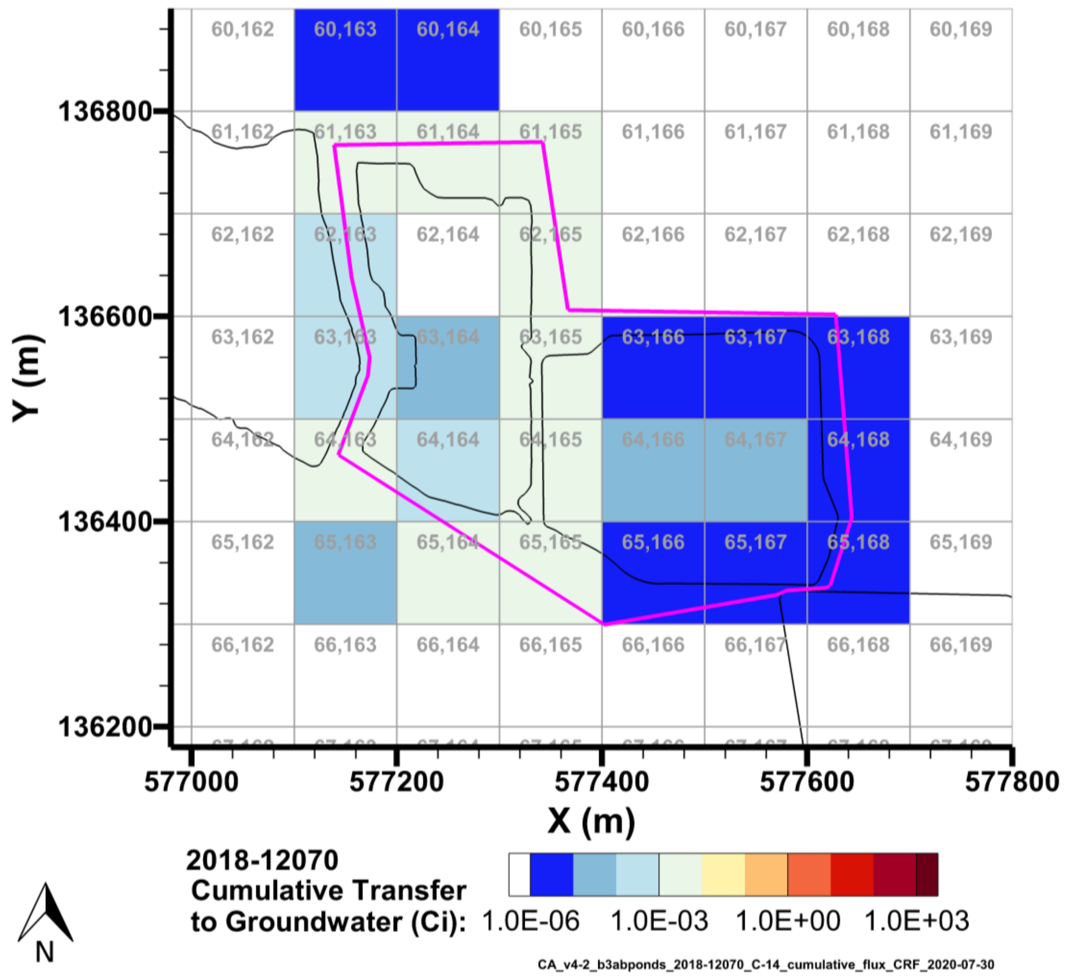

Note: source zone outlined in pink.

Figure 7-2. Cumulative C-14 Activity Discharged to Groundwater from the B-3A/B Ponds Model from 2018–12070 per P2R Grid Cell

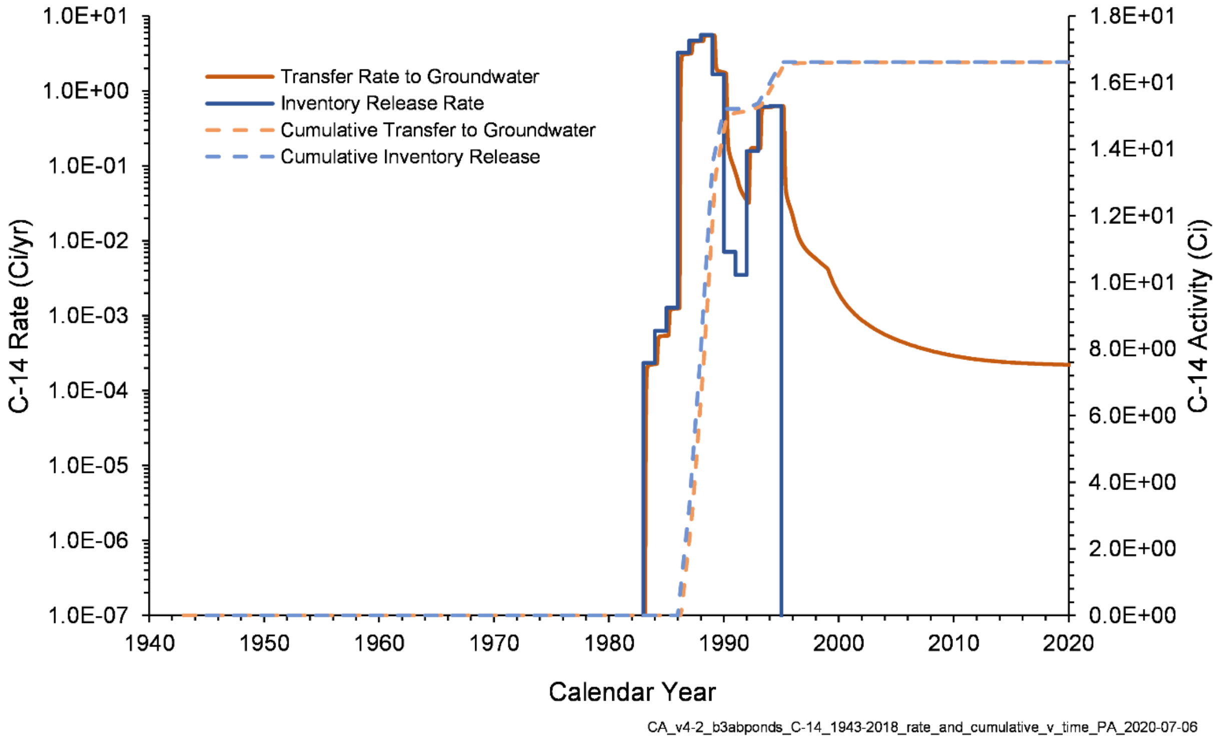

Figure 7-3. C-14 Inventory Release from Waste Sites and Transfer to Groundwater for the B-3A/B Ponds Model from 1943–2018

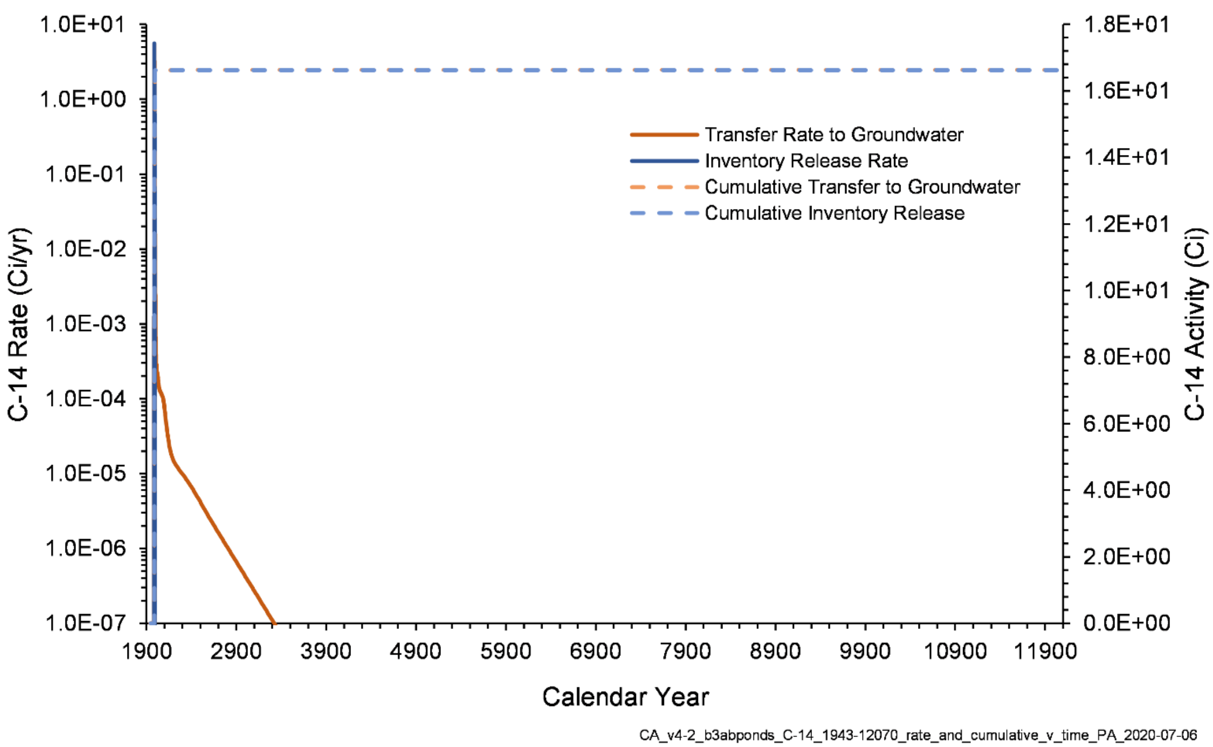

Figure 7-4. C-14 Inventory Release from Waste Sites and Transfer to Groundwater for the B-3A/B Ponds Model from 1943–12070

7.2 Cl-36 Fate and Transport Results

Due to a lack of inventory, transport of Cl-36 was not calculated in this model.

7.3 H-3 Fate and Transport Results

This model simulated release and transport of H-3. The cumulative discharge of H-3 into groundwater is shown aggregated by P2R grid cell in Figure 7-5 and Figure 7-6 for 1943–2018 and 2018–12070, respectively. The inventory released to the B-3A/B Ponds model and the transfer of H-3 to groundwater are shown from 1943–2018 in Figure 7-7 and from 1943–12070 in Figure 7-8. Figure 7-9 through Figure 7-15 show the flux of H-3 to groundwater in Ci/yr. These figures are generated at times with peak fluxes (local maxima) and during periods with gradual decline, as shown in Figure 7-7 and Figure 7-8. A figure for 2018, Figure 7-12, is also included to demonstrate the initial flux conditions for the 2018–12070 simulation.

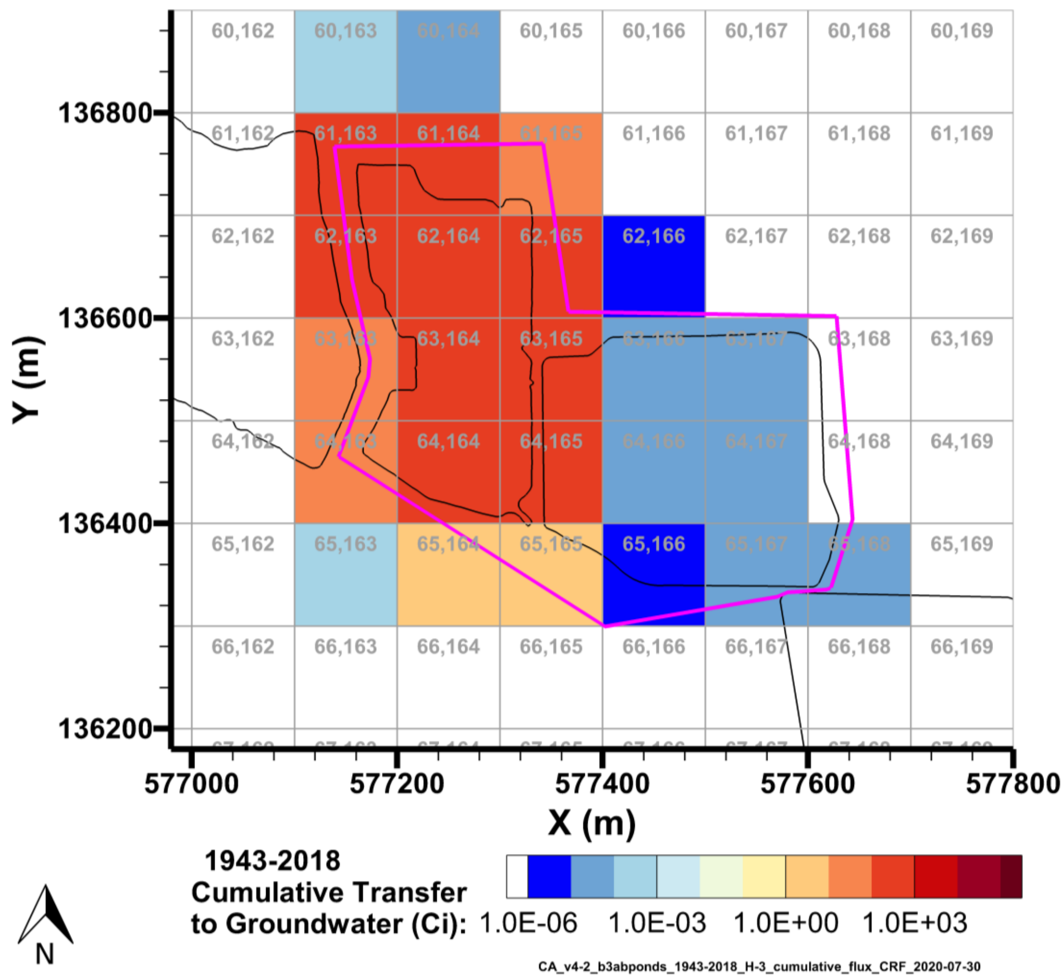

Note: source zone outlined in pink.

Figure 7-5. Cumulative H-3 Activity Discharged to Groundwater from the B-3A/B Ponds Model from 1943–2018 per P2R Grid Cell

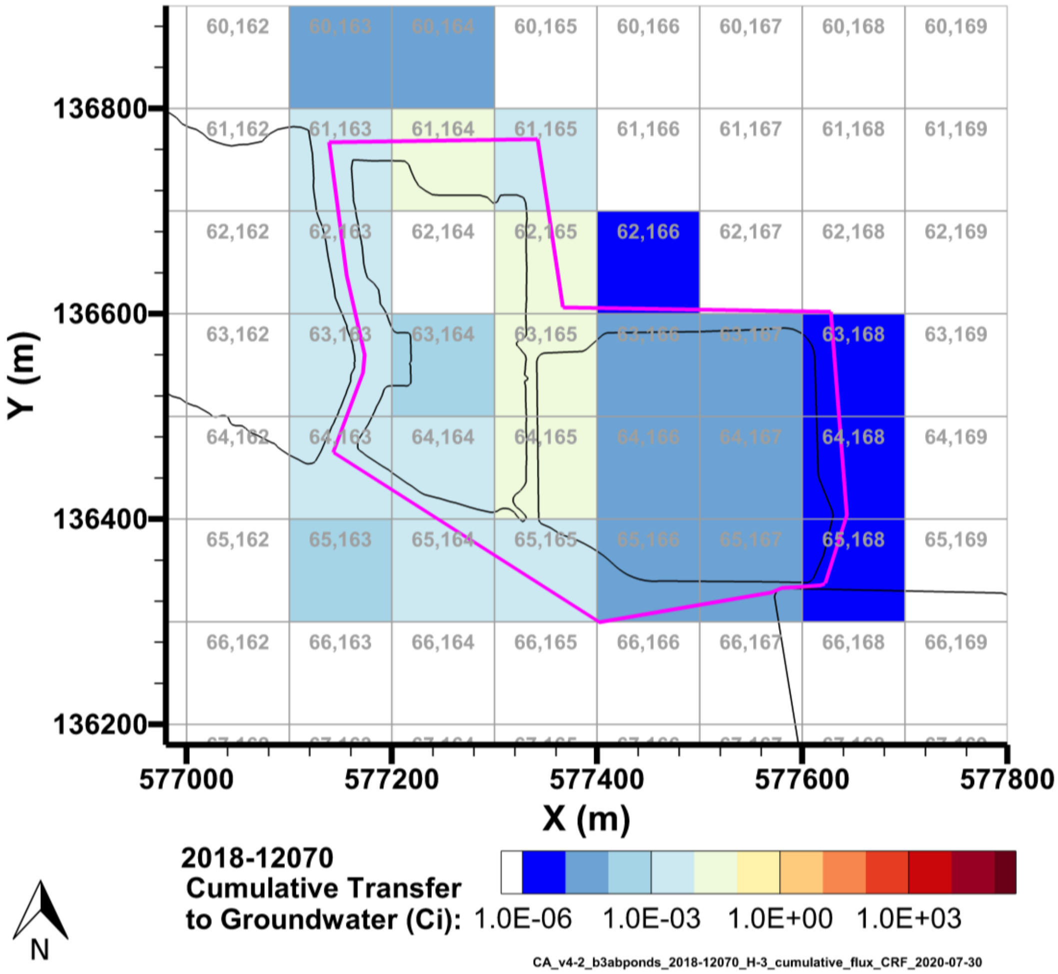

Note: source zone outlined in pink.

Figure 7-6. Cumulative H-3 Activity Discharged to Groundwater from the B-3A/B Ponds Model from 2018–12070 per P2R Grid Cell

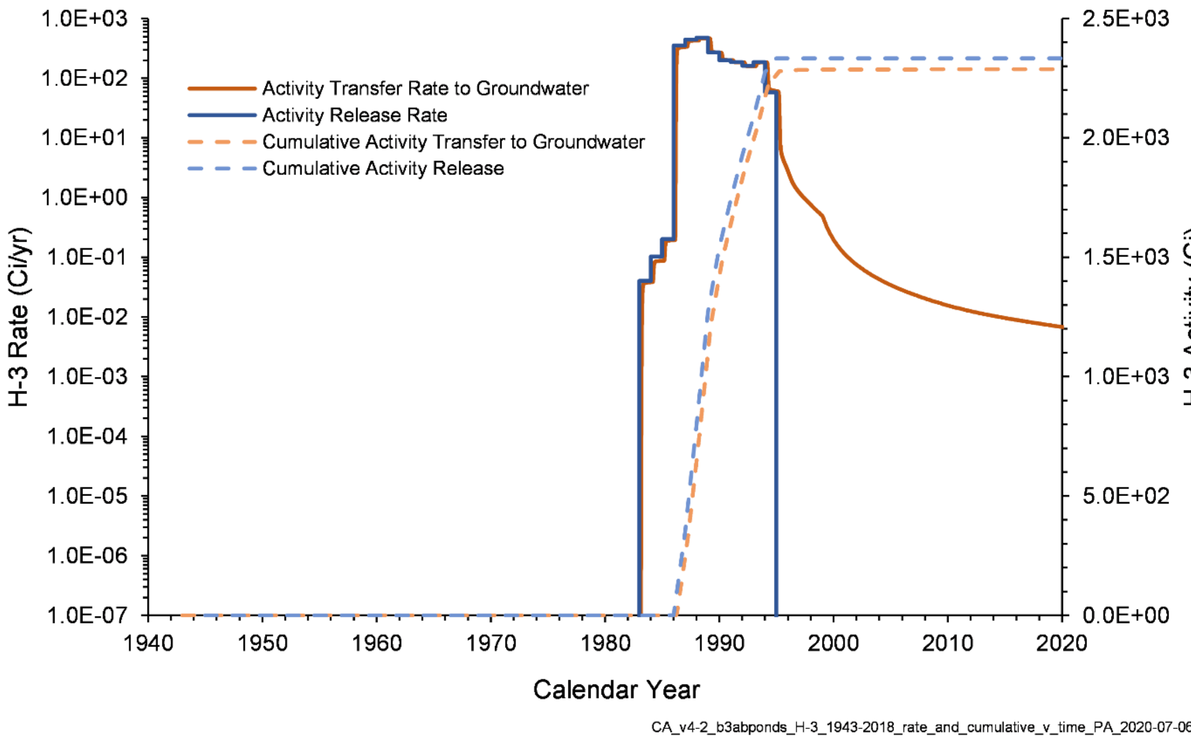

Figure 7-7. H-3 Inventory Release from Waste Sites and Transfer to Groundwater for the B-3A/B Ponds Model from 1943–2018

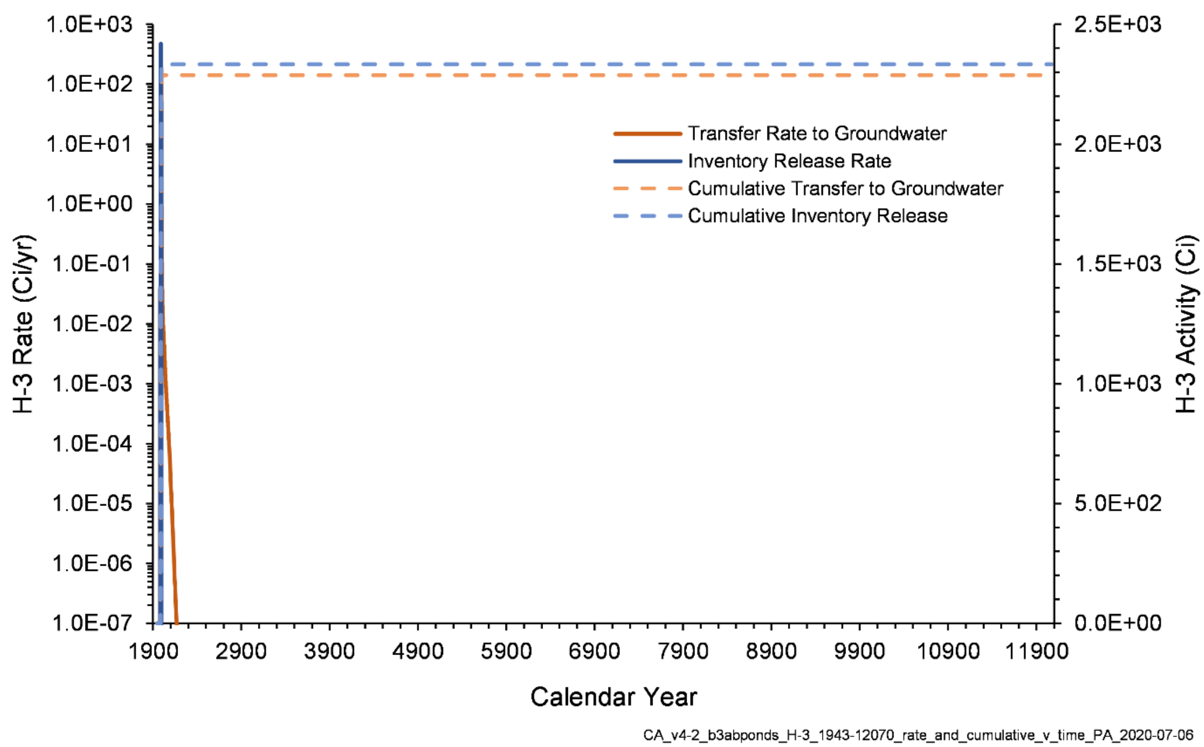

Figure 7-8. H-3 Inventory Release from Waste Sites and Transfer to Groundwater for the B-3A/B Ponds Model from 1943–12070

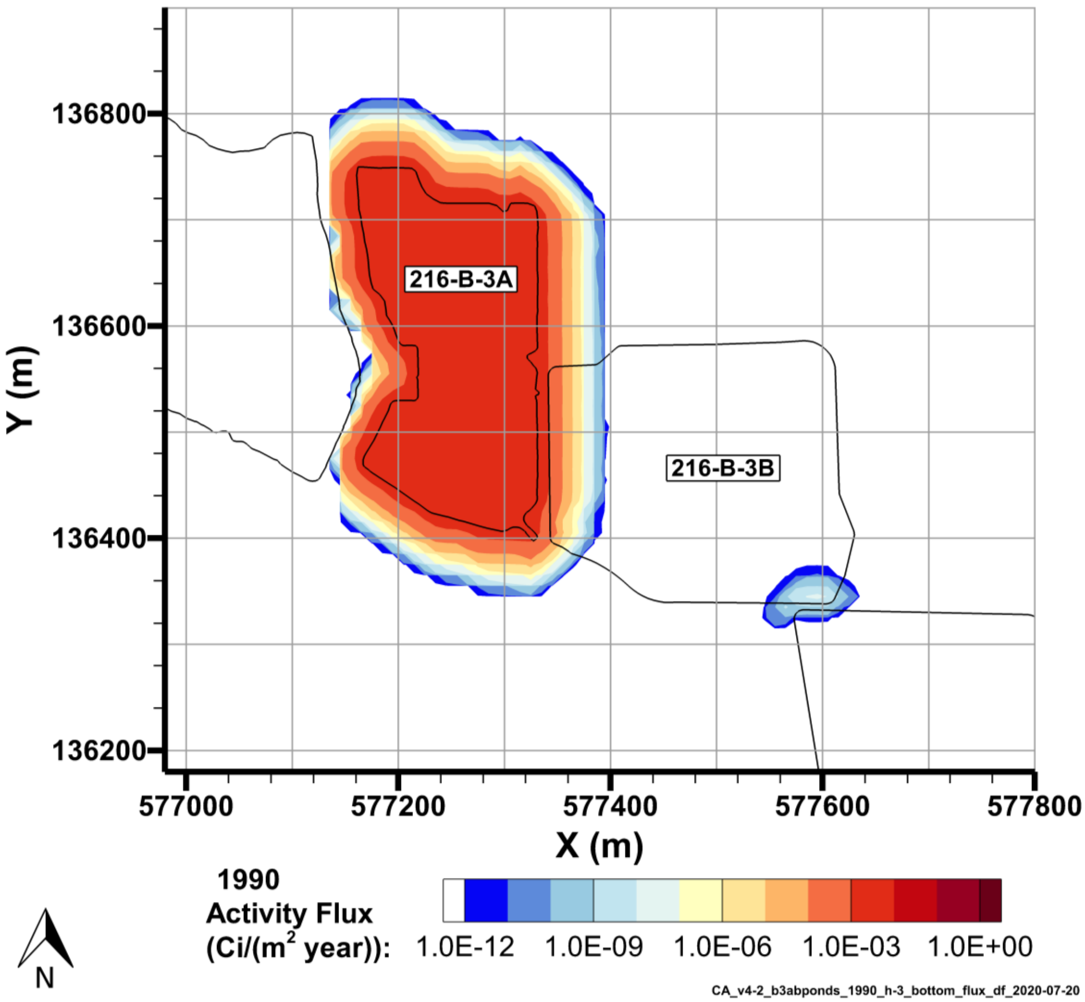

Figure 7-9. H-3 Flux to Groundwater, 1990

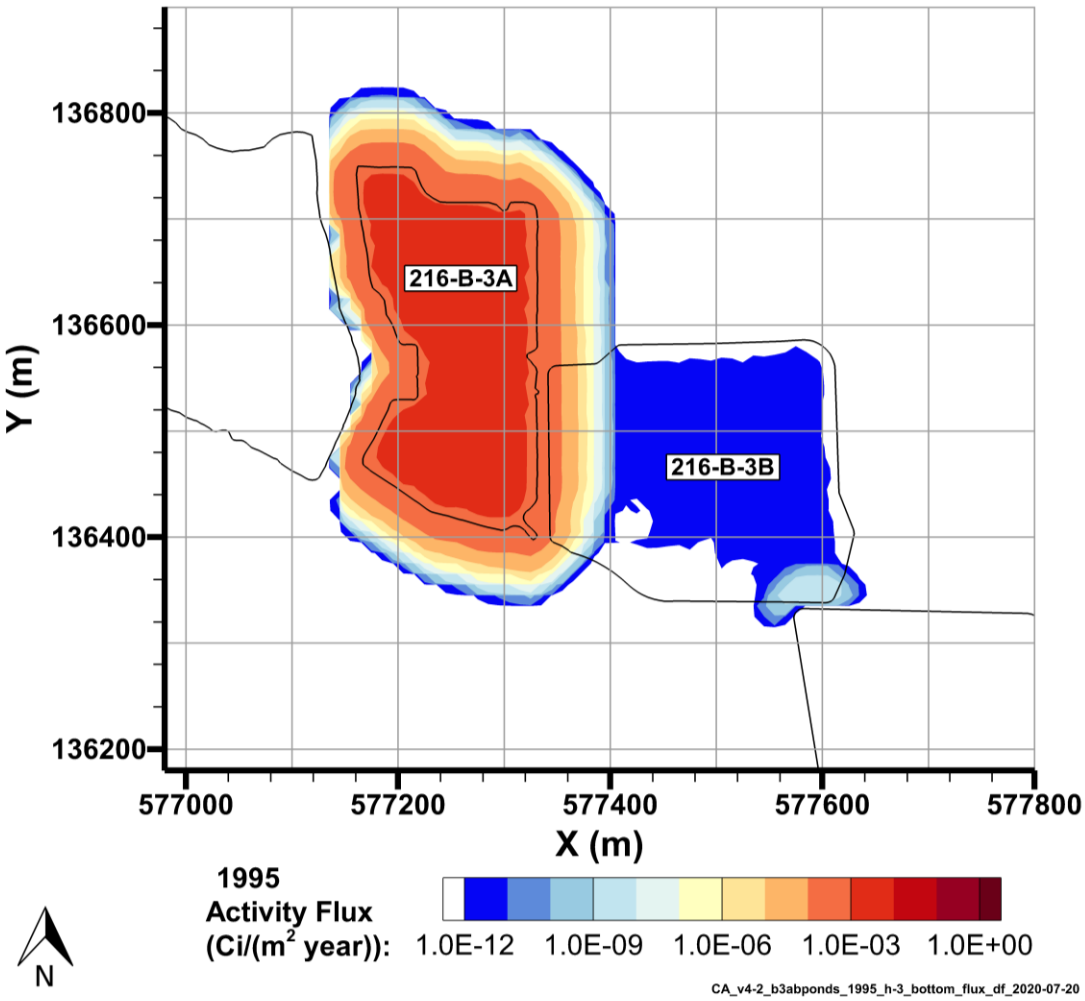

Figure 7-10. H-3 Flux to Groundwater, 1995

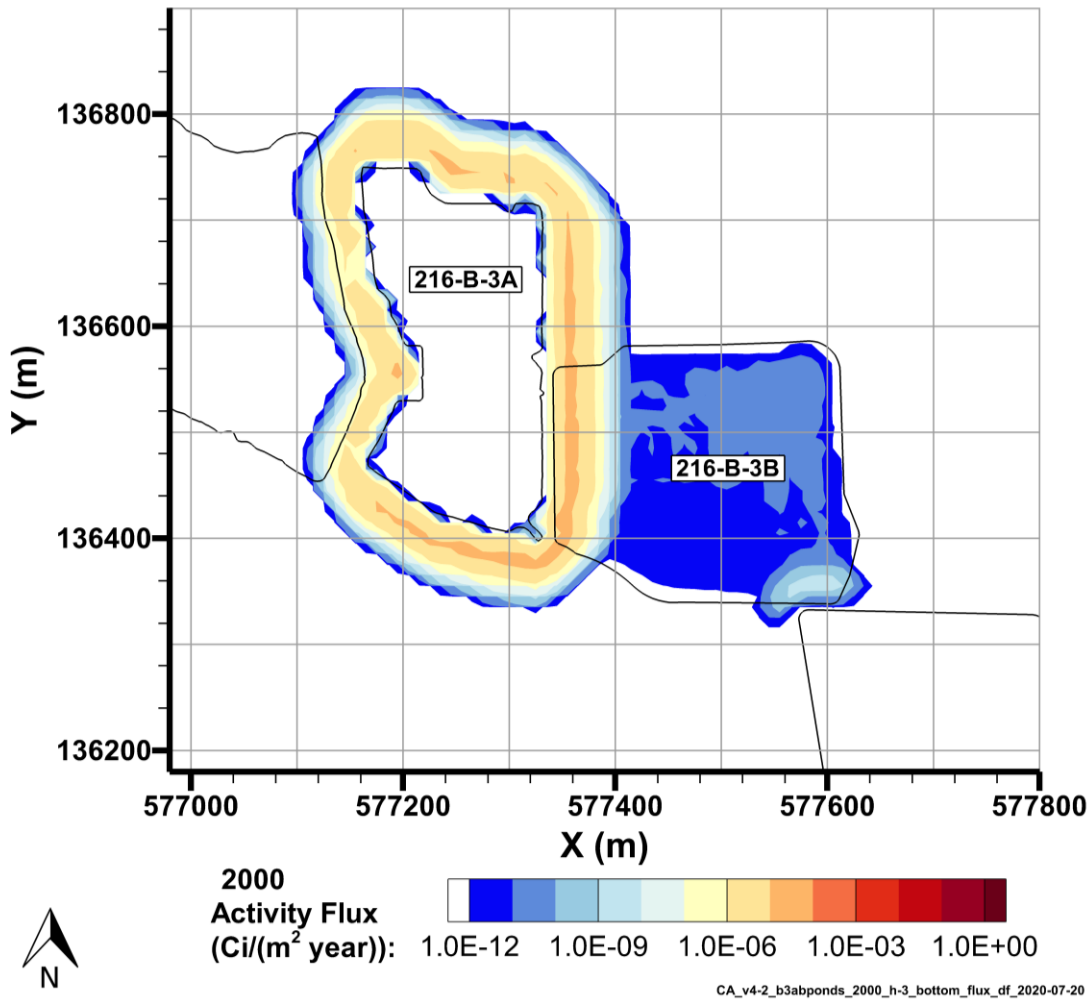

Figure 7-11. H-3 Flux to Groundwater, 2000

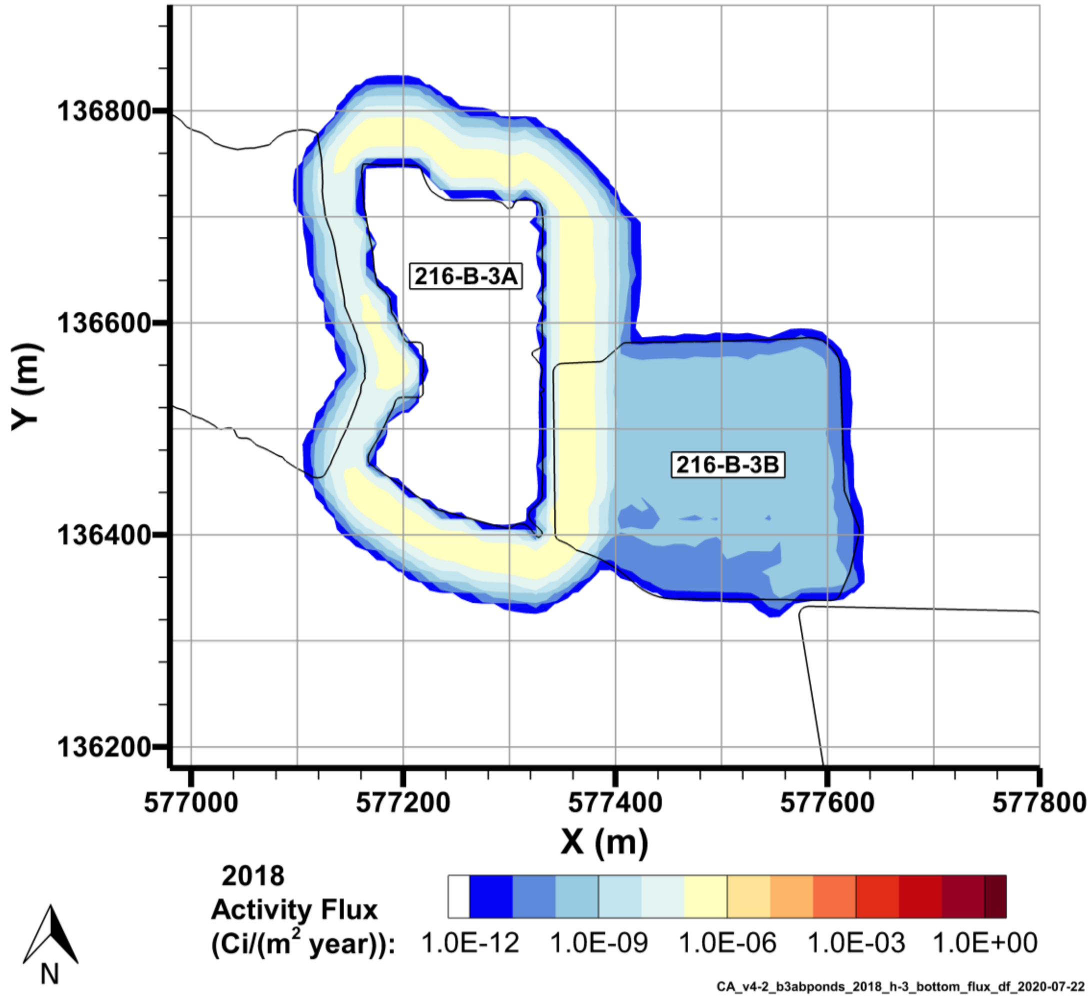

Figure 7-12. H-3 Flux to Groundwater, 2018

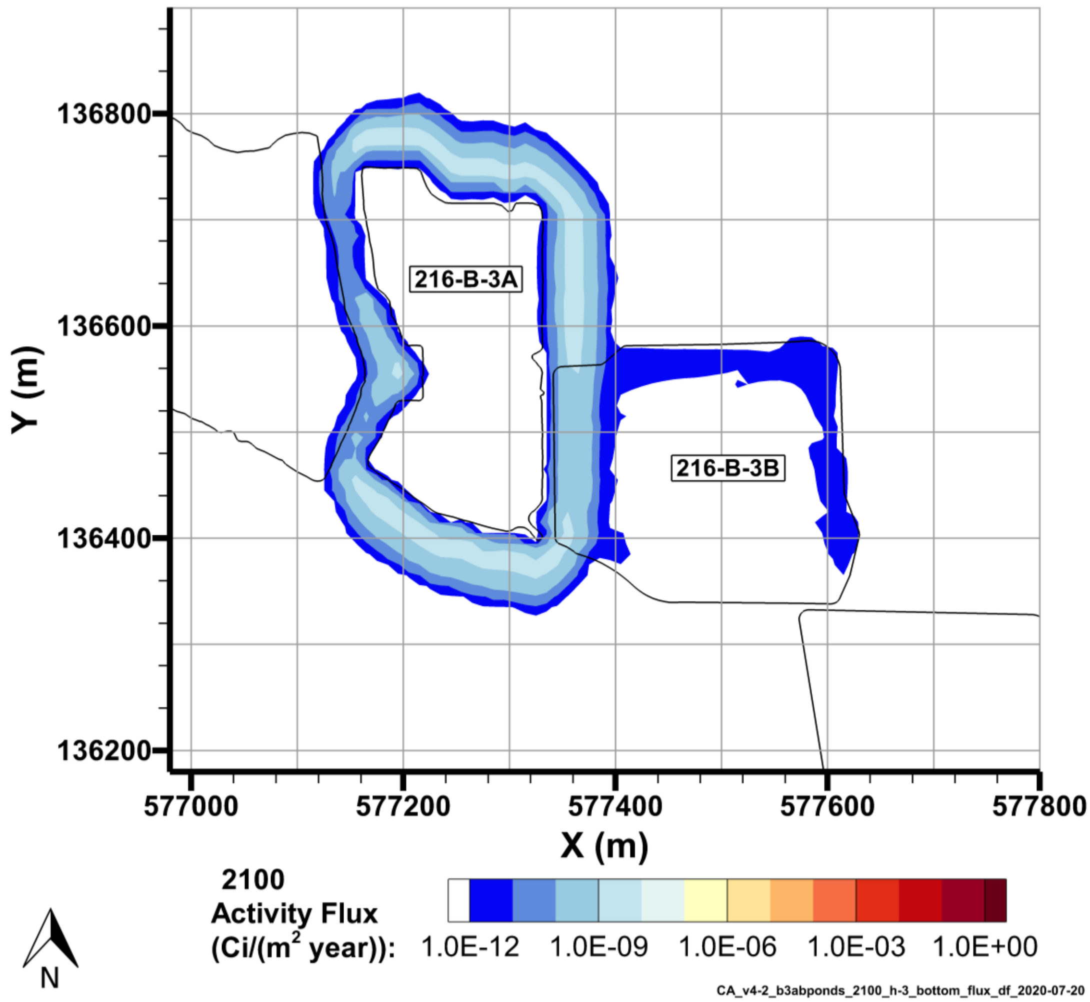

Figure 7-13. H-3 Flux to Groundwater, 2100

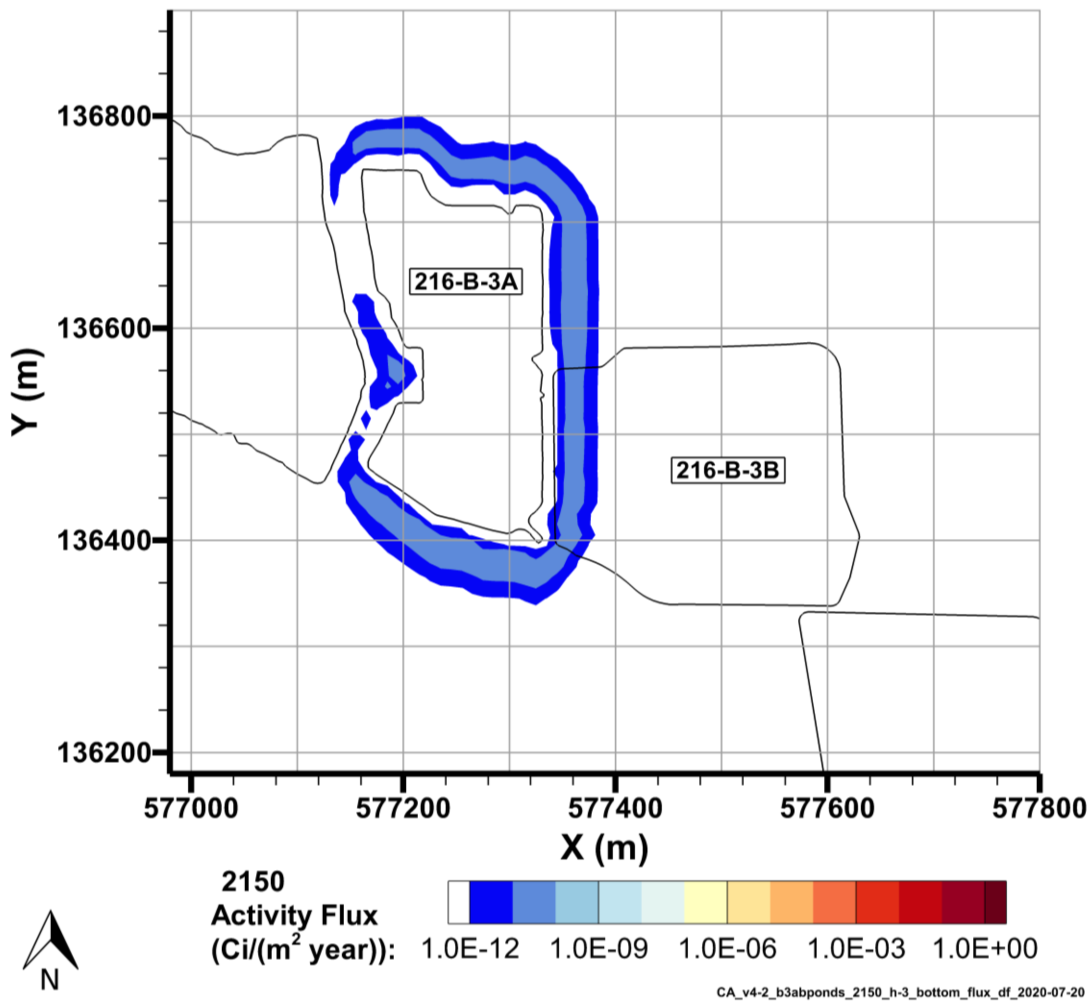

Figure 7-14. H-3 Flux to Groundwater, 2150

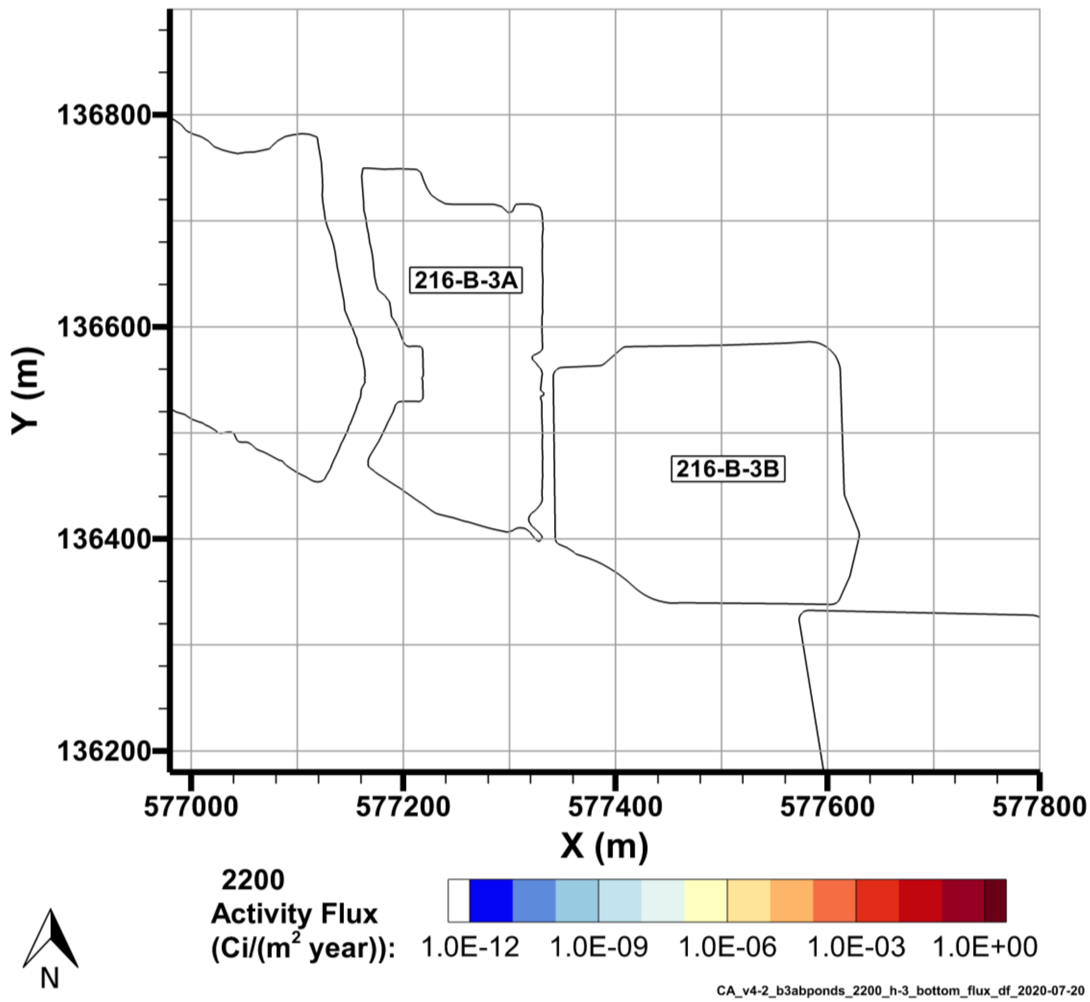

Figure 7-15. H-3 Flux to Groundwater, 2200

7.4 I-129 Fate and Transport Results

This model simulated release and transport of I-129. The cumulative discharge of I-129 into groundwater is shown aggregated by P2R grid cell in Figure 7-16 for 1943–2018. No I-129 was released into groundwater at a cumulative activity above 1.0E-6 Ci per P2R grid cell from 2018–12070. The inventory released to the B-3A/B Ponds model and the transfer of I-129 to groundwater are shown from 1943–2018 in Figure 7-17 and from 1943–12070 in Figure 7-18.

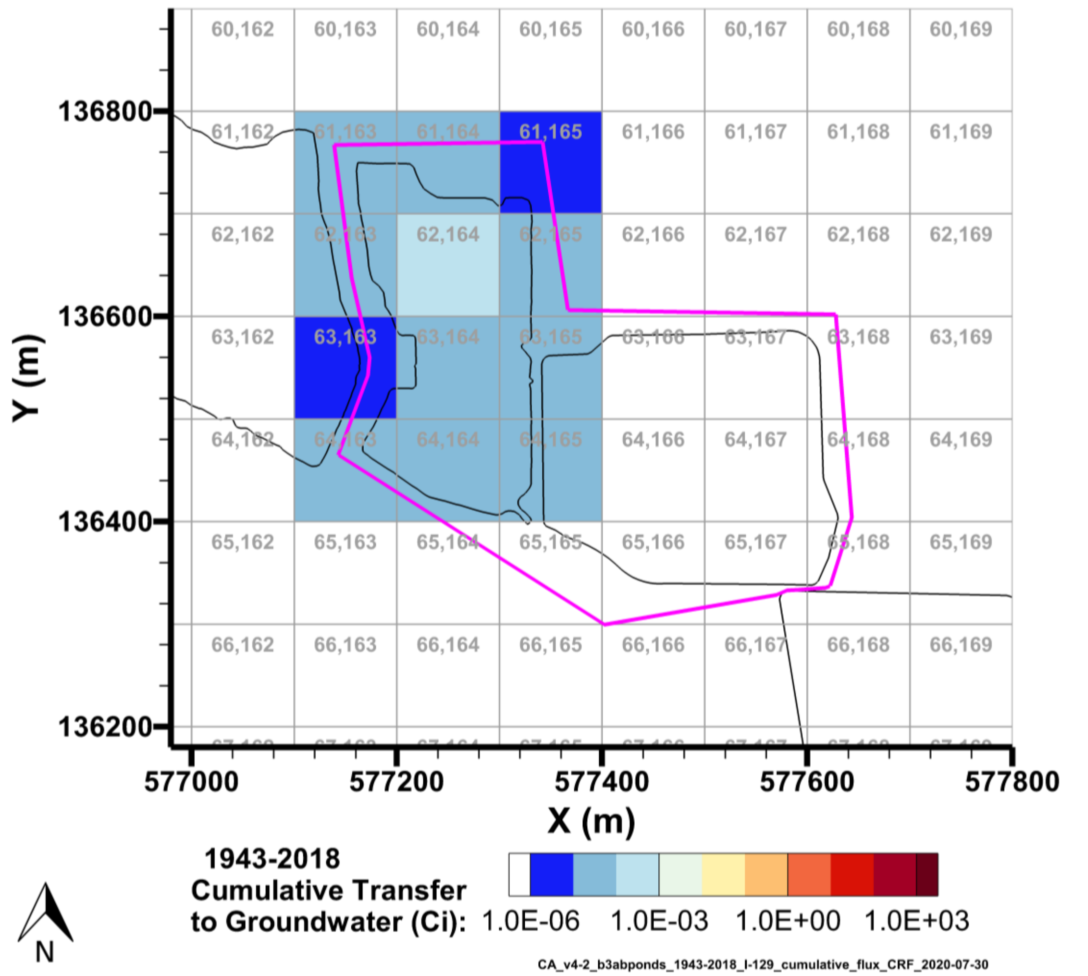

Note: source zone outlined in pink.

Figure 7-16. Cumulative I-129 Activity Discharged to Groundwater from the B-3A/B Ponds Model from 1943–2018 per P2R Grid Cell

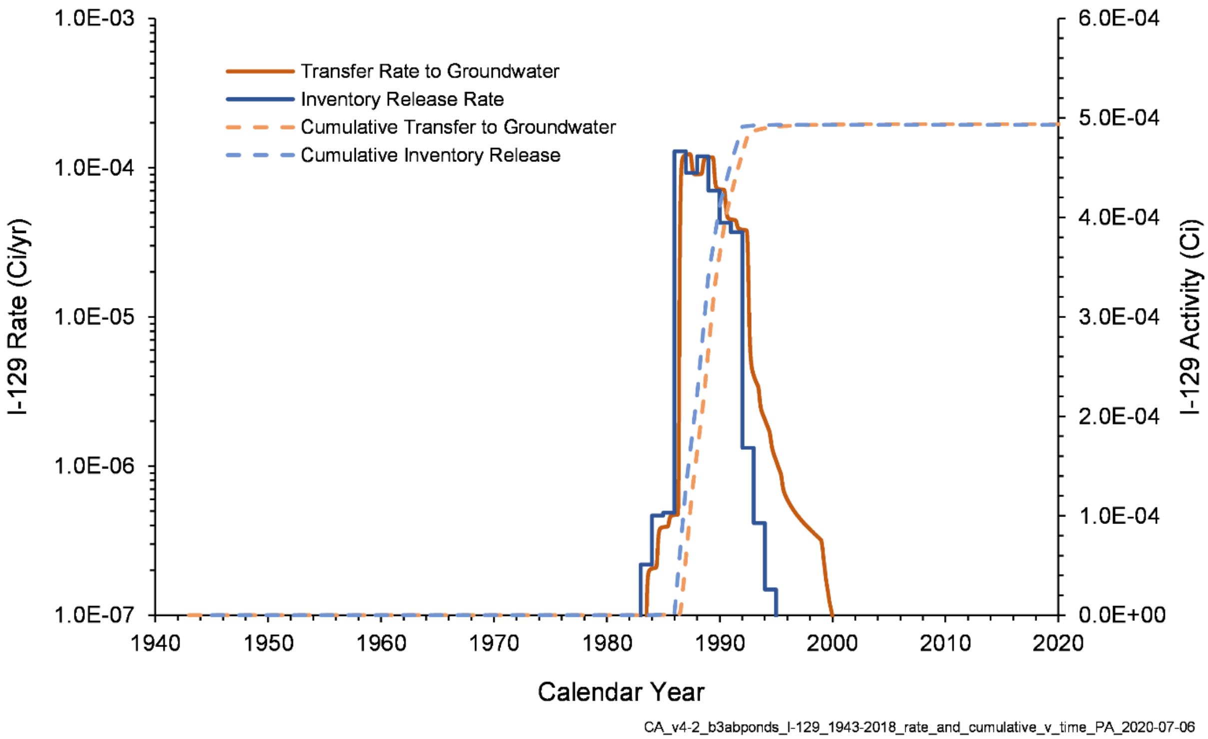

Figure 7-17. I-129 Inventory Release from Waste Sites and Transfer to Groundwater for the B-3A/B Ponds Model from 1943–2018

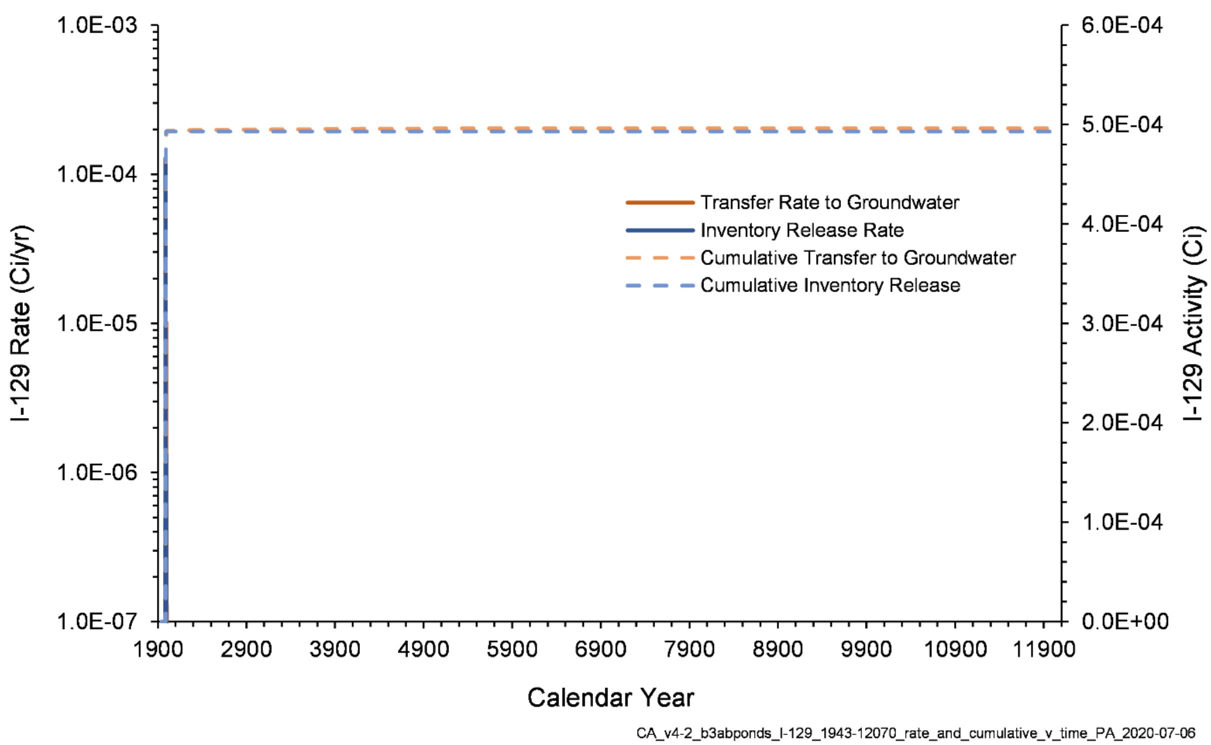

Figure 7-18. I-129 Inventory Release from Waste Sites and Transfer to Groundwater for the B-3A/B Ponds Model from 1943–12070

7.5 Np-237 Fate and Transport Results

This model simulated the release and transport of Np-237. The cumulative discharge of Np-237 into groundwater is shown aggregated by P2R grid cell in Figure 7-19 and Figure 7-20 for 1943–2018 and 2018–12070, respectively. The inventory released to the B-3A/B Ponds model and the transfer of Np-237 to groundwater are shown from 1943–2018 in Figure 7-21 and from 1943–12070 in Figure 7-22.

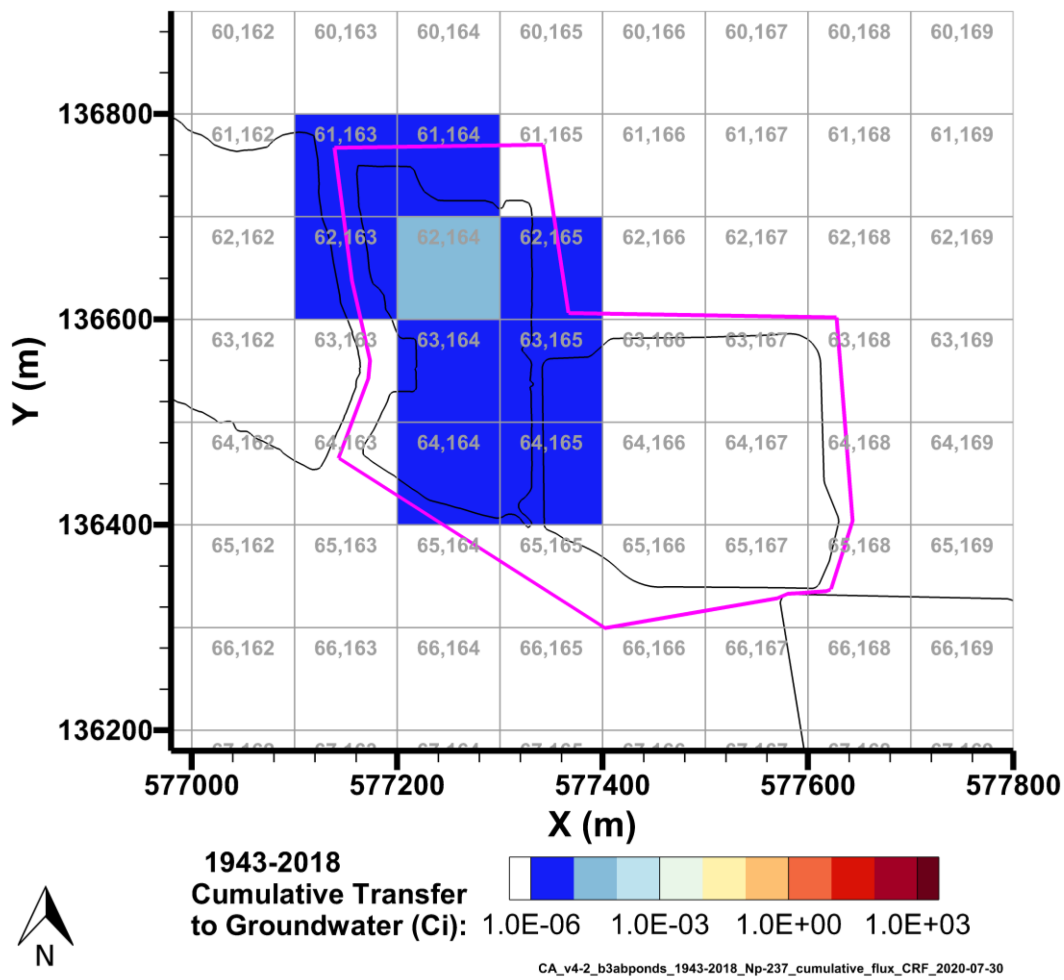

Note: source zone outlined in pink.

Figure 7-19. Cumulative Np-237 Activity Discharged to Groundwater from the B-3A/B Ponds Model from 1943–2018 per P2R Grid Cell

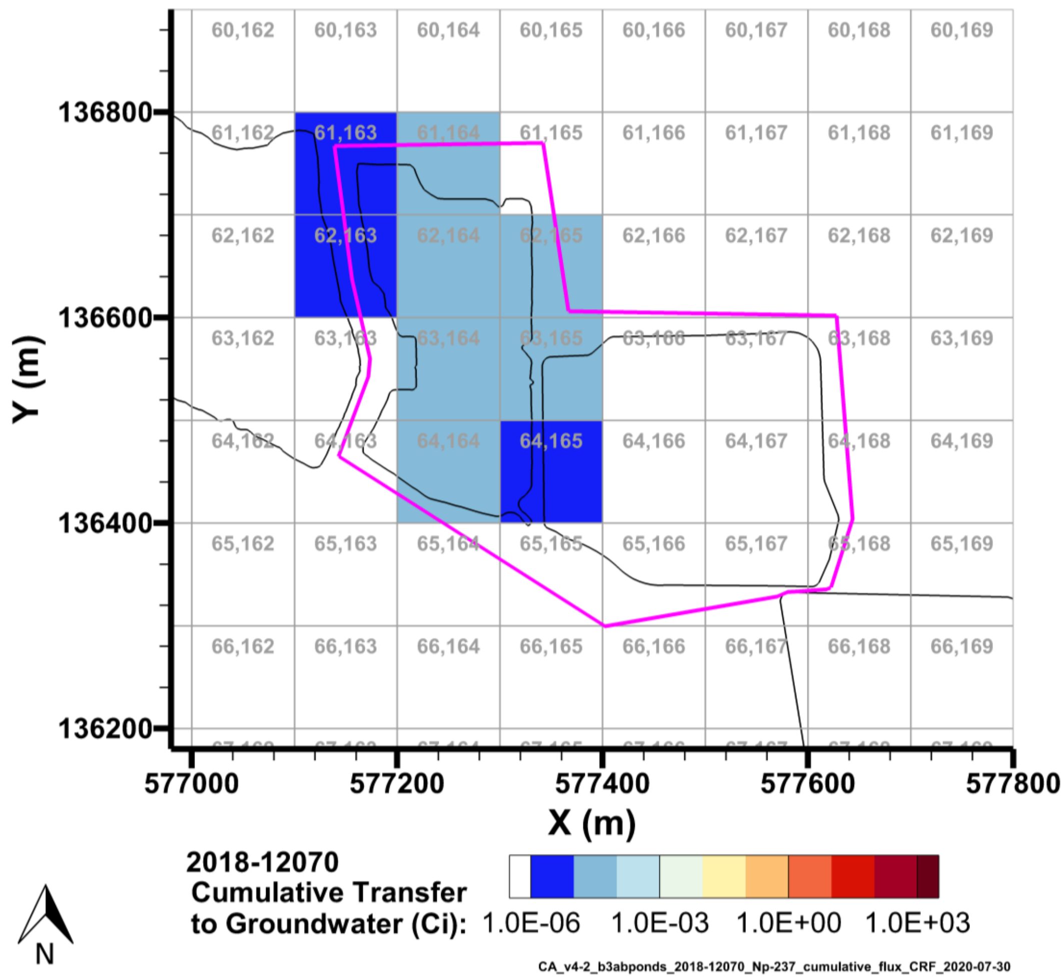

Note: source zone outlined in pink.

Figure 7-20. Cumulative Np-237 Activity Discharged to Groundwater from the B-3A/B Ponds Model from 2018–12070 per P2R Grid Cell

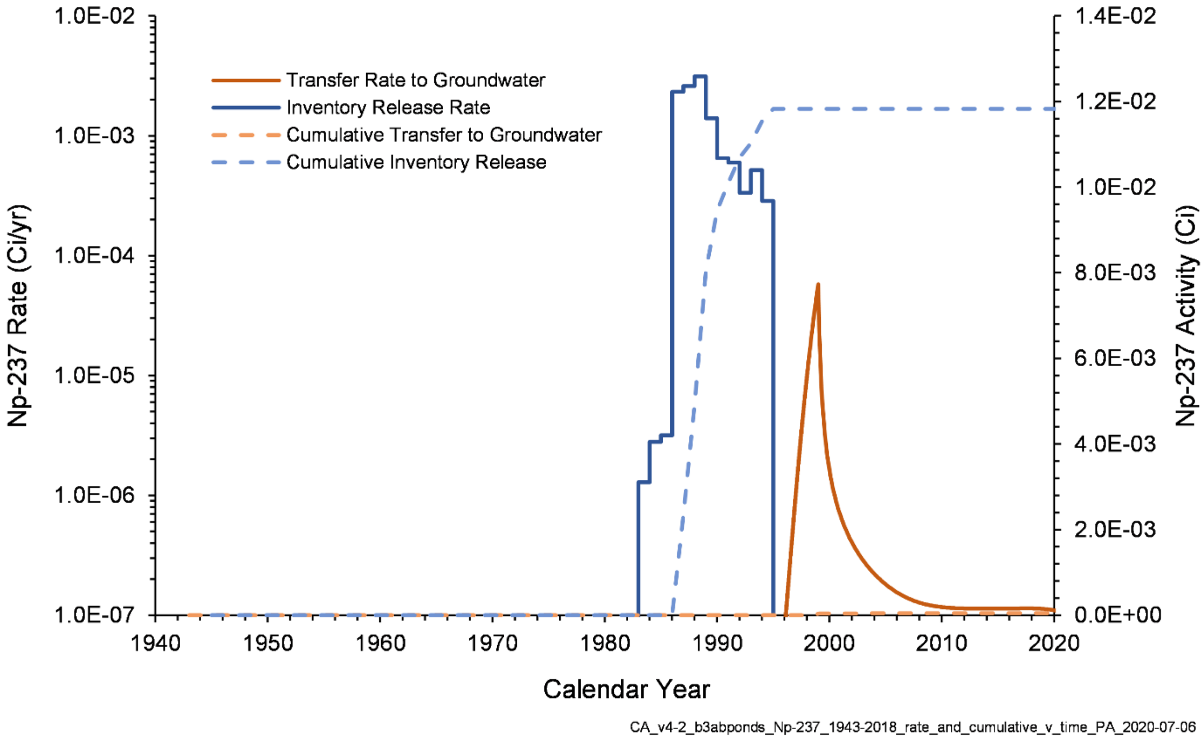

Figure 7-21. Np-237 Inventory Release from Waste Sites and Transfer to Groundwater for the B-3A/B Ponds Model from 1943–2018

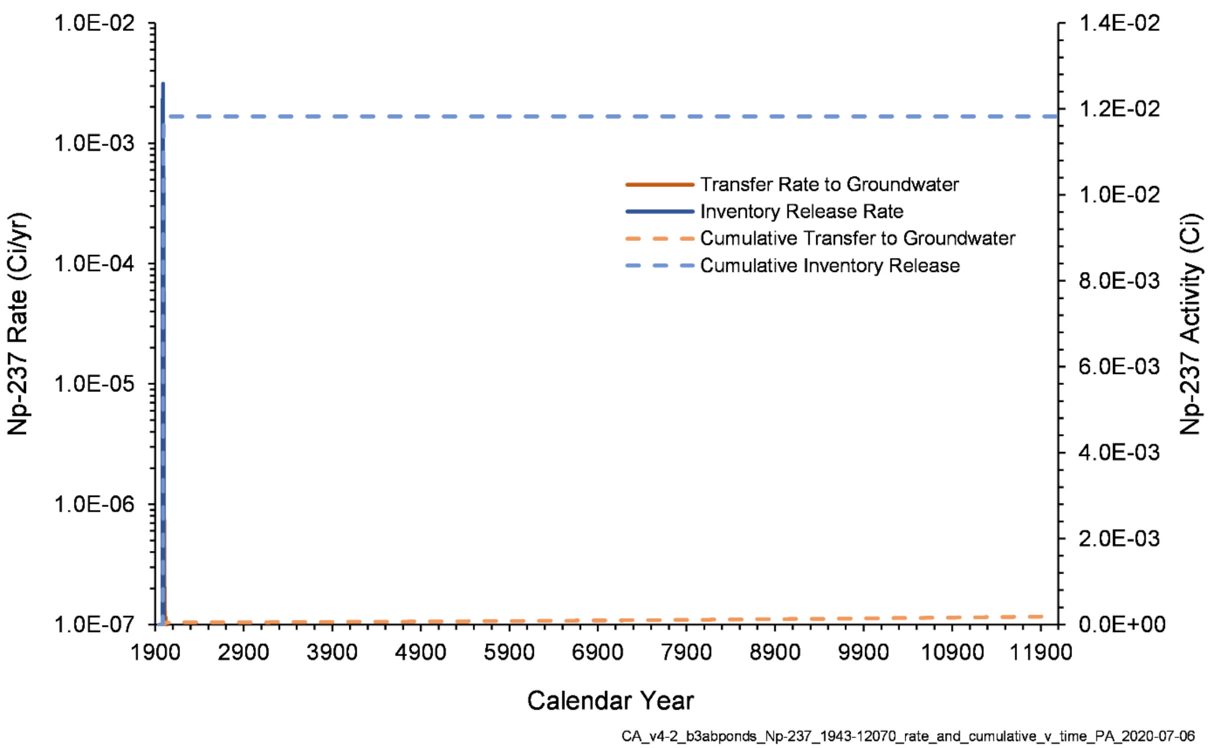

Figure 7-22. Np-237 Inventory Release from Waste Sites and Transfer to Groundwater for the B-3A/B Ponds Model from 1943–12070

7.6 Re-187 Fate and Transport Results

Due to a lack of inventory, transport of Re-187 was not calculated in this model.

7.7 Sr-90 Fate and Transport Results

This model simulated the release and transport of Sr-90. No Sr-90 was discharged to groundwater at a cumulative activity above 1.0E-6 Ci per P2R grid cell at any point during modeling. The inventory released to the B-3A/B Ponds model and the transfer of Sr-90 to groundwater are shown from 1943–2018 in Figure 7-23 and from 1943–12070 in Figure 7-24.

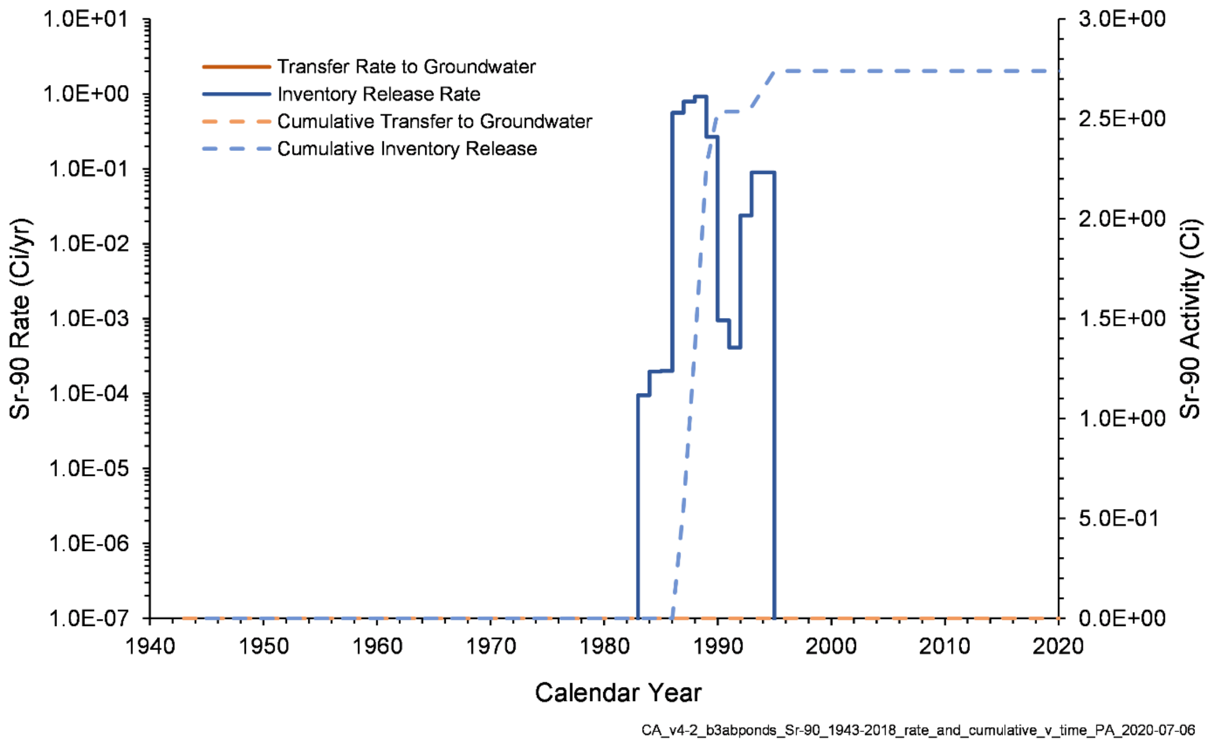

Figure 7-23. Sr-90 Inventory Release from Waste Sites and Transfer to Groundwater for the B-3A/B Ponds Model from 1943–2018

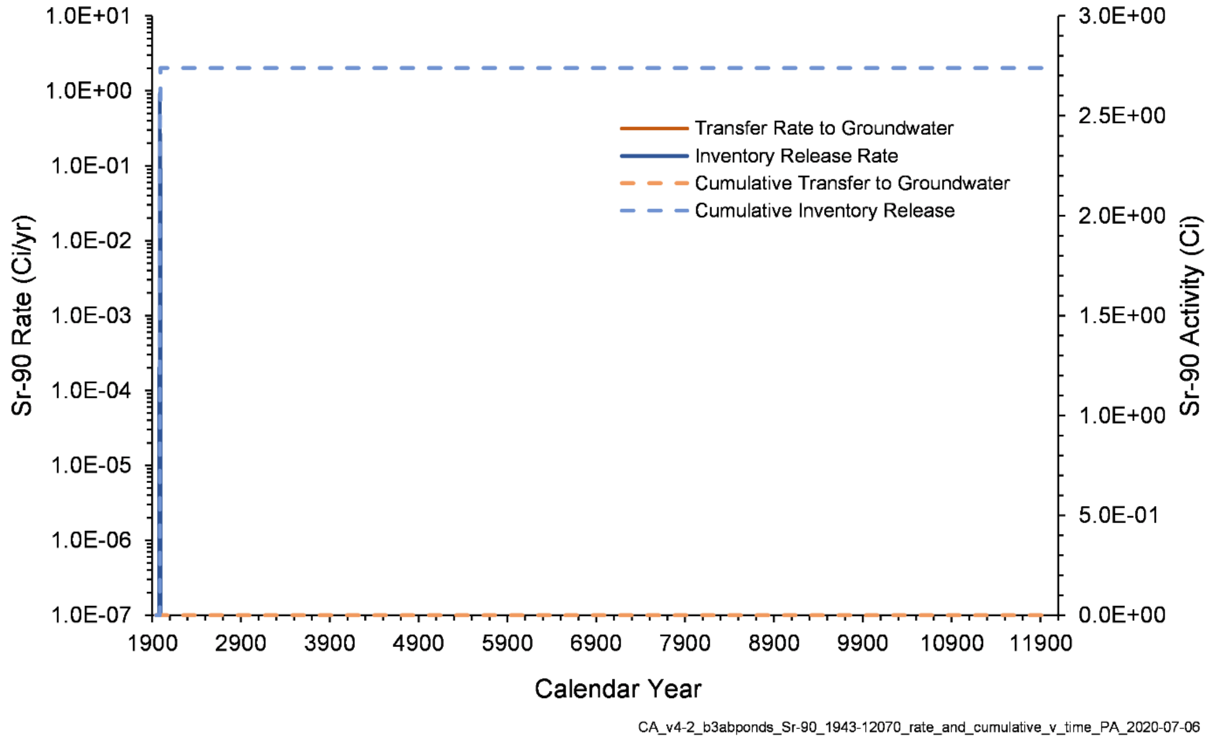

Figure 7-24. Sr-90 Inventory Release from Waste Sites and Transfer to Groundwater for the B-3A/B Ponds Model from 1943–12070

7.8 Tc-99 Fate and Transport Results

This model simulated release and transport of Tc-99. The cumulative discharge of Tc-99 into groundwater is shown aggregated by P2R grid cell in Figure 7-25 and Figure 7-26 for 1943–2018 and 2018–12070, respectively. The inventory released to the B-3A/B Ponds model and the transfer of Tc-99 to groundwater are shown from 1943–2018 in Figure 7-27 and from 1943–12070 in Figure 7-28.

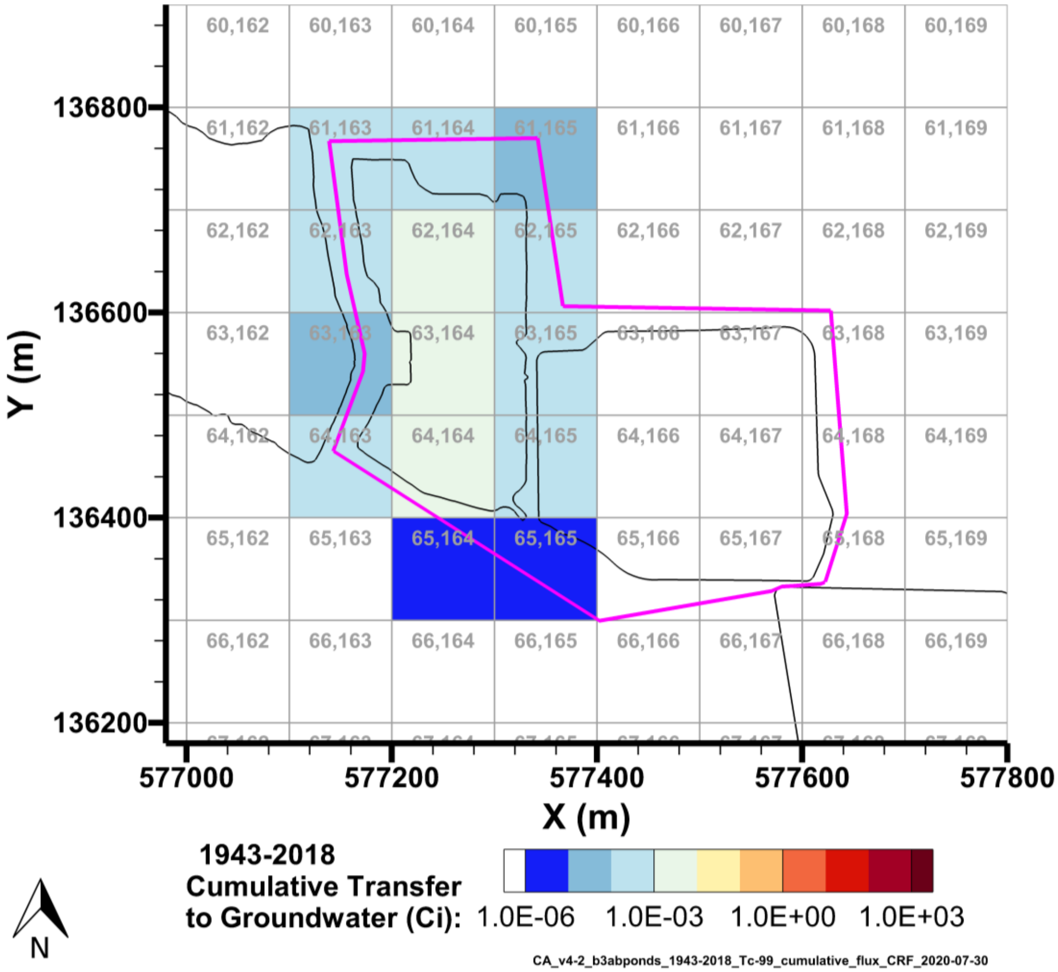

Note: source zone outlined in pink.

Figure 7-25. Cumulative Tc-99 Activity Discharged to Groundwater from the B-3A/B Ponds Model from 1943–2018 per P2R Grid Cell

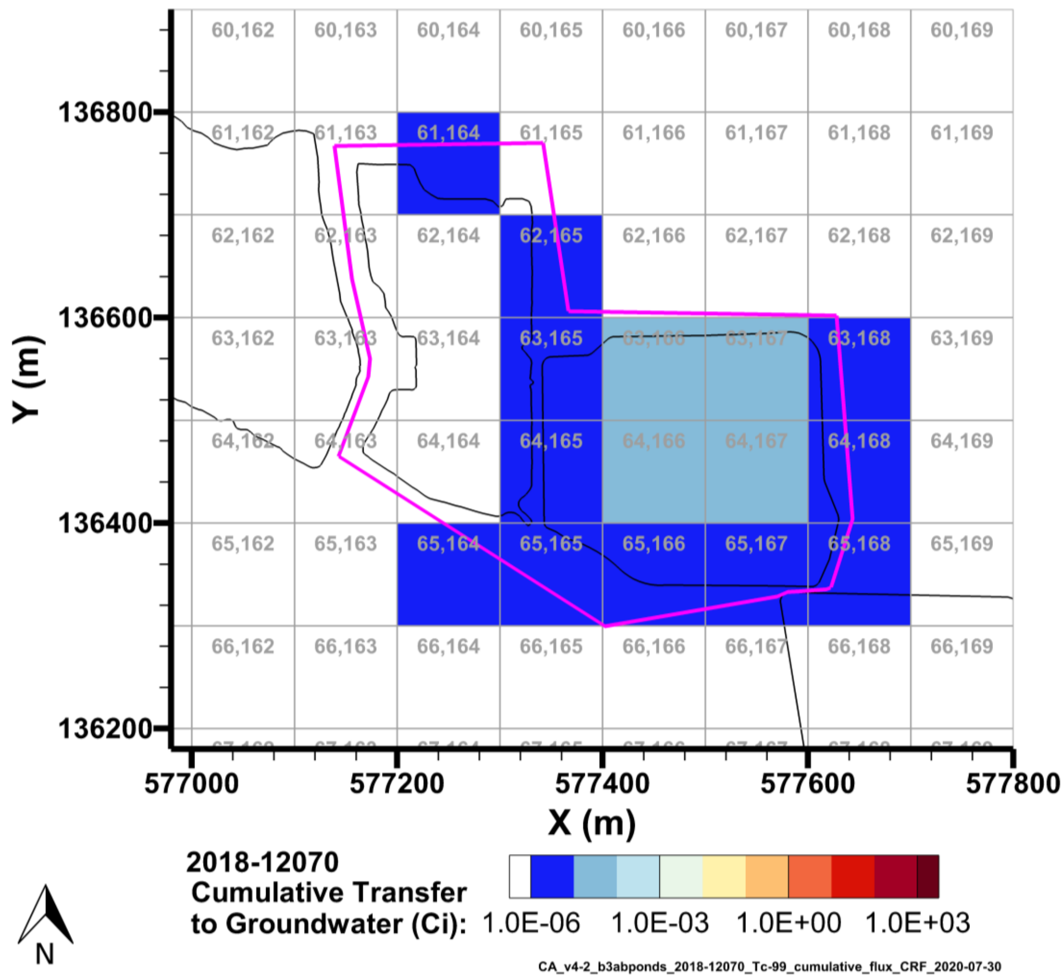

Note: source zone outlined in pink.

Figure 7-26. Cumulative Tc-99 Activity Discharged to Groundwater from the B-3A/B Ponds Model from 2018–12070 per P2R Grid Cell

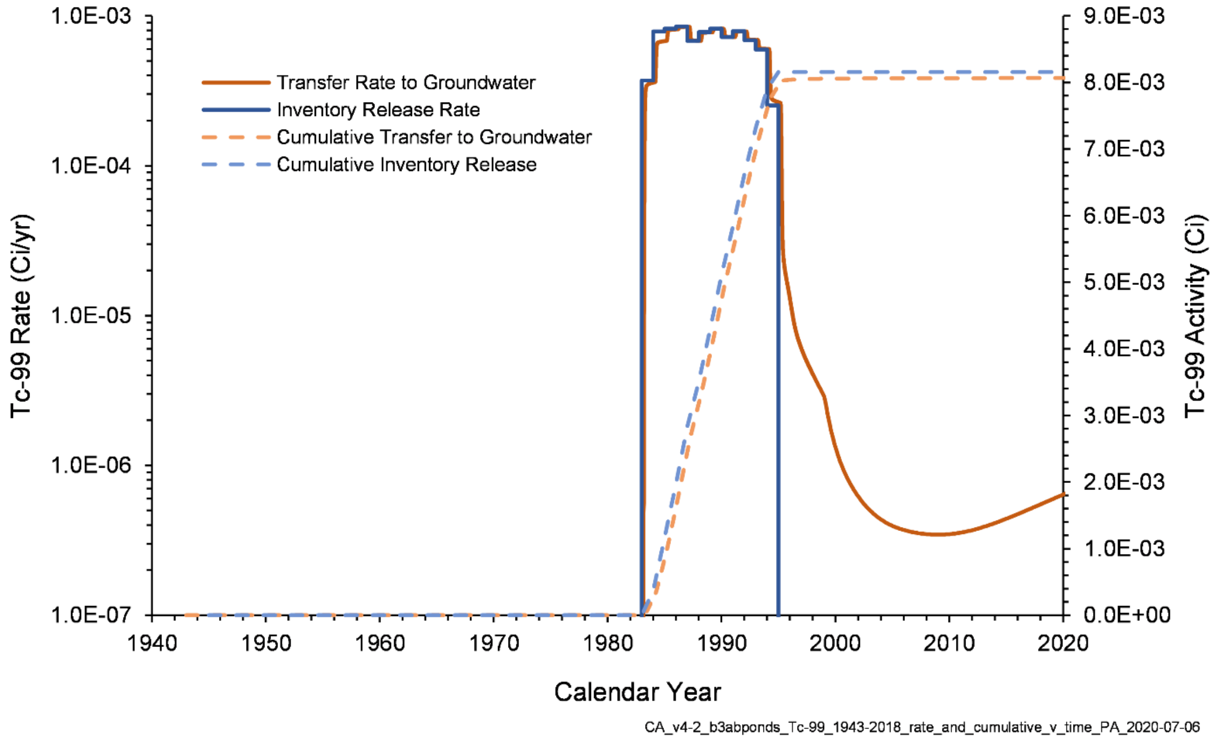

Figure 7-27. Tc-99 Inventory Release from Waste Sites and Transfer to Groundwater for the B-3A/B Ponds Model from 1943–2018

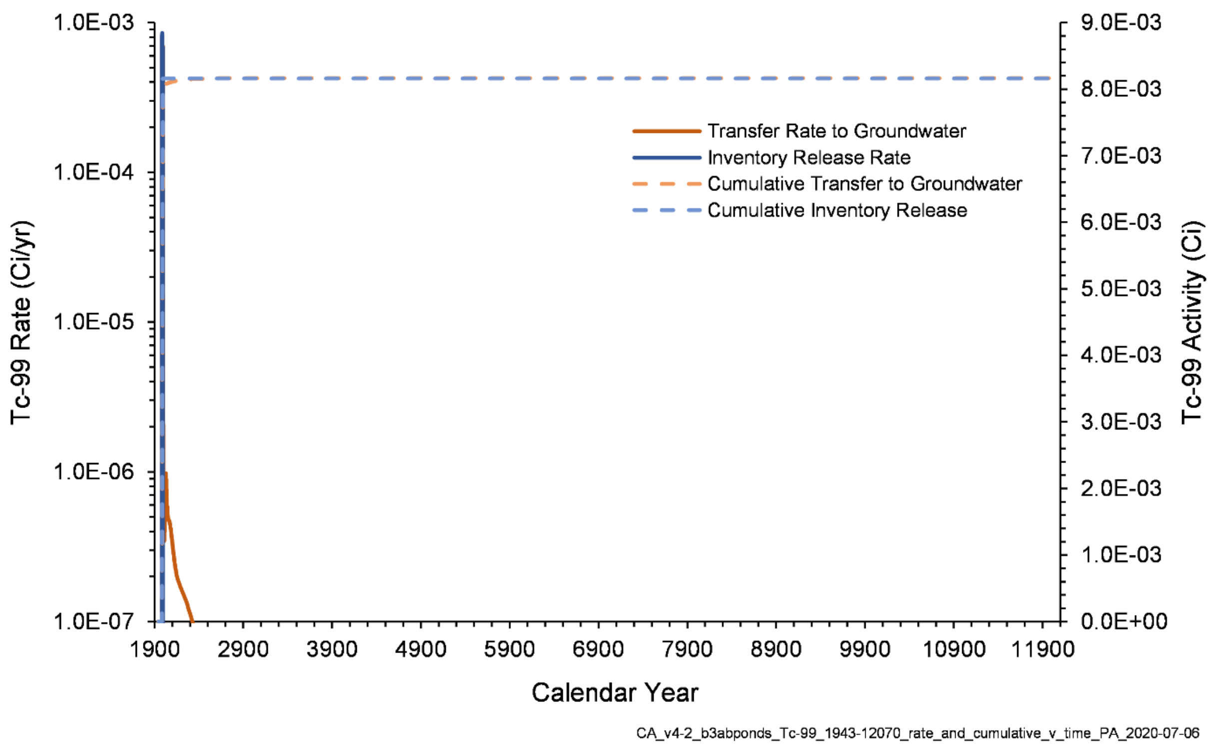

Figure 7-28. Tc-99 Inventory Release from Waste Sites and Transfer to Groundwater for the B-3A/B Ponds Model from 1943–12070

7.9 U-232 Fate and Transport Results

This model simulated the release and transport of U-232. The cumulative discharge of U-232 into groundwater is shown aggregated by P2R grid cell in Figure 7-29 for 1943–2018. No U-232 was discharged to groundwater at a cumulative activity above 1.0E-6 Ci per P2R grid cell from 2018–12070. The inventory released to the B-3A/B Ponds model and the transfer of U-232 to groundwater are shown from 1943–2018 in Figure 7-30 and from 1943–12070 in Figure 7-31.

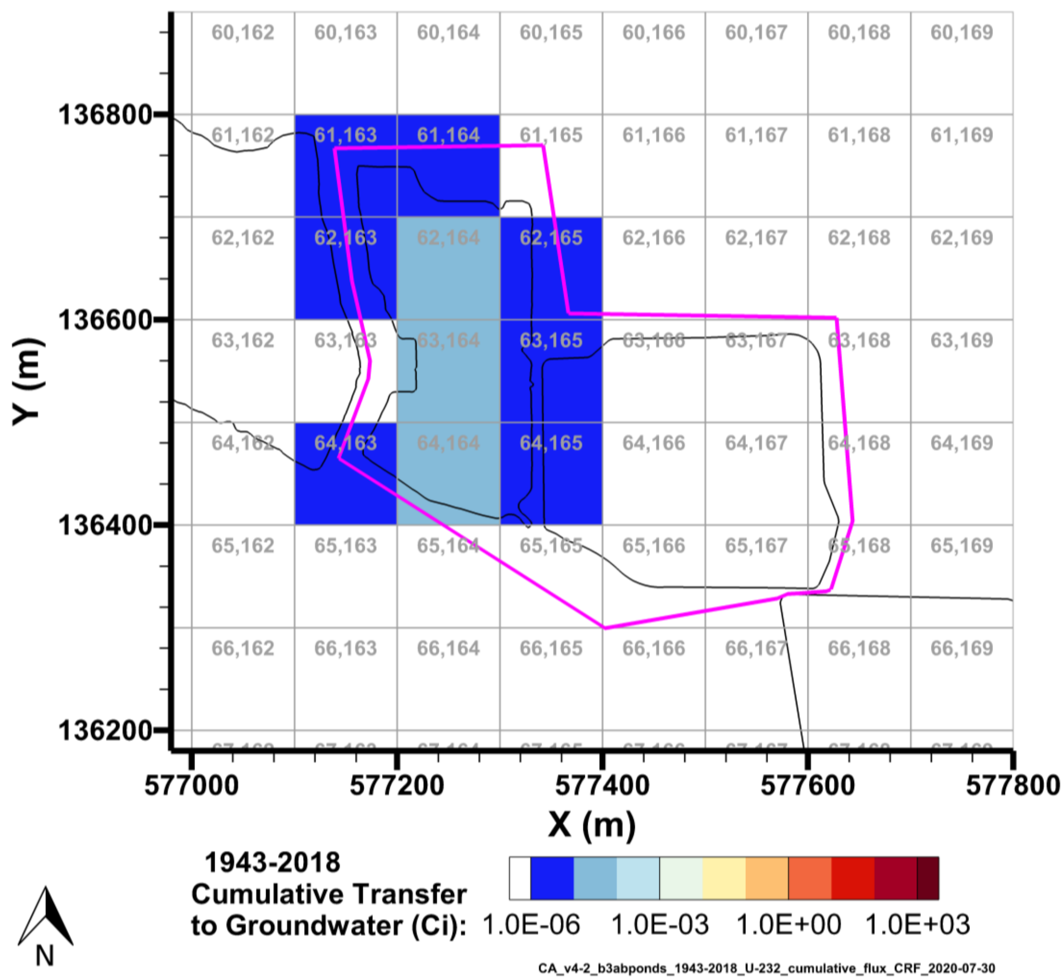

Note: source zone outlined in pink.

Figure 7-29. Cumulative U-232 Activity Discharged to Groundwater from the B-3A/B Ponds Model from 1943–2018 per P2R Grid Cell

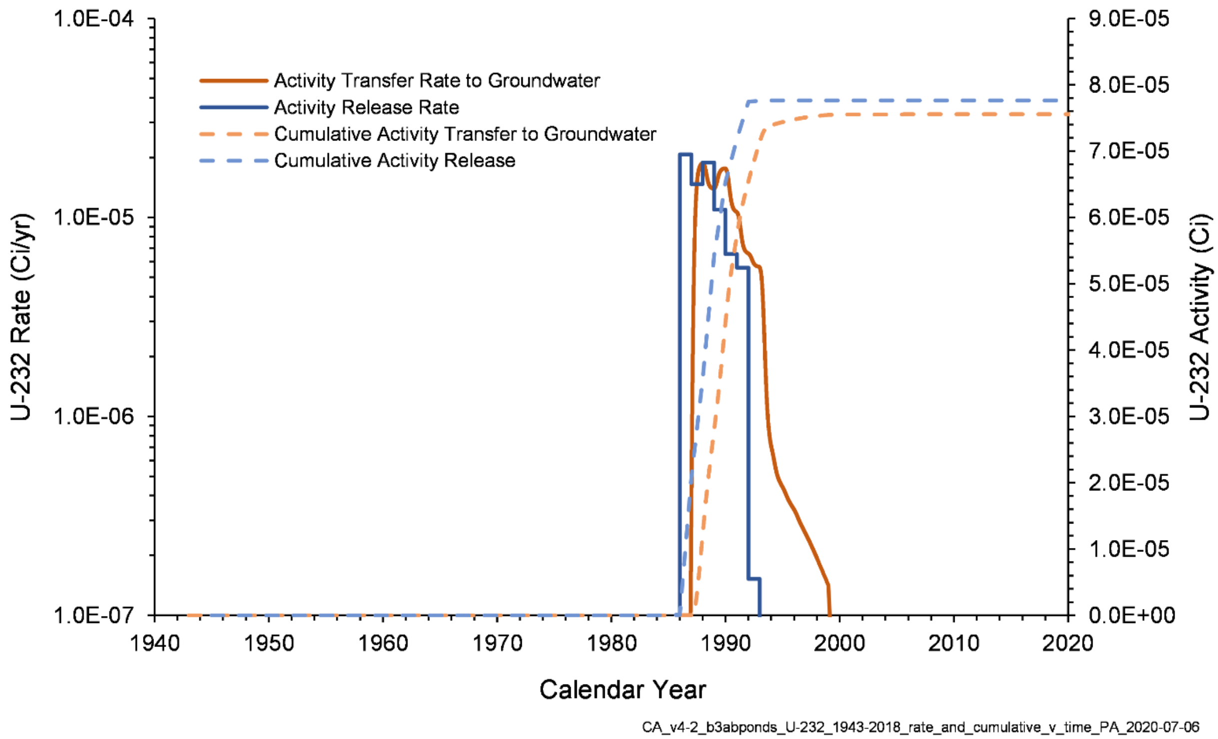

Figure 7-30. U-232 Inventory Release from Waste Sites and Transfer to Groundwater for the B-3A/B Ponds Model from 1943–2018

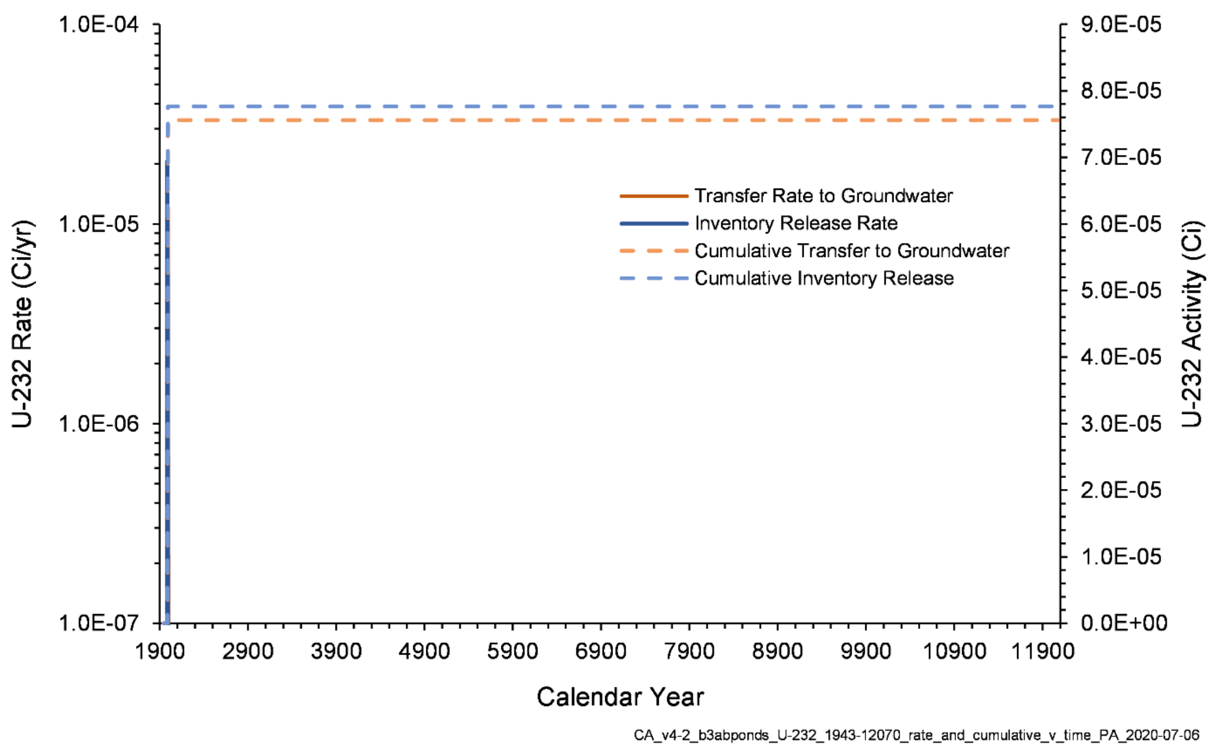

Figure 7-31. U-232 Inventory Release from Waste Sites and Transfer to Groundwater for the B-3A/B Ponds Model from 1943–12070

7.10 U-233 Fate and Transport Results

This model simulated the release and transport of U-233. The cumulative discharge of U-233 into groundwater is shown aggregated by P2R grid cell in Figure 7-32 for 1943–2018. No U-233 was discharged to groundwater at a cumulative activity above 1.0E-6 Ci per P2R grid cell from 2018–12070. The inventory released to the B-3A/B Ponds model and the transfer of U-233 to groundwater are shown from 1943–2018 in Figure 7-33 and from 1943–12070 in Figure 7-34.

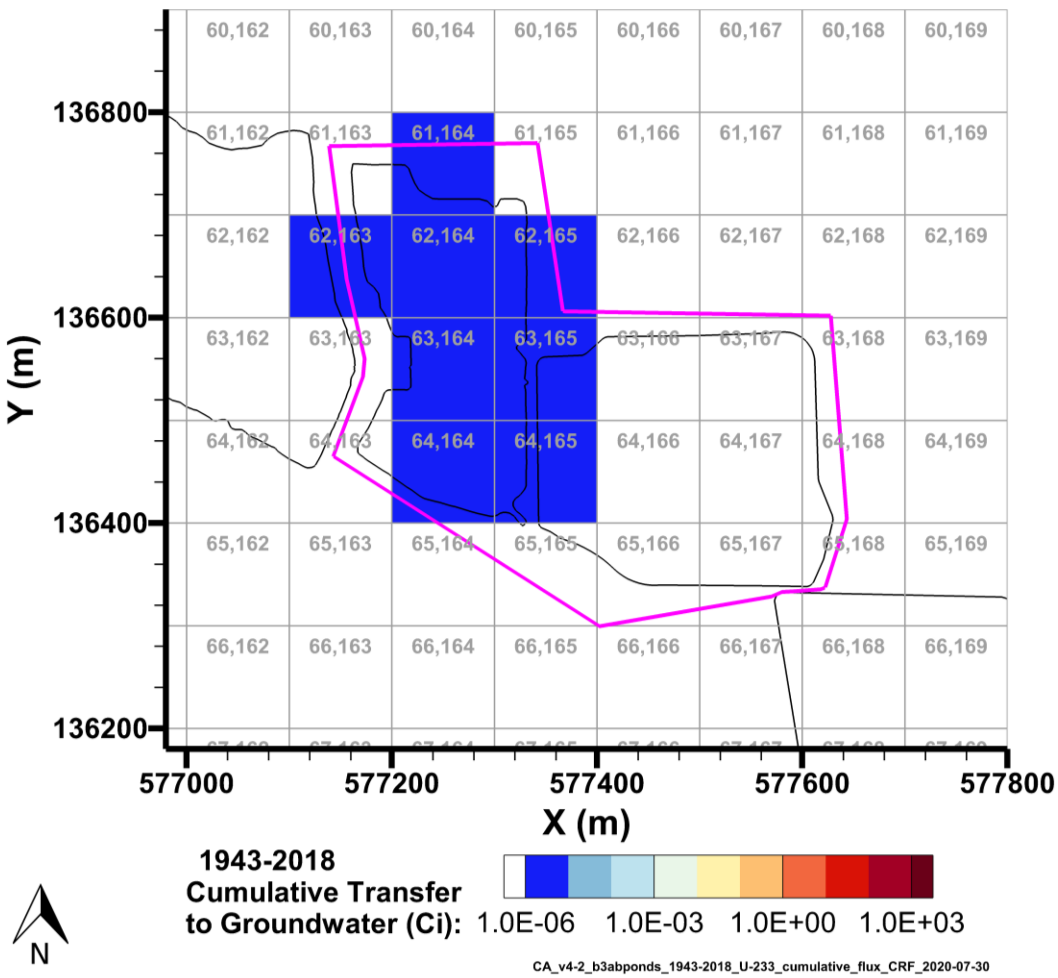

Note: source zone outlined in pink.

Figure 7-32. Cumulative U-233 Activity Discharged to Groundwater from the B-3A/B Ponds Model from 1943–2018 per P2R Grid Cell

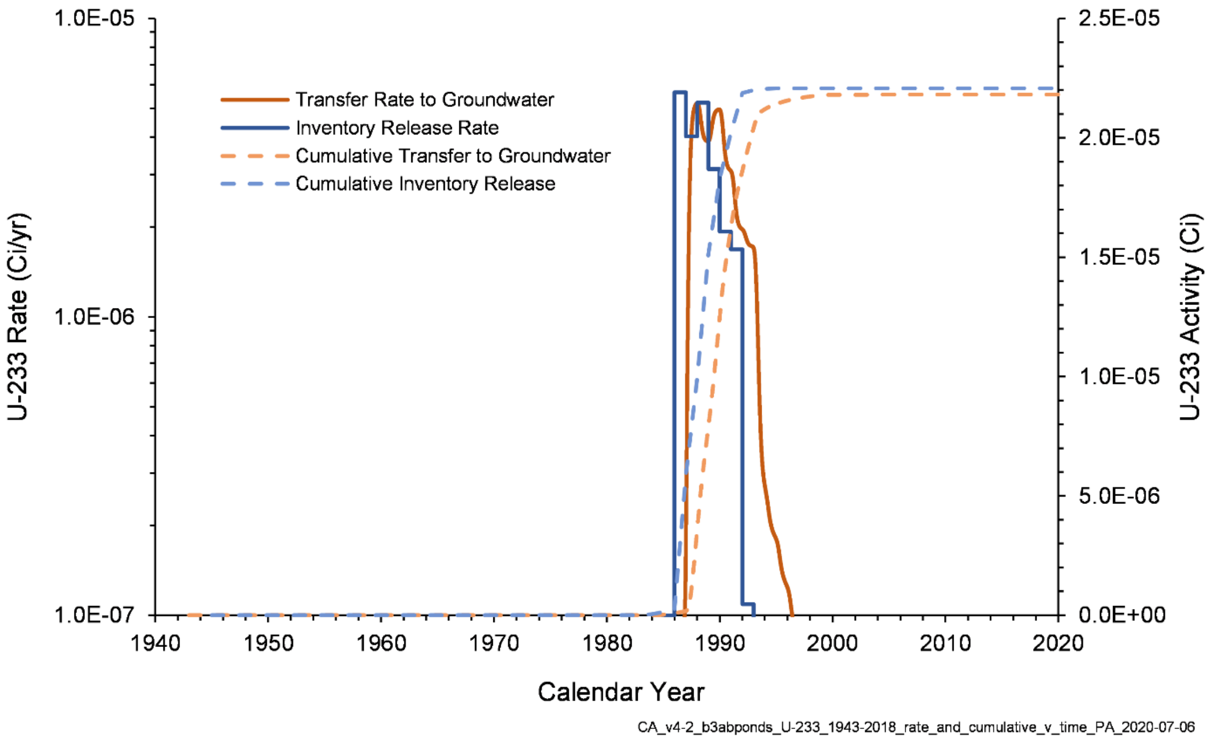

Figure 7-33. U-233 Inventory Release from Waste Sites and Transfer to Groundwater for the B-3A/B Ponds Model from 1943–2018

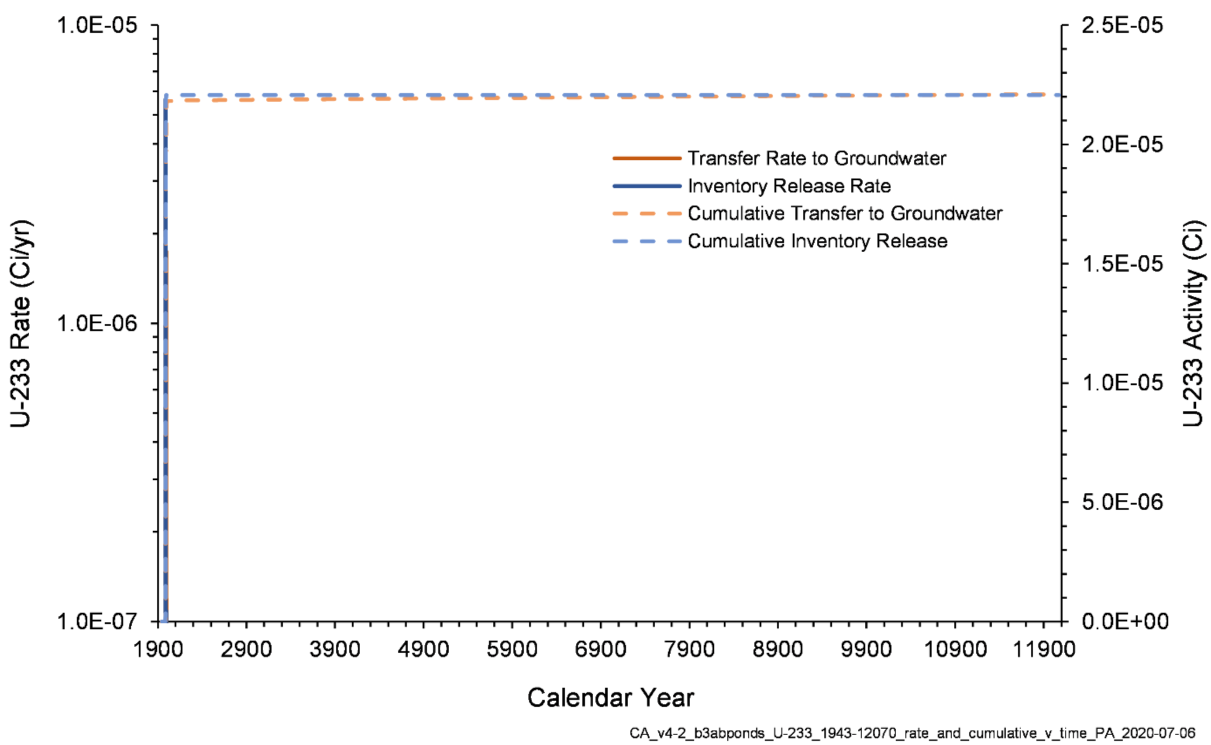

Figure 7-34. U-233 Inventory Release from Waste Sites and Transfer to Groundwater for the B-3A/B Ponds Model from 1943–12070

7.11 U-234 Fate and Transport Results

This model simulated the release and transport of U-234. The cumulative discharge of U-234 into groundwater is shown aggregated by P2R grid cell in Figure 7-35 and Figure 7-36 for 1943–2018 and 2018–12070, respectively. The inventory released to the B-3A/B Ponds model and the transfer of U-234 to groundwater are shown from 1943–2018 in Figure 7-37 and from 1943–12070 in Figure 7-38.

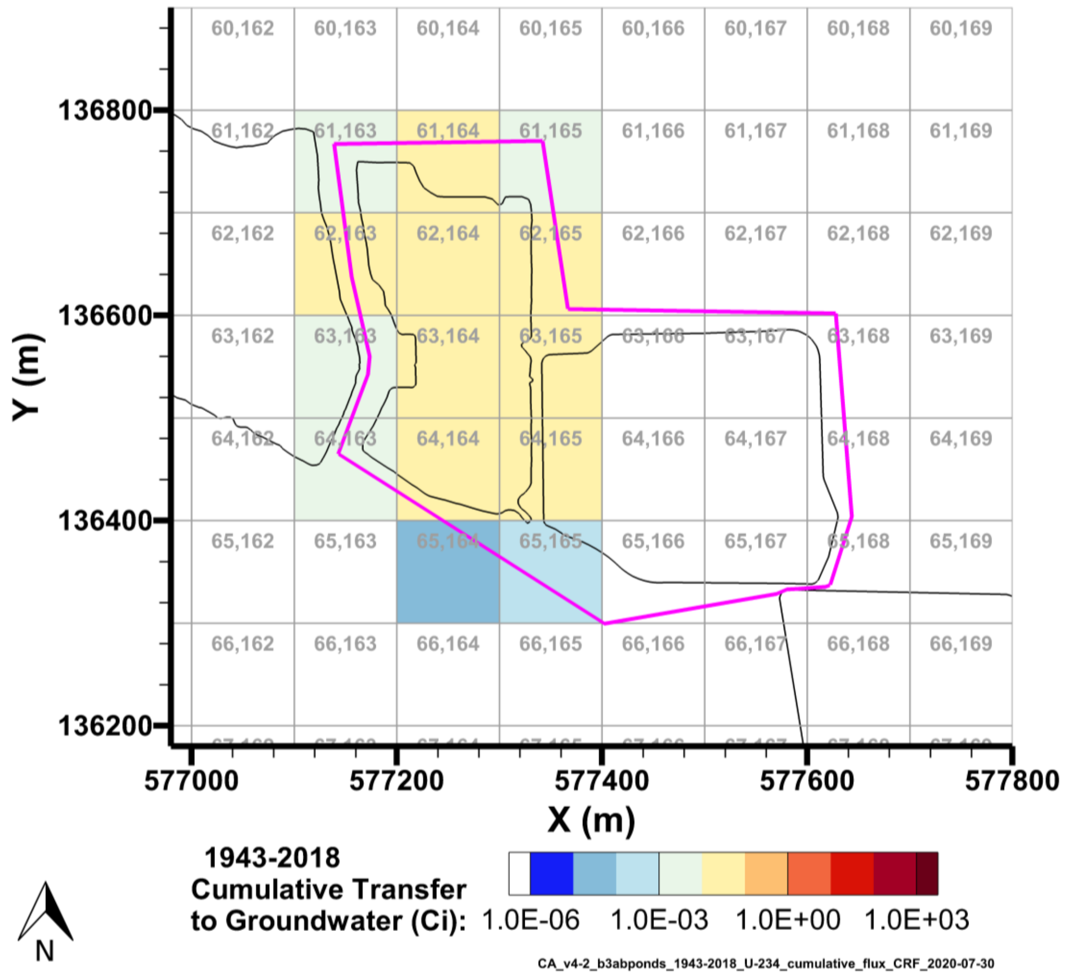

Note: source zone outlined in pink.

Figure 7-35. Cumulative U-234 Activity Discharged to Groundwater from the B-3A/B Ponds Model from 1943–2018 per P2R Grid Cell

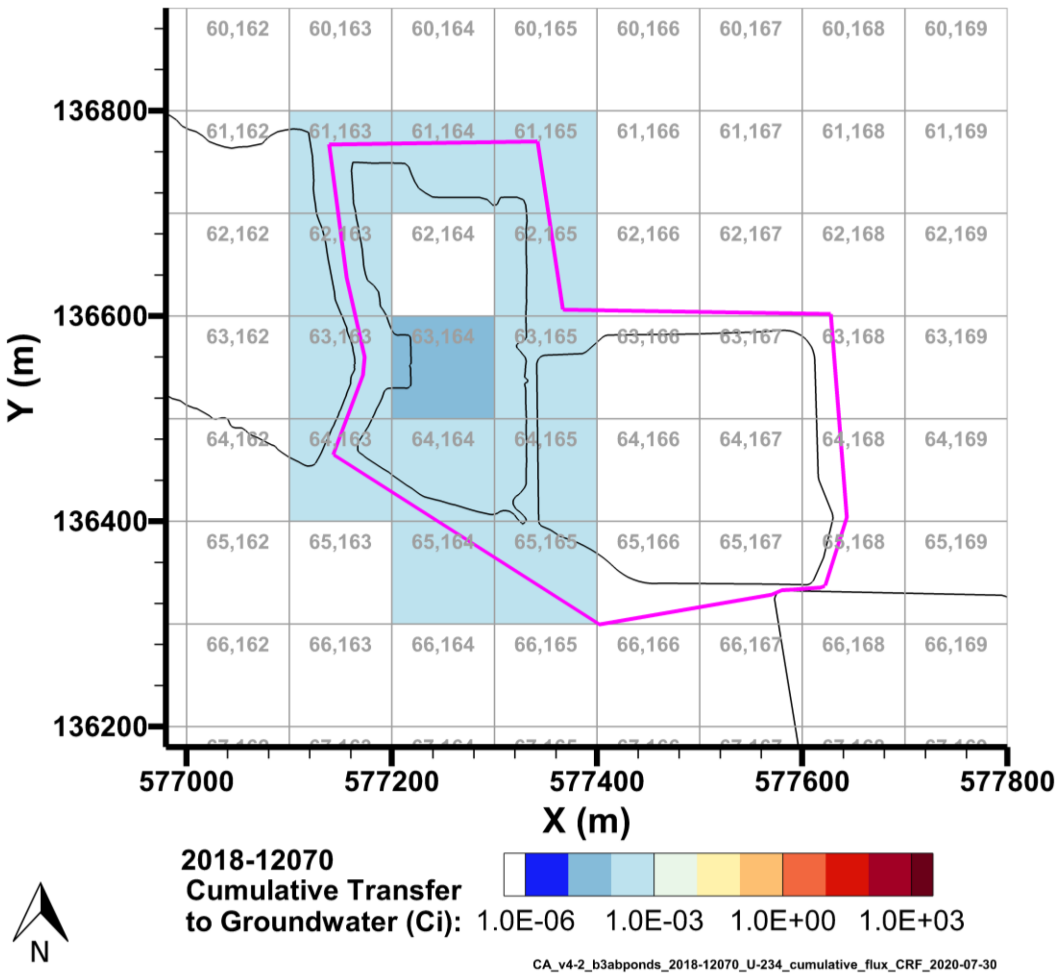

Note: source zone outlined in pink.

Figure 7-36. Cumulative U-234 Activity Discharged to Groundwater from the B-3A/B Ponds Model from 2018–12070 per P2R Grid Cell

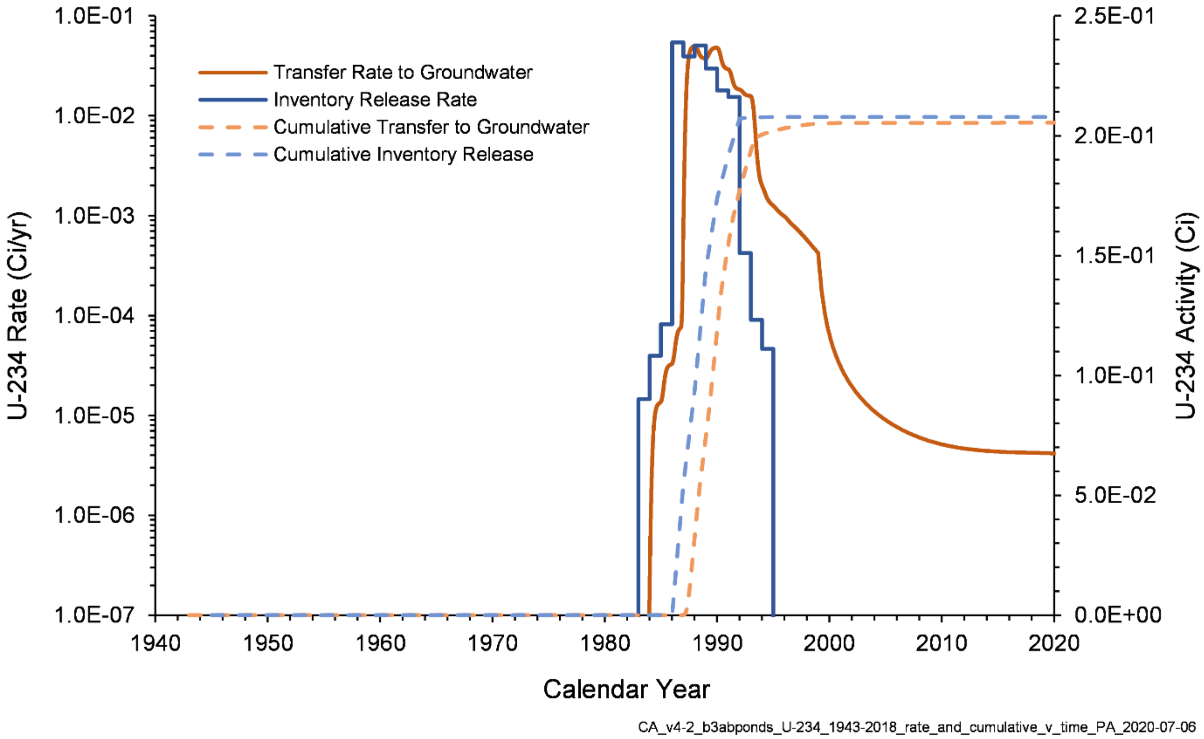

Figure 7-37. U-234 Inventory Release from Waste Sites and Transfer to Groundwater for the B-3A/B Ponds Model from 1943–2018

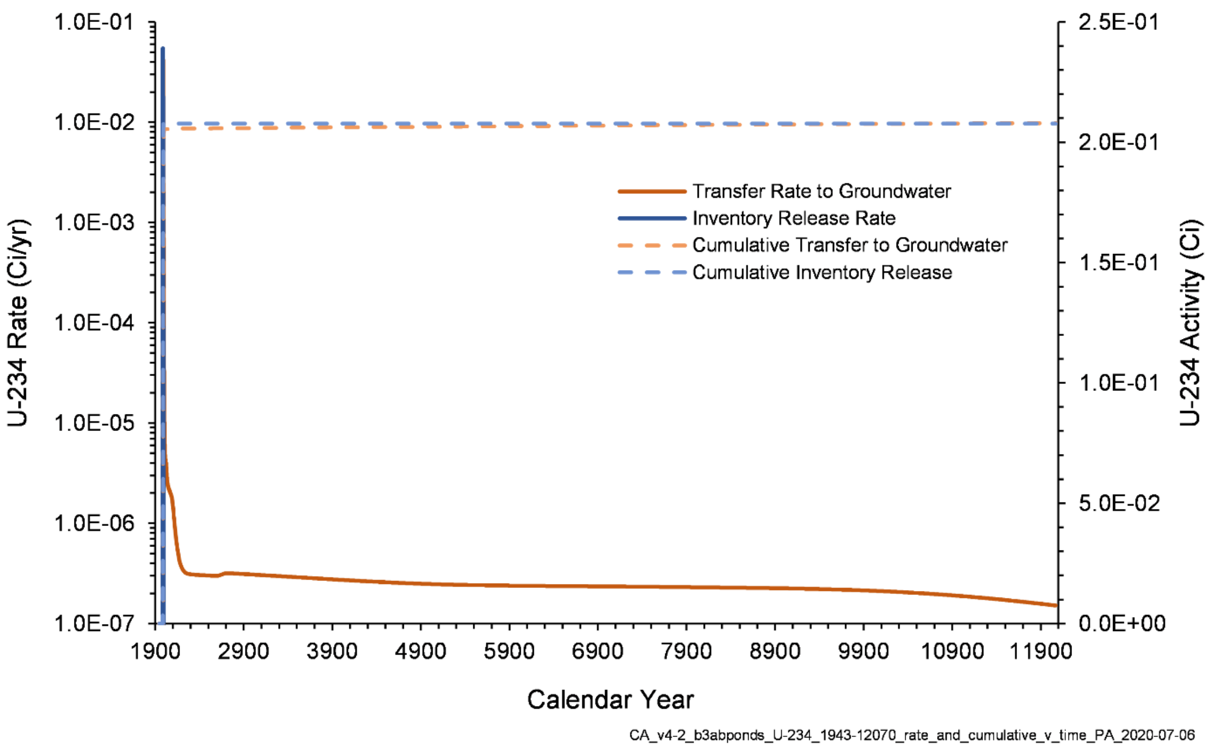

Figure 7-38. U-234 Inventory Release from Waste Sites and Transfer to Groundwater for the B-3A/B Ponds Model from 1943–12070

7.12 U-235 Fate and Transport Results

This model simulated the release and transport of U-235. The cumulative discharge of U-235 into groundwater is shown aggregated by P2R grid cell in Figure 7-39 and Figure 7-40 for 1943–2018 and 2018–12070, respectively. The inventory released to the B-3A/B Ponds model and the transfer of U-235 to groundwater are shown from 1943–2018 in Figure 7-41 and from 1943–12070 in Figure 7-42.

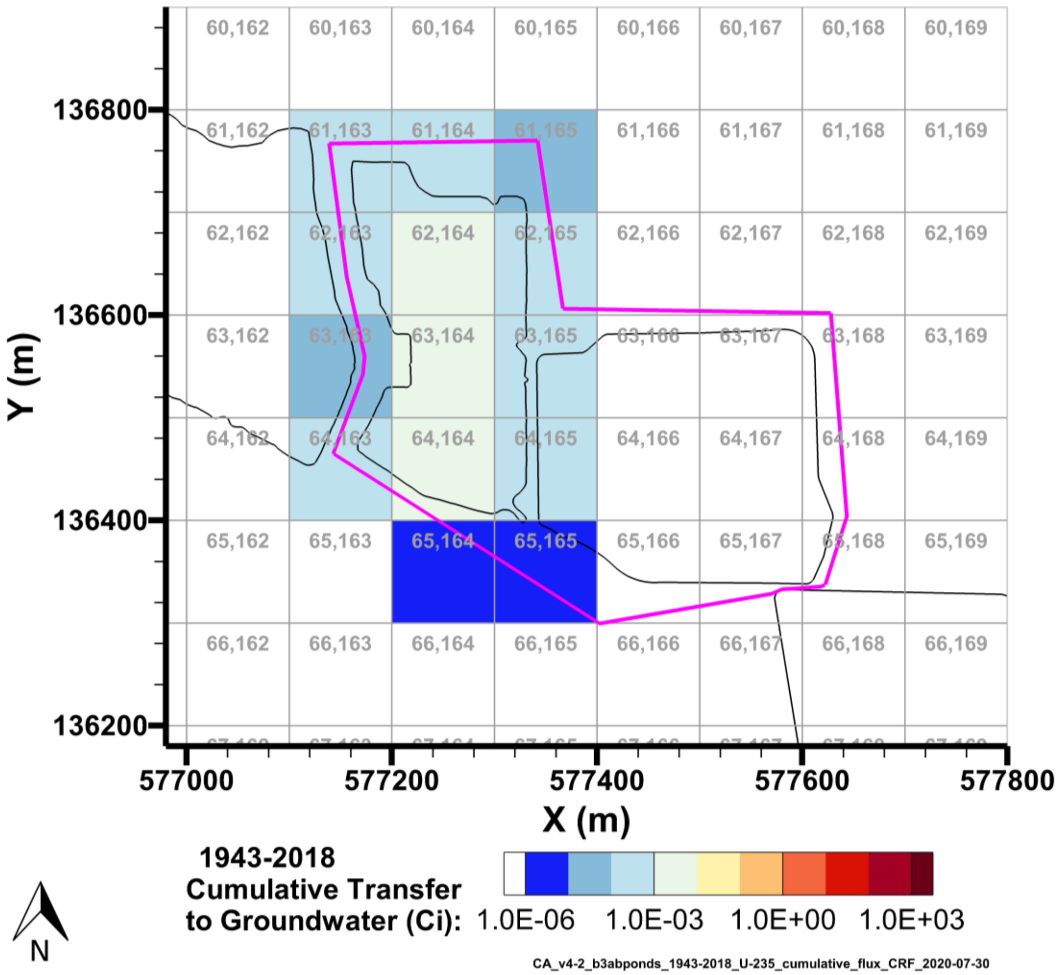

Note: source zone outlined in pink.

Figure 7-39. Cumulative U-235 Activity Discharged to Groundwater from the B-3A/B Ponds Model from 1943–2018 per P2R Grid Cell

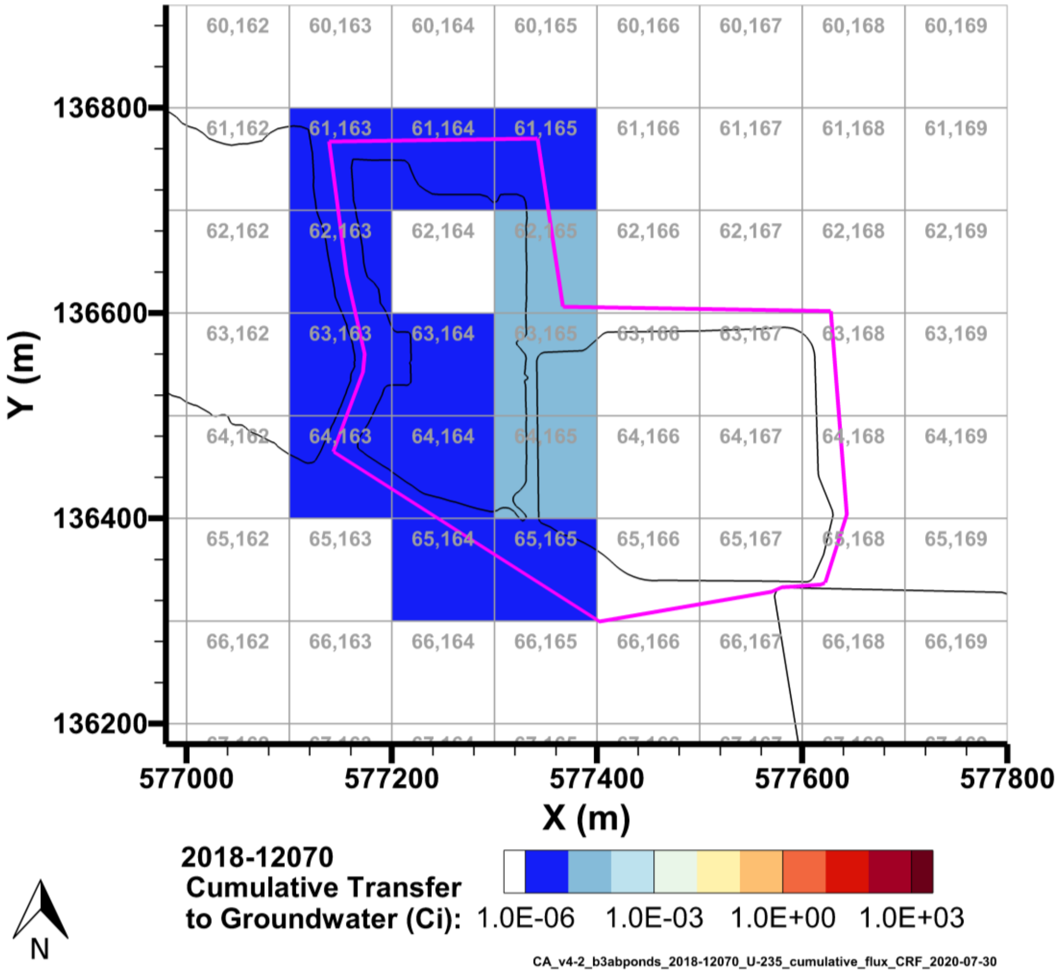

Note: source zone outlined in pink.

Figure 7-40. Cumulative U-235 Activity Discharged to Groundwater from the B-3A/B Ponds Model from 2018–12070 per P2R Grid Cell

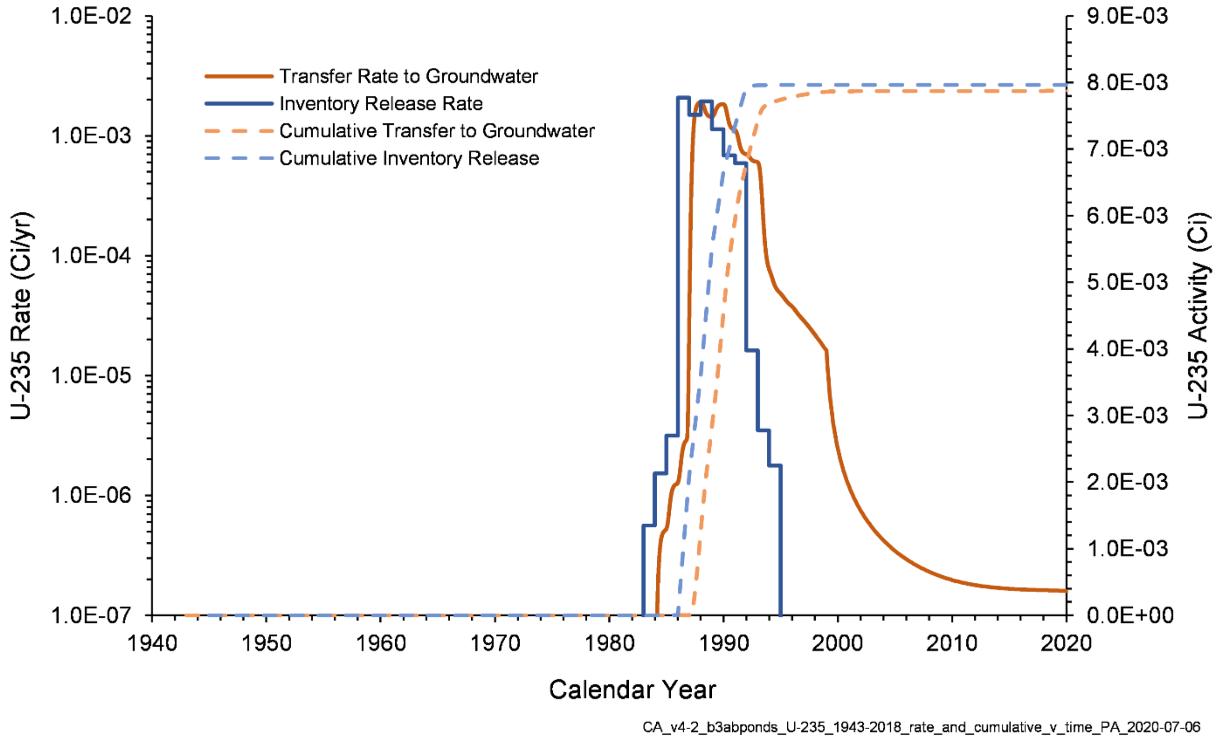

Figure 7-41. U-235 Inventory Release from Waste Sites and Transfer to Groundwater for the B-3A/B Ponds Model from 1943–2018

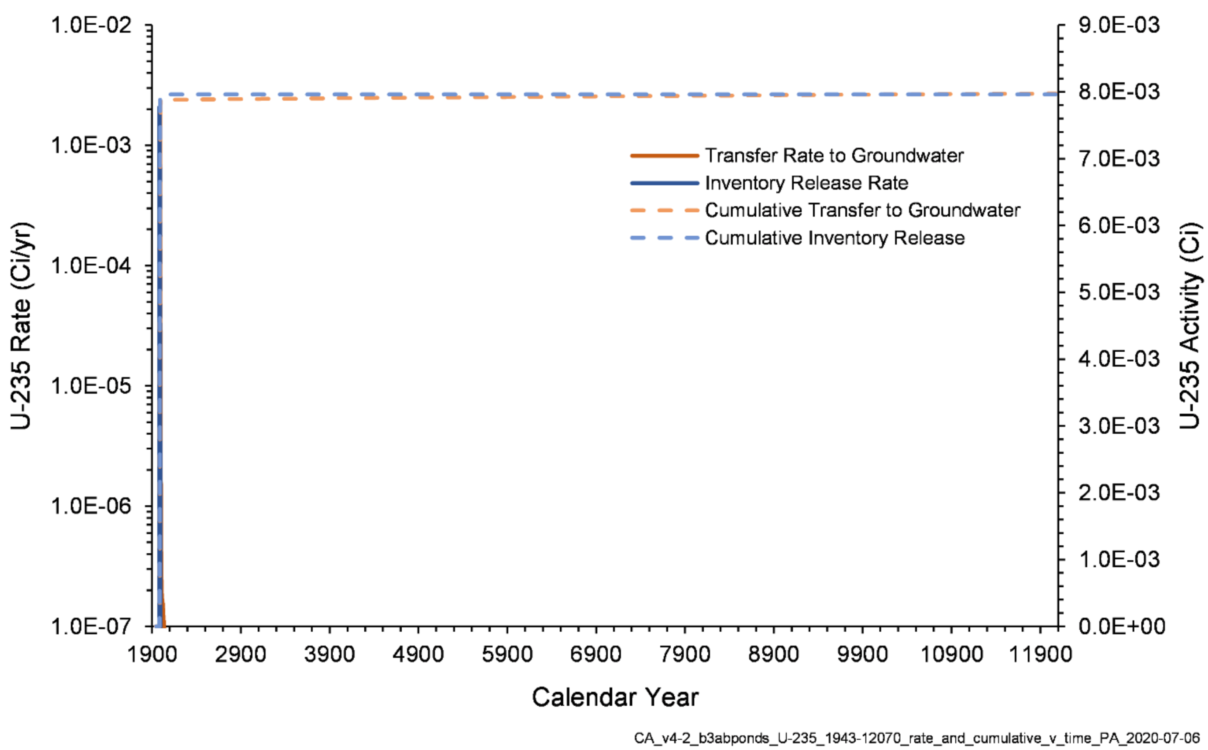

Figure 7-42. U-235 Inventory Release from Waste Sites and Transfer to Groundwater for the B-3A/B Ponds Model from 1943–12070

7.13 U-236 Fate and Transport Results

This model simulated the release and transport of U-236. The cumulative discharge of U-236 into groundwater is shown aggregated by P2R grid cell in Figure 7-43 and Figure 7-44 for 1943–2018 and 2018–12070, respectively. The inventory released to the B-3A/B Ponds model and the transfer of U-236 to groundwater from 1943–2018 in Figure 7-45 and from 1943–12070 in Figure 7-46.

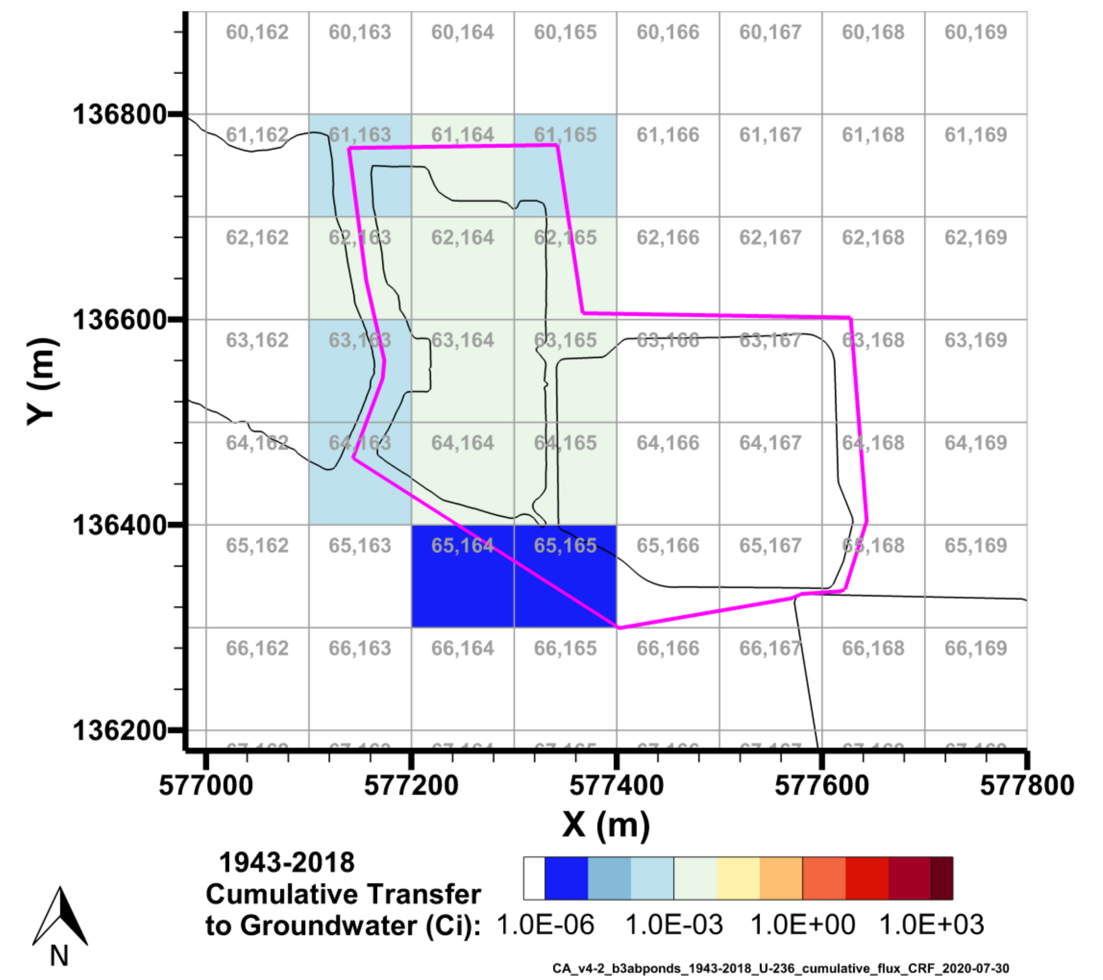

Note: source zone outlined in pink.

Figure 7-43. Cumulative U-236 Activity Discharged to Groundwater from the B-3A/B Ponds Model from 1943–2018 per P2R Grid Cell

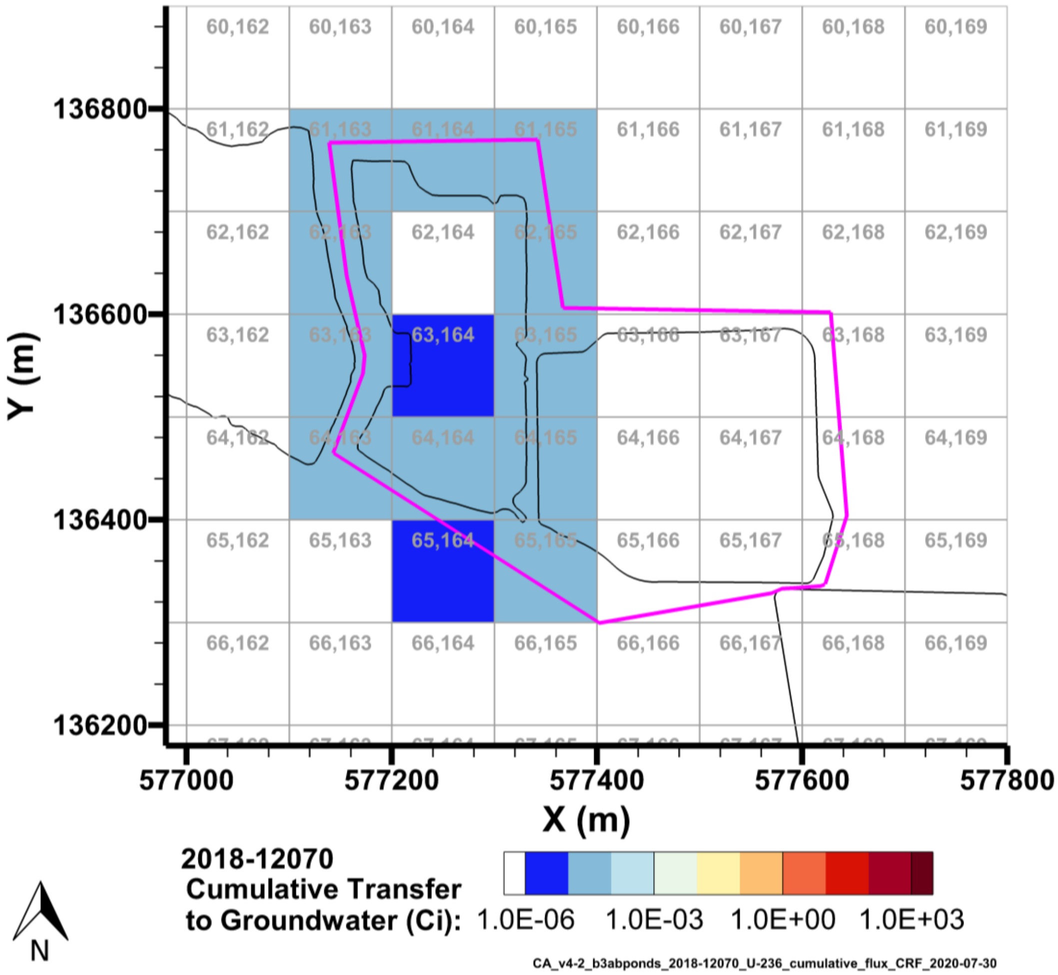

Note: source zone outlined in pink.

Figure 7-44. Cumulative U-236 Activity Discharged to Groundwater from the B-3A/B Ponds Model from 2018–12070 per P2R Grid Cell

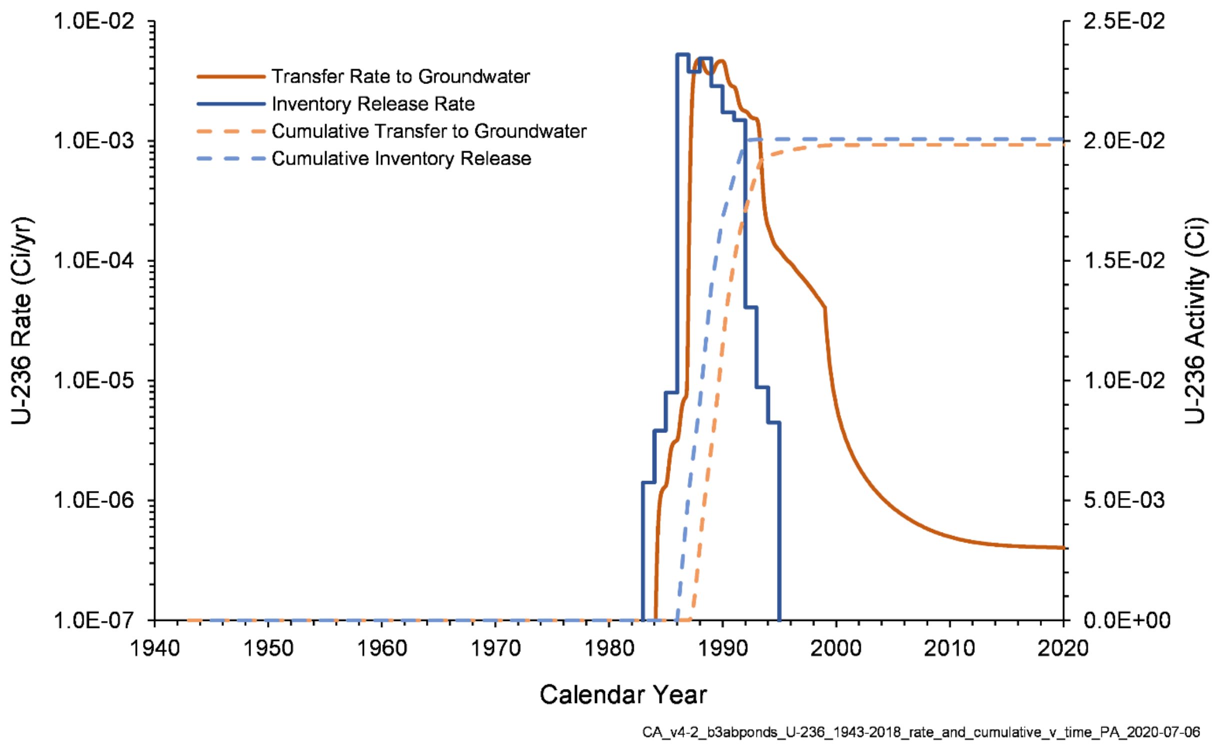

Figure 7-45. U-236 Inventory Release from Waste Sites and Transfer to Groundwater for the B-3A/B Ponds Model from 1943–2018

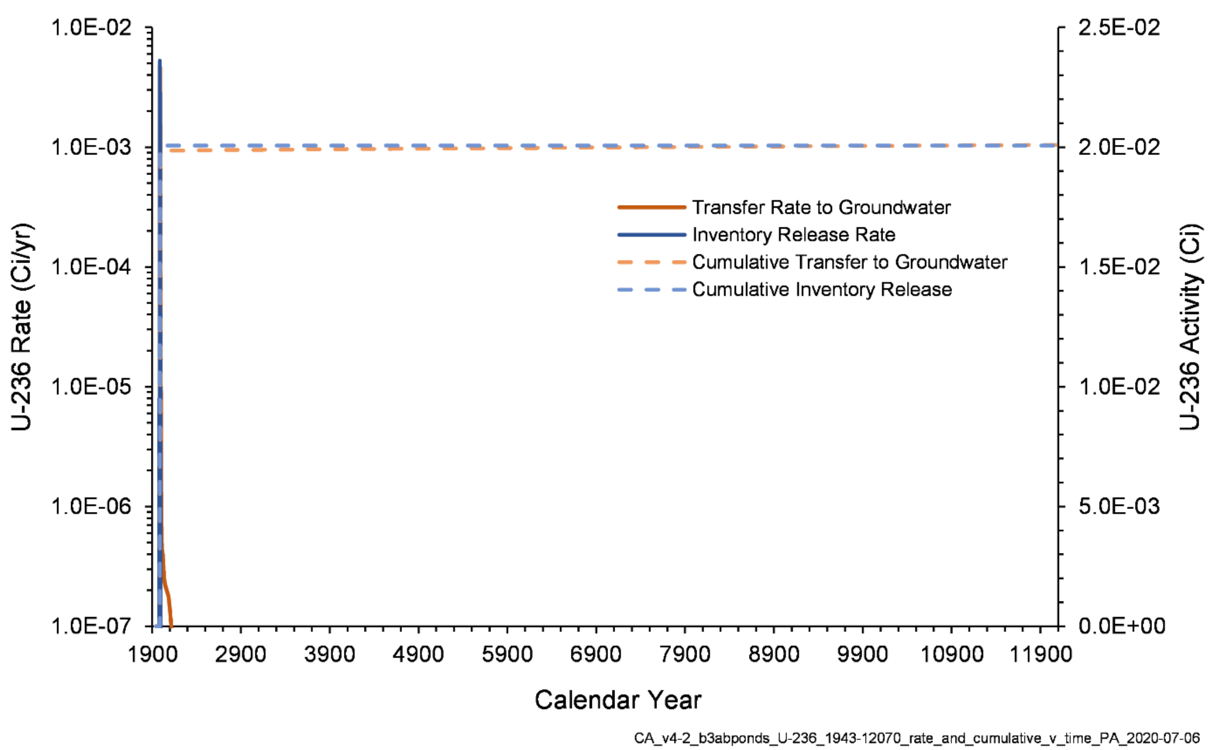

Figure 7-46. U-236 Inventory Release from Waste Sites and Transfer to Groundwater for the B-3A/B Ponds Model from 1943–12070

7.14 U-238 Fate and Transport Results

This model simulated release and transport of U-238. The cumulative discharge of U-238 into groundwater is shown aggregated by P2R grid cell in Figure 7-47 and Figure 7-48 for 1943–2018 and 2018–12070, respectively. The inventory released to the B-3A/B Ponds model and the transfer of U-238 to groundwater are shown from 1943–2018 in Figure 7-49 and from 1943–12070 in Figure 7-50.

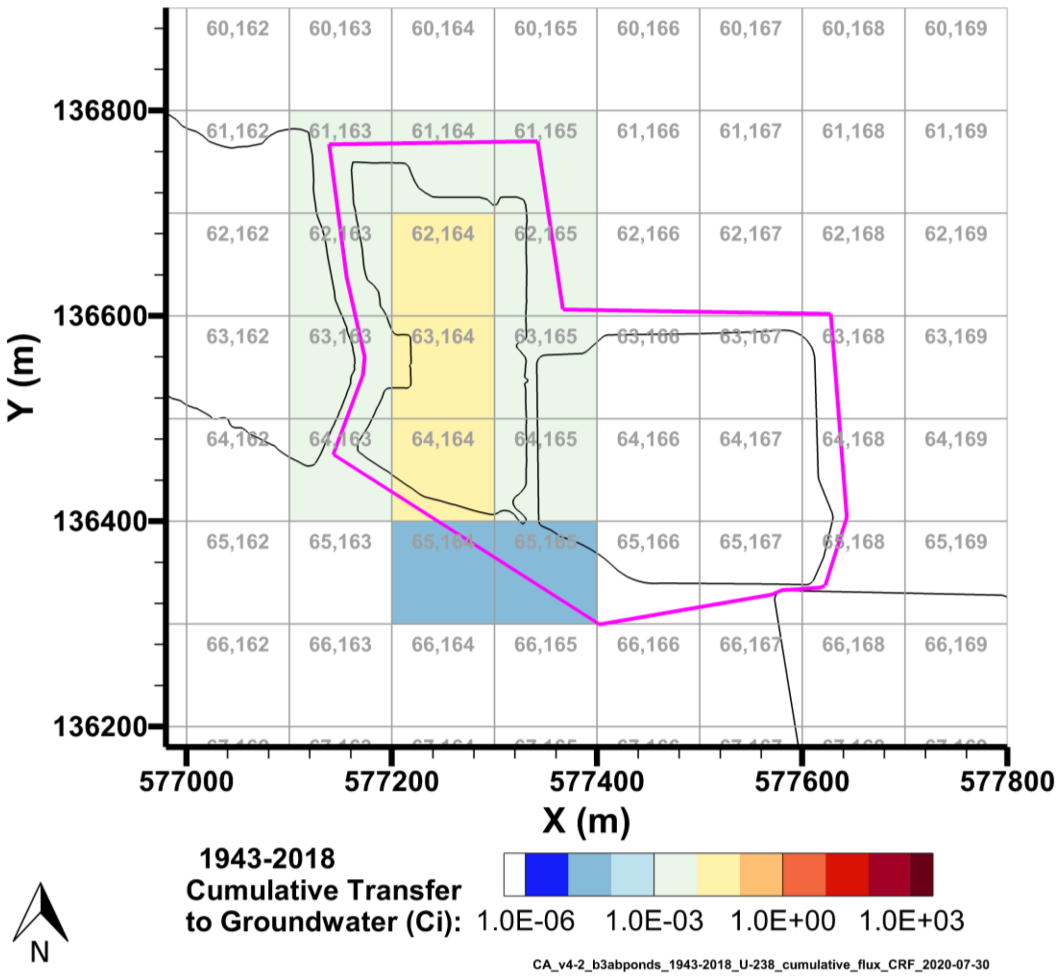

Note: source zone outlined in pink.

Figure 7-47. Cumulative U-238 Activity Discharged to Groundwater from the B-3A/B Ponds Model from 1943–2018 per P2R Grid Cell

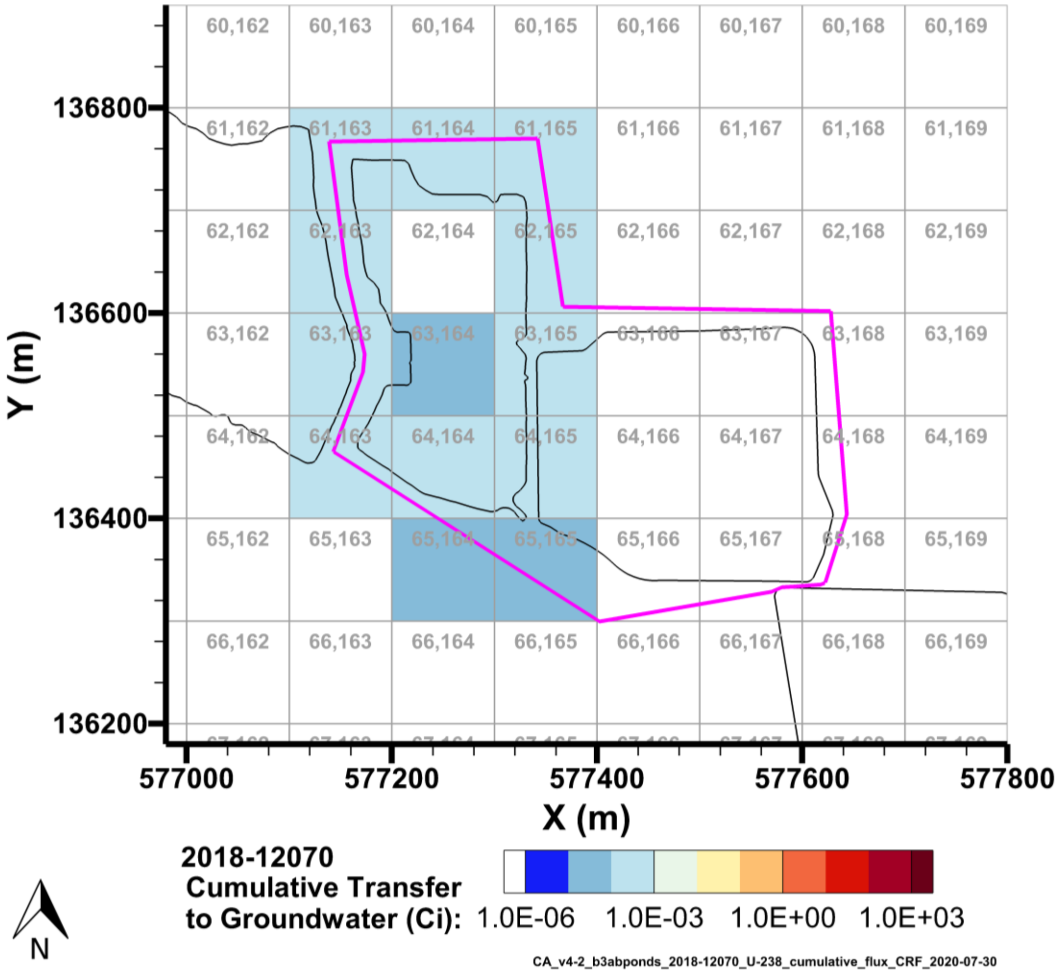

Note: source zone outlined in pink.

Figure 7-48. Cumulative U-238 Activity Discharged to Groundwater from the B-3A/B Ponds Model from 2018–12070 per P2R Grid Cell

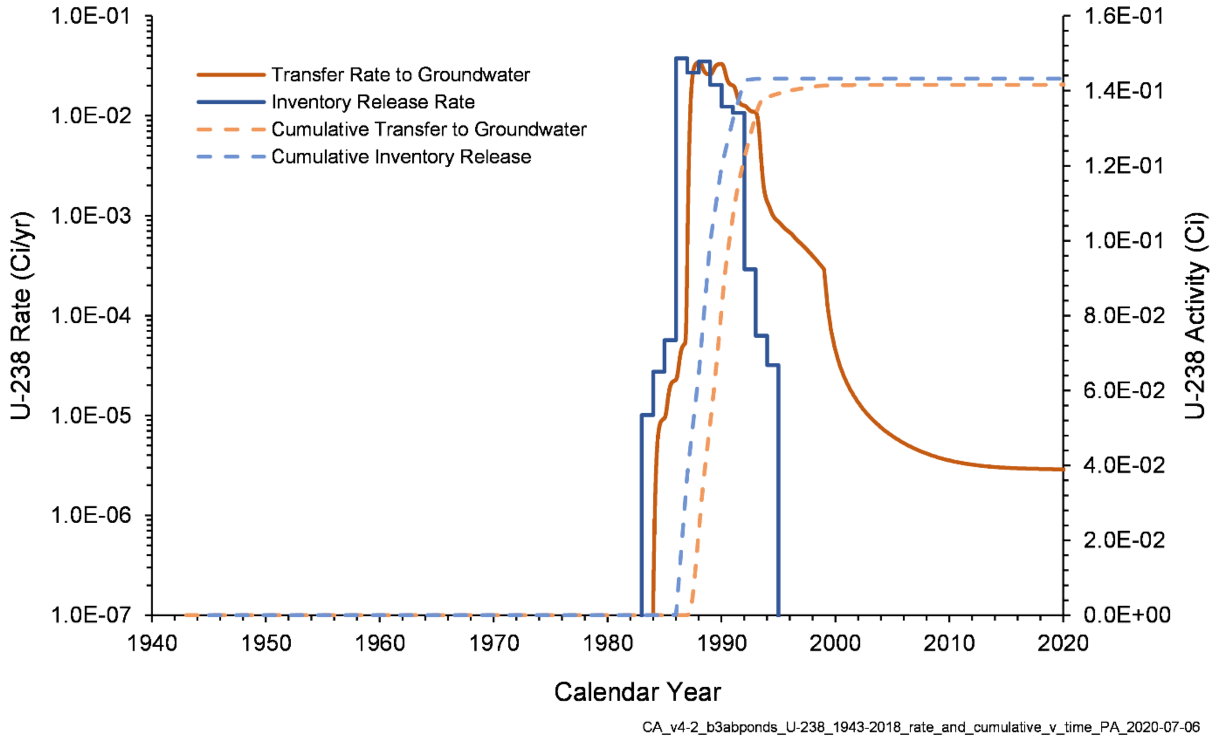

Figure 7-49. U-238 Inventory Release from Waste Sites and Transfer to Groundwater for the B-3A/B Ponds Model from 1943–2018

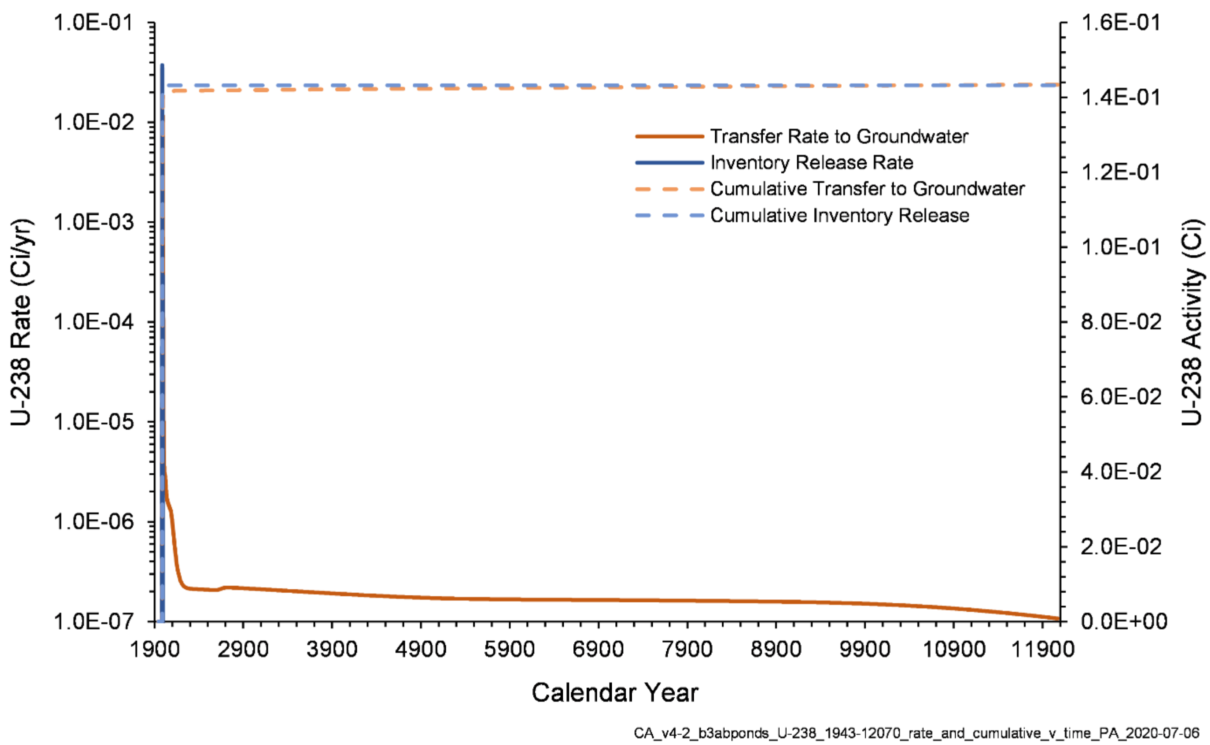

Figure 7-50. U-238 Inventory Release from Waste Sites and Transfer to Groundwater for the B-3A/B Ponds Model from 1943–12070

7.15 Ra-226 Fate and Transport Results

Ra-226 has no inventory but is present as a decay product of U-234. Flux to groundwater of Ra-226 is so low it is not presented in figures in this section.

7.16 Th-230 Fate and Transport Results

Th-230 has no inventory but it is present as a decay product of U-234. Flux to groundwater of Th-230 is so low it is not presented in figures in this section.

This page intentionally left blank.

8 References

CHPRC-00176, 2016, *STOMP Software Management Plan*, Rev. 4, CH2M HILL Plateau Remediation Company, Richland, Washington.

CHPRC-00211, 2016, *STOMP Software Test Plan*, Rev 3, CH2M HILL Plateau Remediation Company, Richland, Washington.

CHPRC-00222, 2016, *STOMP Functional Requirements Document* Rev 2, CH2M HILL Plateau Remediation Company, Richland, Washington.

CHPRC-00269, 2017, *STOMP Requirement Traceability Matrix*, Rev. 5, CH2M HILL Plateau Remediation Company, Richland, Washington.

CHPRC-00515, 2017, *STOMP Acceptance Test Report*, Rev. 5, CH2M HILL Plateau Remediation Company, Richland, Washington.

CHPRC-04032, 2020, *Composite Analysis / Cumulative Impact Evaluation (CACIE) Utility Codes Integrated Software Management Plan*, Rev. 1, CH2M HILL Plateau Remediation Company, Richland, Washington.

CP-57037, 2020, *Model Package Report: Plateau to River Groundwater Model Version 8.3*, Rev. 2, CH2M HILL Plateau Remediation Company, Richland, Washington. Available at: https://www.osti.gov/servlets/purl/1601635.

CP-60925, 2018, *Model Package Report: Central Plateau Vadose Zone Geoframework*, Rev. 0, CH2M HILL Plateau Remediation Company, Richland, Washington. Available at: https://www.osti.gov/servlets/purl/1432798.

CP-61786, 2019, *Inventory Data Package for the Hanford Site Composite Analysis*, Rev. 1, CH2M HILL Plateau Remediation Company, Richland, Washington. Available at: https://www.osti.gov/servlets/purl/1576745.

CP-62184, 2019, *Hanford Site Composite Analysis: Radionuclide Selection for Groundwater Pathway Evaluation*, Rev. 0, CH2M HILL Plateau Remediation Company, Richland, Washington. Available at: https://www.osti.gov/servlets/purl/1491467.

CP-62766, 2020, *Model Package Report: Composite Analysis Solid Waste Release Model (CASWR Model)*, Rev. 0, CH2M HILL Plateau Remediation Company, Richland, Washington. Available at: https://www.osti.gov/servlets/purl/1595469.

CP-63515, *Model Package Report: Central Plateau Vadose Zone Models*, Rev. 0 pending, CH2M HILL Plateau Remediation Company, Richland, Washington.

CP-63883, 2020, *Vadose Zone Flow and Transport Parameters Data Package for the Hanford Site Composite Analysis*, Rev. 0, CH2M HILL Plateau Remediation Company, Richland, Washington. Available at: https://www.osti.gov/servlets/purl/1608425.

DOE O 414.1D Chg 1 (Admin Chg), 2013, *Quality Assurance*, U.S. Department of Energy, Washington, D.C. Available at: https://www.directives.doe.gov/directives-documents/400-series/0414.1-BOrder-d-admchg1.

DOE/RL-89-28, 1994, *216-B-3 Expansion Ponds Closure Plan*, Rev. 2, U.S. Department of Energy, Richland Operations Office, Richland, Washington. Available at: https://pdw.hanford.gov/document/D196043318

DOE/RL-2008-59, 2017, *Interim Status Groundwater Monitoring Plan for the 216-B-3 Pond*, Rev. 2, U.S. Department of Energy, Richland Operations Office, Richland, Washington. Available at: https://pdw.hanford.gov/document/0066771H.

ECF-HANFORD-15-0019, 2020, *Hanford Site-wide Natural Recharge Boundary Condition for Groundwater Models*, Rev. 2, CH2M HILL Plateau Remediation Company, Richland, Washington. Available at: https://www.osti.gov/servlets/purl/1633785.

ECF-HANFORD-17-0079, 2018, *Hanford Soil Inventory Model (SIM-v2) Calculated Radionuclide Inventory of Direct Liquid Discharges to Soil in the Hanford Site's 200 Areas*, Rev. 0, CH2M HILL Plateau Remediation Company, Richland, Washington. Available at: https://www.osti.gov/servlets/purl/1441375.

ECF-HANFORD-17-0120, 2017, *Preparation of the March 2017 Hanford Site Water Table and Potentiometric Surface Maps*, Rev. 0, CH2M HILL Plateau Remediation Company, Richland, Washington. Available at: https://pdw.hanford.gov/document/0066758H.

ECF-HANFORD-18-0035, 2020, *Central Plateau Vadose Zone Geoframework*, Rev. 0, CH2M HILL Plateau Remediation Company, Richland, Washington. Available at: https://www.osti.gov/servlets/purl/1603767.

ECF-HANFORD-19-0032, *Distribution of Infiltration in the 216-U-10 and 216-B-3 Pond Systems 1944-1997*, pending, CH2M HILL Plateau Remediation Company, Richland, Washington.

ECF-HANFORD-19-0041, *Vadose Zone Model for B-3 Pond for Composite Analysis*, pending, CH2M HILL Plateau Remediation Company, Richland, Washington.

ECF-HANFORD-19-0043, *Vadose Zone Model for B-3C Pond for Composite Analysis*, pending, CH2M HILL Plateau Remediation Company, Richland, Washington.

ECF-HANFORD-19-0094, 2020, *Calculation of Moisture-Dependent Anisotropic Parameters Supporting the Hanford Site's Composite Analysis, Cumulative Impact Evaluation, and Performance Assessments*, Rev. 0, CH2M HILL Plateau Remediation Company, Richland, Washington. Available at: https://www.osti.gov/servlets/purl/1595470.

ECF-HANFORD-19-0112, 2020, *Solid Waste Release Calculations for the Composite Analysis Baseline Assessment*, Rev. 0, CH2M HILL Plateau Remediation Company, Richland, Washington. Available at: https://www.osti.gov/servlets/purl/1617041.

ECF-HANFORD-19-0121, 2020, *Selection of Vadose Zone Flow and Transport Properties with Gravel Fraction Corrections for the Hanford Site Composite Analysis and Cumulative Impact Evaluation*, Rev. 0, CH2M HILL Plateau Remediation Company, Richland, Washington. Available at: https://www.osti.gov/servlets/purl/1605425.

ECF-HANFORD-20-0006, 2020, *Composite Analysis Solid Waste Release Data Reduction of Activity Flux from Waste Sites to the Vadose Zone*, Rev. 0, CH2M HILL Plateau Remediation Company, Richland, Washington. Available at: https://www.osti.gov/servlets/purl/1644636.

EMDT-GR-0035, 2019, *Waste Site and Structure Footprint Shapefiles for Inclusion in Updated Composite Analysis*, Rev. 0, CH2M HILL Plateau Remediation Company, Richland, Wshington.

Farrow, C.R., M. Williams, M. Oostrom, P. Allena, and D. Fryar, 2019, “Prediction of Long-Term Contaminant Flux from the Vadose Zone to Groundwater for Fluctuating Water Table Conditions at the Hanford Site,” AGU Fall Meeting Abstracts.

Green, T.R., J.E. Constantz, and D.L. Freyberg, 1996, “Upscaled Soil-Water Retention Using Van Genuchten’s Function,” Journal of Hydrologic Engineering 1(3):123–130.

Khaleel, R., T.C.J. Yeh, and Z. Lu, 2002, “Upscaled Flow and Transport Properties for Heterogeneous Unsaturated Media,” Water Resources Research 38(5):11-1–11-12.

Mualem, Y., 1976, “A New Model for Predicting the Hydraulic Conductivity of Unsaturated Porous Media,” *Water Resources Research* 12(3):513-522.

NQA-1, 2008, *Quality Assurance Requirements for Nuclear Facility Applications*, American Society of Mechanical Engineers, New York, New York.

NUREG/CR-5965, 1994, *Modeling Field Scale Unsaturated Flow and Transport Processes*, Office of Nuclear Regulatory Research, U.S. Nuclear Regulatory Commission, Washington, D.C.

Oostrom, M., M.J. Truex, M.L. Rockhold, and T.C. Johnson, 2017, “Deep Vadose Zone Contaminant Flux Evaluation at the Hanford BY-Cribs Site Using Forward and Imposed Concentration Modeling Approaches,” Environmental Processes 4(4):771–797.

PNNL-11216, 1997, *STOMP: Subsurface Transport Over Multiple Phases Application Guide*, Pacific Northwest National Laboratory, Richland, Washington. Available at: http://stomp.pnl.gov/documentation/application.pdf.

PNNL-12030, 2000, *STOMP: Subsurface Transport Over Multiple Phases Version 2.0 Theory Guide*, Pacific Northwest National Laboratory, Richland, Washington. Available at: http://stomp.pnnl.gov/documentation/guides/theory.pdf.

PNNL-13895, 2003, *Hanford Contaminant Distribution Coefficient Database and Users Guide*, Rev. 1, Pacific Northwest National Laboratory, Richland, Washington.

PNNL-14702, 2006, *Vadose Zone Hydrogeology Data Package for Hanford Assessments*, Rev. 1, Pacific Northwest National Laboratory, Richland, Washington. Available at: https://www.pnnl.gov/main/publications/external/technical_reports/PNNL-14702rev1.pdf.

PNNL-15782, 2006, *STOMP: Subsurface Transport Over Multiple Phases Version 4.0: User’s Guide*, Pacific Northwest National Laboratory, Richland, Washington. Available at: http://stomp.pnl.gov/documentation/userguide.pdf.

PNNL-17154, 2008, *Geochemical Characterization Data Package for the Vadose Zone in the Single-Shell Tank Waste Management Areas at the Hanford Site*, Pacific Northwest National Laboratory, Richland, Washington.

PNNL-25146, 2016, *Scale-Dependent Solute Dispersion in Variably Saturated Porous Media,* RPT-IGTP-009, Rev. 0, Pacific Northwest National Laboratory, Richland, Washington.

RPP-ENV-58782, 2016, *Performance Assessment of Waste Management Area C, Hanford Site, Washington*, Rev. 0, Washington River Protection Solutions, Richland, Washington.

RPP-RPT-59197, 2016, *Analysis of Past Waste Tank Leaks and Losses in the Vicinity of Waste Management Area C, Hanford Site, Washington*, Rev. 1, Washington River Protection Solutions, Richland, Washington.

van Genuchten, M.T., 1980, "A Closed-form Equation for Predicting the Hydraulic Conductivity of Unsaturated Soils," *Soil Sci. Soc. Am. J.* 44(5):892-898. Available at: http://ars.usda.gov/sp2UserFiles/Place/53102000/pdf_pubs/P0682.pdf.

Ye, M., R. Khaleel, and T.C.J. Yeh, 2005, "Stochastic Analysis of Moisture Plume Dynamics of a Field Injection Experiment," Water Resources Research 41(3):W03013.1–W03013.13.

Yeh, T.C.J., R. Khaleel, and K.C. Carroll, 2015, Flow Through Heterogeneous Geologic Media, Cambridge University Press, New York, New York.

Zhang, Z.F. and R. Khaleel, 2010, "Simulating Field-Scale Moisture Flow Using a Combined Power-Averaging and Tensorial Connectivity-Tortuosity Approach," Water Resources Research 46(9):W09505, 14 pp.

Zhang, Z.F., A.L. Ward, and G.W. Gee, 2003, "A Tensorial Connectivity–Tortuosity Concept to Describe the Unsaturated Hydraulic Properties of Anisotropic Soils," Vadose Zone Journal 2(3):313–321.

Appendix A

Checking Documentation for the B-3A/B Ponds Model

This page intentionally left blank.

Contents

This page intentionally left blank.

A1 Introduction

This appendix is a folder of portable document files. These files contain documentation of checks completed by the modeling team and from qualified employees outside of the modeling team.

This page intentionally left blank.

Model Check 2 – Transport XPRT Part A				
Model (full name):	B-3 A/B Ponds			
Modeler Name:	Praveena Allena			
Peer Reviewer Name:	Sandra Mondragon			
Task/Action/Operation	***Modeler***		***Peer Reviewer***	
	Status	Comment	Status	Comment
Surface Card Checks				
Completed tool qualification check (Surface Flux Cards Check 1)	☒		☒	
Completed P2R fingerprint check (Surface Flux Cards Check 2)	☒		☒	
Completed *input_SS* fingerprint check (Surface Flux Cards Check 3)	☒		☒	
Completed check of Rad1 and Rad2 list in *rad#_surface_flux.txt* files and proper sequence (Surface Flux Cards Check 4)	☒		☒	
Completed comparison of *rad#_surface_flux.txt* files (Surface Flux Cards Check 5)	☒		☒	
Completed check on TSFF computation (Surface Flux Cards Check 6)	☒		☒	DeltaA = 7, DeltaB = 6
Completed check to ensure correct domain bottom is used (Surface Flux Cards Check 7)	☒		☒	
Completed check on correct use of P2R area (Surface Flux Cards Check 8)	☒		☒	
Completed check on correct STOMP-P2R grid mapping (Surface Flux Cards Check 9)	☒		☒	
Output Card Checks				
Completed tool qualification check (Output Cards Check 1)	☒		☒	
Completed *input.nij* fingerprint check (Output Cards Check 2)	☒		☒	
Completed *input.sij* fingerprint check (Output Cards Check 3)	☒		☒	

Model Check 2 – Transport XPRT Part A				
Model (full name):	B-3 A/B Ponds			
Modeler Name:	Praveena Allena			
Peer Reviewer Name:	Sandra Mondragon			
Task/Action/Operation	***Modeler***		***Peer Reviewer***	
	Status	Comment	Status	Comment
Completed *input.top* fingerprint check (Output Cards Check 4)	☒		☒	
Completed *plot_times.txt* check (Output Cards Check 5)	☒		☒	
Completed comparison of *rad#_Output_Control.dat* files (Output Cards Check 6)	☒		☒	
Completed comparison of *rad#_Mass_Balance_Output_Control.dat* files (Output Cards Check 7)	☒		☒	
Completed comparison of *rad1_Output_Control.dat* and *rad1_Mass_Balance_Output_Control.dat* files (Output Cards Check 8)	☒		☒	
Completed spot check of specified node locations (Output Cards Check 9)	☒		☒	
Boundary Card Checks				
Completed high-level check of recharge plots (Boundary Conditions Card Check 1)	☒		☒	
Completed recharge spot check and time-series comparison. Write down the checked i,j locations and time-series comparison results (OK; not OK) (Boundary Conditions Card Check 2)	☒	RET Nodes checked: 10,15 – OK 22,55 – OK 42,50 – OK 65,39 - OK 75,20 - OK	☒	I,J Values: 36, 28; OK 59, 14; OK 74, 14; OK 33, 39; OK 22, 49; OK
After completion by both the modeler and peer-reviewer, the form should be moved to the CompletedForms folder. The form should not be signed until both have completed the check and all issues have been resolved.				
Date Completed	***Modeler: 03-23-2020***		***Peer Reviewer: 3-21-2020***	

Model Check 2 – Transport XPRT Part A				
Model (full name):	B-3 A/B Ponds			
Modeler Name:	Praveena Allena			
Peer Reviewer Name:	Sandra Mondragon			
Task/Action/Operation	***Modeler***		***Peer Reviewer***	
	Status	Comment	Status	Comment
Name	Praveena Allena		Sandra Mondragon	
Signature				

Model Check 2 – Transport XPRT Part B				
Model (full name):	B-3A/B Ponds Model			
Modeler Name:	G. Tartakovsky			
Peer Reviewer Name:	Christian Hall			
Task/Action/Operation	***Modeler***		***Peer Reviewer***	
	Status	Comment	Status	Comment
Check list follows sections in CA-XPRT-2018-Input-File-Check-PartB-*.pptx Modelers: \CAVE\v4-2\supportfiles\CheckingDocs\xprt-PartB Peer Reviewers: \Rel.061\vadose\Peer-Checking-xprt-B\CheckingDocs				
Completed tool qualification checks (pages 11-17 of *CA-XPRT-2018-Input-File-Check-PartB-*.pptx*)	☒		☒	
Completed *ca-src2stomp.pl* tool input check (Pages 18-22)	☒		☒	
Completed *xprt_2018_input_gen.f for xprt-1 Simulations* tool input check (Pages 23-32)	☒		☒	
Completed *xprt_2018_input_gen.f for xprt-2 Simulations* tool input check (Pages 33-42)	☒		☒	
Completed Source Card site list comparison with maps (Page 43-45)	☒		☒	
Completed construction of all source-check spreadsheets (Page 49)	☒		☒	
Completed site areas comparison (Page 50)	☒		☒	
Completed operation years comparison (Page 51)	☒		☒	
Completed cumulative inventory comparison (Page 52)	☒		☒	
For sfarms model only: Completed special case check for SX-115 site (Page 53)	☐	NA	☐	N/A
For bcomplex model only: Completed special case check for BX-102 site (Page 54)	☐	NA	☐	N/A

Model Check 2 – Transport XPRT Part B				
Model (full name):	B-3A/B Ponds Model			
Modeler Name:	G. Tartakovsky			
Peer Reviewer Name:	Christian Hall			
Task/Action/Operation	***Modeler***		***Peer Reviewer***	
	Status	Comment	Status	Comment
For tfarms model only: Completed special case check for T-106 site (Page 55-56)	☐	NA	☐	N/A
Input File Check – xprt-1 simulation				
Completed Simulation Title Card Check (Page 59)	☒		☒	
Completed Solution Control Card Check (Page 60-62)	☒		☒	
Completed Direct input_SS Copy Check (Page 63)	☒		☒	
Completed Water Table Boundary Check (Page 64)	☒		☒	
Completed Solute/Fluid Interaction Card Check (Page 65)	☒		☒	
Completed Solute/Porous Media Interaction Card Check (Page 66-67)	☒		☒	
Completed Initial Conditions Card Check (Page 68)	☒		☒	
Input File Check – xprt-2 simulation				
Completed Simulation Title Card Check (Page 71)	☒		☒	
Completed Solution Control Card Check (Page 72-74)	☒		☒	
Completed Direct input_SS Copy Check (Page 75)	☒		☒	
Completed Water Table Boundary Check (Page 76)	☒		☒	

Model Check 2 – Transport XPRT Part B				
Model (full name):	B-3A/B Ponds Model			
Modeler Name:	G. Tartakovsky			
Peer Reviewer Name:	Christian Hall			
Task/Action/Operation	***Modeler***		***Peer Reviewer***	
	Status	Comment	Status	Comment
Completed Solute/Fluid Interaction Card Check (Page 77)	☒		☒	
Completed Solute/Porous Media Interaction Card Check (Page 78-79)	☒		☒	
Completed Initial Conditions Card Check (Page 80)	☒		☒	
After completion by both the modeler and peer-reviewer, the form should be moved to the CompletedForms folder. The form should not be signed until both have completed the check and all issues have been resolved.				
	Modeler		***Peer Reviewer***	
Date Completed	***05/29/2020***		***06/09/2020***	
Name	***G. Tartakovsky***		**Christian Hall**	
Signature and Date	06/09/2020		06/09/20	

Model Check 3 – Transport XPRT Part C				
Model (full name):	B-3A/B Ponds Model			
Modeler Name:	G. Tartakovsky			
Peer Reviewer Name:	Christian Hall			
Task/Action/Operation	***Modeler***		***Peer Reviewer***	
	Status	Comment	Status	Comment
Check list follows sections in CA-XPRT-MB-Input-File-Check-PartC-*.pptx Modelers: \CAVE\v4-2\supportfiles\CheckingDocs\xprt-PartC Peer Reviewers: \Rel.061\vadose\Peer-Checking-xprt-C\CheckingDocs				
Completed tool qualification checks (pages 12-13 of *CA-XPRT-MB-Input-File-Check-PartC-*.pptx*)	☒		☒	
Completed *xprt_mb_input_gen.f* tool input check (Pages 15-18)	☒		☒	
Input File Check – MB1 simulation				
Completed Simulation Title Card Check (Page 21)	☒		☒	
Completed Solution Control Card Check (Page 22-24)	☒		☒	
Completed Direct *input_XPRT-1* Copy Check (Page 25)	☒		☒	
Completed Solute/Fluid Interaction Card Check (Page 26)	☒		☒	
Completed Output Control Card Check (Page 27)	☒		☒	
Completed Surface Card Check (Page 28)	☒		☒	
Input File Check – MB2 simulation				
Completed Simulation Title Card Check (Page 31)	☒		☒	
Completed Solution Control Card Check (Page 32-234)	☒		☒	

Model Check 3 – Transport XPRT Part C				
Model (full name):	B-3A/B Ponds Model			
Modeler Name:	G. Tartakovsky			
Peer Reviewer Name:	Christian Hall			
Task/Action/Operation	***Modeler***		***Peer Reviewer***	
	Status	Comment	Status	Comment
Completed Direct *input_XPRT-1* Copy Check (Page 35)	☒		☒	
Completed Solute/Fluid Interaction Card Check (Page 36)	☒		☒	
Completed Output Control Card Check (Page 37)	☒		☒	
Completed Surface Card Check (Page 38)	☒		☒	
After completion by both the modeler and peer-reviewer, the form should be moved to the CompletedForms folder. The form should not be signed until both have completed the check and all issues have been resolved.				
	Modeler		***Peer Reviewer***	
Date Completed	***06/08/2020***		***06/09/2020***	
Name	***G. Tartakovsky***		**Christian Hall**	
Signature and Date	06/09/2020		06/09/20	

Model Check 4– Transport XPRT Part D				
Model (full name):	B-3A/B Ponds Model			
Modeler Name:	Guzel Tartakovsky			
Peer Reviewer Name:	Christian Hall			
Task/Action/Operation	***Modeler***		***Peer Reviewer***	
	Status	Comment	Status	Comment
Check list follows sections in CA-XPRT-12070-Input-File-Check-PartD-*.pptx Modelers: \CAVE\v4-2\supportfiles\CheckingDocs\xprt-PartD Peer Reviewers: \Rel.061\vadose\Peer-Checking-xprt-D\CheckingDocs				
Completed tool qualification checks (pages 11-12 of *CA-XPRT-12070-Input-File-Check-PartD-*.pptx*)	☒		☒	
Completed *xprt_12070_input_gen.f* tool input check (Pages 14-15)	☒		☒	
Input File Check: xprt-1-12070 simulation				
Completed Simulation Title Card Check (Page 18)	☒		☒	
Completed Solution Control Card Check (Page 19)	☒		☒	
Completed Direct *input_XPRT-1* Copy Check (Page 20)	☒		☒	
Completed Output Control Card Check (Page 21)	☒		☒	
Input File Check: xprt-2-12070 simulation				
Completed Simulation Title Card Check (Page 24)	☒		☒	
Completed Solution Control Card Check (Page 25)	☒		☒	
Completed Direct *input_XPRT-2* Copy Check (Page 26)	☒		☒	
Completed Output Control Card Check (Page 27)	☒		☒	

Model Check 4– Transport XPRT Part D				
Model (full name):	B-3A/B Ponds Model			
Modeler Name:	Guzel Tartakovsky			
Peer Reviewer Name:	Christian Hall			
Task/Action/Operation	***Modeler***		***Peer Reviewer***	
	Status	Comment	Status	Comment
After completion by both the modeler and peer-reviewer, the form should be moved to the CompletedForms folder. The form should not be signed until both have completed the check and all issues have been resolved.				
	Modeler		***Peer Reviewer***	
Date Completed	***05/27/2020***		***06/09/2020***	
Name	***Guzel Tartakovsky***		**Christian Hall**	
Signature and Date	06/09/2020		06/09/2020	

Appendix B

Cross-Sections of the Hydrostratigraphy in the B-3A/B Ponds Model

(Electronic Appendix)

This page intentionally left blank.

Contents

This page intentionally left blank.

B1 Introduction

This appendix is a folder containing two subfolders, SouthToNorth and WestToEast. Both contain images of cross-sections through the model showcasing the hydrostratigraphy; the first from south to north and the second from west to east.

The contents of this electronic appendix are stored in the Environmental Modeling Management Archive (EMMA) indexed to this ECF by document number.

This page intentionally left blank.

Appendix C

Charts of Recharge to the B-3A/B Ponds Model as Defined by the Recharge Evolution Tool

(Electronic Appendix)

This page intentionally left blank.

Contents

This page intentionally left blank.

C1 Introduction

This appendix is a folder of images. Each image is a map of the annual recharge rate at the surface of the model, as assigned by the Recharge Evolution Tool, per grid cell in the model for each year where any recharge rate is different than the preceding year.

The contents of this electronic appendix are stored in the Environmental Modeling Management Archive (EMMA) indexed to this ECF by document number.

This page intentionally left blank.

Appendix D

Software Installation and Checkout Forms

This page intentionally left blank.

Contents

This page intentionally left blank.

D1 Introduction

This appendix is a portable document file showing the completed Software Installation and Checkout form.

This page intentionally left blank.

CHPRC SOFTWARE INSTALLATION AND CHECKOUT FORM

Software Owner Instructions:

Complete Fields 1-13, then run test cases in Field 14. Compare test case results listed in Field 15 to corresponding Test Report outputs. If results are the same, sign and date Field 19. If not, resolve differences and repeat above steps.

Software Subject Matter Expert Instructions:

Assign test personnel. Approve the installation of the code by signing and dating Field 21, then maintain form as part of the software support documentation.

GENERAL INFORMATION:

1. Software Name: STOMP (Subsurface Transport Over Multiple Phases) Software Version No.: Bld 6

EXECUTABLE INFORMATION:

2. Executable Name (include path):

Following STOMP serial and parallel mode executable files in directory [REDACTED]/bin on head node and each compute node (compute-0-0 through compute-0-8, inclusive):

```
--------------------------------  --------------------------
MD5 File Signature                Executable File Name
--------------------------------  --------------------------
4a0f738b74620bc8df4d05290b513a44  eSTOMP1-chprc06-20200204-gaia.x
6536b8e12d8c5b83dca76f2c947b6153  stomp-wae-bcg-chprc06i.x
e0cdf04bc1a2f6c55c5a1b499939f663  stomp-wae-bcg-chprc06l.x
86c58db6fac5d1b4e6cbe13041b2568b  stomp-wae-bcg-chprc07i.x
6e72340bb39f6056e232fe5ff241c4d4  stomp-wae-bd-chprc06i.x
3f837a0fb8d9f47dbcada686f542d7fc  stomp-wae-bd-chprc06l.x
7e5b4cc36a8991b3d5a8ea2ed155ce47  stomp-wae-cgsq-chprc06i.x
00a898c0c3ec06817485781ad1c9ec46  stomp-wae-cgsq-chprc06l.x
f18ff5ab5667065d8ab12657344fb6a0  stomp-wae-cgst-chprc06i.x
061af86cf21ad8435b046d0efabe971b  stomp-wae-cgst-chprc06l.x
3c8111a9855dc0e430bf3c8a7abcf37e  stomp-w-bcg-chprc06i.x
20436d615a94955a2ce8eecdb8cba546  stomp-w-bcg-chprc06l.x
8b3df29df21d040189c3e2a50ef823bb  stomp-w-bd-chprc06i.x
066a289a75aedb933eb2536da5d7d1ff  stomp-w-bd-chprc06l.x
c8e62ad7a0d9b6fca39d8a8952ef5d8e  stomp-w-cgsq-chprc06i.x
28ad16806e1307aca51fd7bf89793e75  stomp-w-cgsq-chprc06l.x
6c25051016db2fe1f883a7caaaab1e97  stomp-w-cgst-chprc06i.x
ff9ff6f29b3469419ffaece87d7e772b  stomp-w-cgst-chprc06l.x
0c3e3fba40f5b93e71bcf9586432fd27  stomp-w-r-bcg-chprc06i.x
78492aee80a8c2d0a4e82aabf4a9c213  stomp-w-r-bcg-chprc06l.x
84b129786aba9c4be884e15e45a67389  stomp-w-r-bd-chprc06i.x
e990f1566c8099a8d54508de3da9cd88  stomp-w-r-bd-chprc06l.x
18a589a2b55aab2db290efea19b39351  stomp-w-r-cgsq-chprc06i.x
6569959476772a137df35ce874821889  stomp-w-r-cgsq-chprc06l.x
```

3. Executable Size (bytes): MD5 signatures above uniquely identify each executable file

COMPILATION INFORMATION:

4. Hardware System (i.e., property number or ID):

Tellus Subsurface Modeling Platform (serial STOMP executables) and compiled directly on Gaia for eSTOMP.

5. Operating System (include version number):

[REDACTED] 2.6.18-308.4.1.el5 #1 SMP Tue Apr 17 17:08:00 EDT 2012 x86_64 x86 64 x86 64 GNU/Linux (for serial STOMP executables).

INSTALLATION AND CHECKOUT INFORMATION:

6. Hardware System (i.e., property number or ID):

GAIA Subsurface Flow and Transport Modeling Platform (Linux Cluster)

CHPRC SOFTWARE INSTALLATION AND CHECKOUT FORM (continued)

1. Software Name: STOMP (Subsurface Transport Over Multiple Phases) Software Version No.: Bld 6

7. Operating System (include version number):

[REDACTED] 3.10.0-693.5.2.el7.x86_64 #1 SMP Fri Oct 20 20:32:50 UTC 2017 x86_64 x86 64 x86 64 GNU/Linu

8. Open Problem Report? ◉ No ○ Yes PR/CR No.

TEST CASE INFORMATION:

9. Directory/Path:

[REDACTED]/test/stomp/build-6 on head node and each compute node of Gaia

10. Procedure(s):

CHPRC-00211 Rev 3, STOMP Software Test Plan

11. Libraries:

N/A (static linking)

12. Input Files:

Input files for ITC-STOMP-1, ITC-STOMP-2, and ITC-STOMP-2
(Baseline for comparison are results files from ATC-STOMP-1, ATC-STOMP-2, and ATC-STOMP-3 prepared on Tellus during acceptance testing)

13. Output Files:

plot.* files produced by STOMP in testing

14. Test Cases:

ITC-STOMP-1, ITC-STOMP-2, and ITC-STOMP-3

15. Test Case Results:

All PASS, all tests run, on all nodes of Gaia.

16. Test Performed By: WE Nichols

17. Test Results: ◉ Satisfactory, Accepted for Use ○ Unsatisfactory

18. Disposition (include HISI update):

Accepted, entry added to HISI. Installation applicable to all approved Gaia users who have completed STOMP required reading training assignment. Includes all acceptance tested STOMP executables EXCEPT eSTOMP reactive transport (will test this later).

Prepared By:

19. WILLIAM NICHOLS (Affiliate) Digitally signed by WILLIAM NICHOLS (Affiliate) Date: 2020.02.05 11:27:03 -08'00'	WE Nichols	
Software Owner (Signature)	Print	Date

20. Test Personnel:

	WE Nichols	
Sign	Print	Date
Sign	Print	Date
Sign	Print	Date

Approved By:

21.	N/R (per CHPRC-00211 Rev 1)	
Software SME (Signature)	Print	Date

Appendix E

Radionuclide Arrival to the Groundwater Through Time for Plateau to River Grid Cells in the B-3A/B Ponds Model

This page intentionally left blank.

Contents

E1 Introduction

This appendix is a folder of portable document files. These files contain charts showing the radionuclide transfer to groundwater from the model in different configurations, as indicated by the figure titles on the charts.

The contents of this electronic appendix are stored in the Environmental Modeling Management Archive (EMMA) indexed to this ECF by document number.

This page intentionally left blank.